# THE ELECTRODEPOSITION OF POLYMERS AND LUMINESCENT MATERIALS TO CREATE THE NEXT GENERATION OF LIGHTING TECHNOLOGY

by

Samual Gordon Tafara Ngombe BEng



A Thesis

Submitted to the College of Engineering

Swansea University

In Fulfilment of the Requirements

For MSc in Materials Engineering by Research

30th September 2022



Engineering and Physical Sciences Research Council


Swansea University
Prifysgol Abertawe

LUXTEC

# Abstract

This thesis is an account of an experimental investigation into the manufacture of electroluminescent lighting with 3D geometry. The study required extensive experimentation into the electrophoretic deposition process and its suitability to a complex 3D substrate as opposed to 2D. The research required the development of a novel experimental technique in which multiple surfaces of the substrate may be coated. The experimental set-up required alteration from the original design supplied by the sponsoring company to a singular cylindrical electrode developed through literature research. The layers of the emissive source that were experimented on consisted of a Barium Titanate ($BaTiO_3$) dielectric, phosphor trimix (CaS:Eu, ZnS:Ag and ZnS:Cu, Al) emissive layer and a Poly(methyl methacrylate) (PMMA) encapsulating polymer layer. Upon successful results from this novel experimental set up, parameters such as applied voltage, processing time (the period that the substrate is submerged in the suspension and the power source is initiated) and solid concentration were tested in a range of combinations. Extensive experimentation allowed for optimal parameters to be found for each layer. $BaTiO_3$ exhibited preferable deposit morphology at a bulk concentration of 20-25 g/L and the addition of adhesion-promoting polymer Polyvinylpyrrolidone (PVP) formed a high-quality, uniform deposit. The electrophoretic deposition of the phosphor layer was improved through sieving to a particle size range of 4-11 μm. This allowed for a reduction in particle size distribution to make particle mobility more predictable and improve material suspension. Agitation of the phosphor material was found to be important in maximising deposited material. A stirring rate of 315-390 rpm would encourage the most uniform deposit. Electrophoretic deposition of the encapsulating polymer was unsuccessful due to electrolysis causing hole formation in the deposited layer at the anode. Due to this, a dip coating process was established and was successful in achieving material deposit whilst improving the adhesion of the previous layer. Electrophoretic deposition onto a 3D substrate was successful and it is now possible to coat an entire coil from outside to inside face simultaneously. After optimal conditions were found for the individual layers, sequenced deposition of the dielectric, phosphor and encapsulating polymer layers was also carried out successfully. Parameters required further adjustment to account for the increased system resistance due to material deposit. The preliminary stages of testing electrodeposition of the 3 materials have proven to be a promising method in the fabrication of an alternating current electroluminescent (ACEL) device.

# Declarations

This work has not previously been accepted in substance for any degree and is not being concurrently submitted in candidature for any degree.

Signed.....Samual Ngombe.....

Date...30/09/2022.....

This thesis is the result of my own investigations, except where otherwise stated. Other sources are acknowledged by footnotes giving explicit references. A bibliography is appended.

Signed..... Samual Ngombe.....

Date..... 30/09/2022.....

I hereby give consent for my thesis, if accepted, to be available for photocopying and for inter-library loan, and for the title and summary to be made available to outside organisations.

Signed..... Samual Ngombe.....

Date..... 30/09/2022.....

The University's ethical procedures have been followed and, where appropriate, that ethical approval has been granted.

Signed..... Samual Ngombe.....

Date..... 30/09/2022.....

# Contents

# Acknowledgements

I would like to extend my sincere thanks to the Materials and Manufacturing Academy (M2A) for their continued support throughout my process of completing this MSc. Thanks also to the European Social Fund for funding this research.

I would also like to extend my gratitude to Chris Philips. His constant outstanding support as my supervisor has allowed me to improve as an individual researcher and produce a body of work, I am proud to call my own.

I would like to recognise Luxtec Global and Peter Leak for bringing me into their team and allowing me to assist in their research.

Lastly, I would be remiss in not mentioning my family. Their belief in me has kept my spirits and motivation high during this process.

# List of Tables

# List of Figures

# 1.Introduction

This thesis is an account of an experimental investigation into the manufacture of electroluminescent lighting with 3D geometry. This project was sponsored by Luxtec, a company that is looking to launch an alternative to current domestic and industrial lighting using electrophoretic deposition (EPD) on to a 3D scaffold.

### 1.1.Electroluminescent lighting.

From televisions and computer screens to fluorescent lighting in laboratories and classrooms, luminescence surrounds us and is continuously being optimised and remodelled to maximise efficiency and output. A luminescent material, or a phosphor, is defined as a solid which converts certain types of energy into electromagnetic radiation over and above thermal radiation (1). Luminescence is not limited to a single form and the type of output can be defined by the energy that excites the materials in use. For example, photoluminescence is excited by electromagnetic radiation and triboluminescence by mechanical energy. In this study, the focus is on electroluminescence (EL) and its generation of light in response to the passage of an electric current (injection EL) or strong electric field (alternating current EL or ACEL). Depending on the voltage applied, these mechanisms can be distinguished by exhibiting high-field or low-field electroluminescence. Light-emitting diodes (LEDs) characteristically only require a few volts and are typical of low-field electroluminescence, whereas high-field electroluminescence requires electric fields up to $10^6$ V/cm (2). With this, LEDs make use of direct current to operate as opposed to alternating current in ACEL devices.

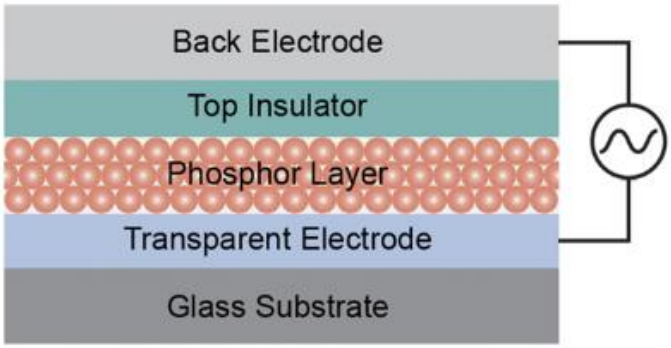


**Figure 1. Schematic illustration of ACEL device [3]**

The build of a traditional ACEL device has two conducting electrodes, one of which is transparent, sandwiching a phosphor and dielectric layer as shown in Figure 1**.** Upon

application of a sufficient AC voltage, a high electric field is developed within the phosphor layer. Electrons trapped at the insulator-phosphor interface are injected into the phosphor layer when this electric field is large enough. Electrons are then transported to the opposite electrode across the phosphor layer. They impact and excite luminance impurities of the phosphor layer to their excited stage from the ground state. As these luminance centres return to their ground states, the excess energy is released in the form of photon emission. As excited luminance particles reach their ground state, the accelerated electrons are trapped at the opposite phosphor-insulator interface (3).

### 1.2.Electrophoretic deposition

Electrophoretic deposition uses an electric field to transport charged particles or colloids towards a substrate. Particles are dispersed in a liquid medium and are charged using a deposition electrode and a counter electrode of opposite polarity. As particles move towards the electrode, they accumulate at the surface and form a deposit. It is a simple and cost-effective method to produce particulate films for solid-state lighting applications(2). Electrophoretic deposition has also proved to be an extremely versatile process. With the ability to alter the deposition time and applied voltage, layer thickness and morphology of deposited film can be altered with ease. Deposition can also be carried out on diverse types of surfaces (flat cylindrical etc.) by changing electrode design and positioning (4). Literature has shown that altering certain processing parameters in the EPD process will cause changes in the final deposited layer. Of these parameters, the main drivers in the system are the charge of the particle and the electrophoretic mobility of the particles in the solvent under the influence of an applied electric field (4). An early investigation by Hamaker (5) and Avgustnik (6) saw the proposal of the following equation to analyse the effect of processing parameters on the deposit yield:

$$w = \int_{t_1}^{t_2} \mu * E * A * C * dt$$ **Equation 1**

This equation relates deposit yield (w) to electrophoretic mobility (μ), electric field strength (E), the surface area of the electrode (A) and particle mass concentration in the suspension (C). The base-level theories for the alteration of the electrodeposition process are mostly drawn from this. EPD currently is widely used in fabrication, most notably for wear-resistant and functional films for advanced microelectronic devices and solid oxide fuel cells. It is also

documented that the process is used for nanoscale assembly of advanced functional materials and development of novel composites or bioactive coatings for medical implants (2).

### 1.3.Luxtec Global project aims

Based on a review of the literature, Luxtec provided provisional working recipes to initiate the study. This research had the fundamental aim of producing a lighting technology that would offer increased efficiency compared to current market offerings. This claim will be enabled by using two three-dimensional emissive sources of different geometries, with alternating current electroluminescence. The increased surface area of the Luxtec global emissive sources is proposed to increase the light output that is usually relatively low in other devices of similar architecture. This project exhibits innovations in multiple aspects of the brief which come with challenges that will later be explored. As previously mentioned, electrophoretic deposition is intended to be used to deposit each of the individual layers of their contemporary alternating current electroluminescent device. As a starting point, Luxtec provided several plastic tanks for the electrophoretic deposition process. These were made from repurposed tanks used for gel electrophoresis and had not been verified for the process. Were these to be successful in depositing the ACEL layers uniformly in sequence through initial experimentation, this project would give innovation in ACEL device design to improve efficiency along with progression in three-dimensional EPD.

### 1.4.Research challenges

Although there is ample evidence for the deposition of the various functional layers on to flat sheets, it has not been tested for 3D geometries and indeed the technique of EPD itself tends to be limited to 2D forms. There are challenges in terms of the deposition of the materials to achieve a comprehensive and consistent coverage over the 3D geometry given that the driving force for deposition is the electric field (V/m) between the substrate and the counter electrode. With flat plates as substrates, it is much easier to maintain an equal electric field between the substrate and counter electrode. With more complex geometries, like the substrate used for this product, this becomes much more difficult with a risk of inconsistent or partial deposition. There is also a lack of evidence for the success of polymer electrophoretic deposition when dissolved in solvent, rather than as particles. As well as the complex 3D geometry, there is the additional complication of sequencing the layers, with modification potentially required when depositing on to already coated substrates. In a working device, all layers would need to be pinhole free to avoid shorting. Sequencing each layer through electrophoretic deposition would

also become a challenge when combined with a complex 3D substrate. Particle suspension is an important factor in effective EPD, and particles such as phosphors which are both relatively large and heavy and have the tendency to settle. This may be addressed through agitation but must not reach a level so high that particle motion through convection supersedes electrophoretic migration to the substrate.

The initial project aims of completion of the entire device with all layers deposited eventually would be adjusted to address each challenge. Due to the challenges that developed throughout experimentation, the primary objective became establishing a method for uniformly depositing onto a 3D substrate. Once this was achieved, the objective then shifted to attaining a uniform deposit that matches the layer weights set by the sponsoring company. Each layer was given a target value for layer weight which has been calculated to reflect total coverage of the substrate with an optimal layer thickness. Given the period of the project, this work will focus on three layers (1) a barium titanate dielectric layer, which will be followed by an encapsulating polymer layer (2), then followed with a phosphor layer (3). These layers were evaluated individually and in sequence.

# 2.Literature review

## 2.1.Electrophoretic deposition

Electrophoretic deposition (EPD) involves the coating of a substrate through the migration of colloidal particles that are suspended in a liquid under the influence of an electric field. This mechanism allows materials to be applied to any form of electrically conductive surface. Besra et al (2) offers an extensive investigation into the electrophoretic deposition process and allows for a greater understanding of methods to improve the results of EPD. From this, it's firstly demonstrated that this process is advantageous due to its short formation time, simple apparatus, and little restriction of the shape of the substrate. The process is very versatile and can be modified easily for a specific application and onto many diverse types of surfaces – flat, cylindrical, or spherical. The thickness and morphology of deposited film can also be altered by changing deposition time and applied potential along with other various combinations of parameters discussed in depth in **Section 2.1.1**. Through literature, it is well demonstrated that electrophoretic deposition is an effective technique that allows the shaping of free-standing objects, and depositing thick films on substrates starting from liquid suspensions of ceramic powders and by application of direct current potentials (7). Cathodic deposition is mainly utilized due to its ability to produce thin films with good adherence to the substrate as compared to anodic deposition. The limitations of the process occur due to the inability to use water as the liquid medium. When a high enough voltage is applied to water, it promotes the evolution of hydrogen and oxygen gases at the electrodes which could adversely affect the quality of the deposits formed. This is due to the onset of electrolysis in the water which is a widely documented phenomenon (8). This is not a major disadvantage as many non-aqueous solvents are available which will be investigated through this review.

It is important to recognise the mechanisms of the electrophoretic deposition technique and how certain control parameters must be set to allow for successful deposition. The factors which influence these conditions and mechanisms are explored in the following section. Before experimentation, the main components of EPD should be identified and optimised: particle dispersion, particle charging, electrophoretic migration and finally the deposition of particles. Particle stabilization ensures that particles do not settle or agglomerate through experimentation. Agglomeration leads to the formation of larger particles that exhibit different physical and chemical properties to the original particles. This will eventually cause inconsistencies in the coating thickness and quality. To assist in the stabilization of the

particles, techniques such as selecting particles of lower density or introducing an energy barrier between particles to prevent them from coming into contact (9) may be used. Effective particle charging is achieved through the selection of a solvent that can enable ionic charge where adsorption/dissolution equilibria for a positive and negative ion are different (10). The next component of EPD is electrophoretic migration which occurs under an electric field. When the electric field is initiated, charged particles migrate in the direction of the oppositely charged electrode to be deposited through the electrophoresis mechanism.

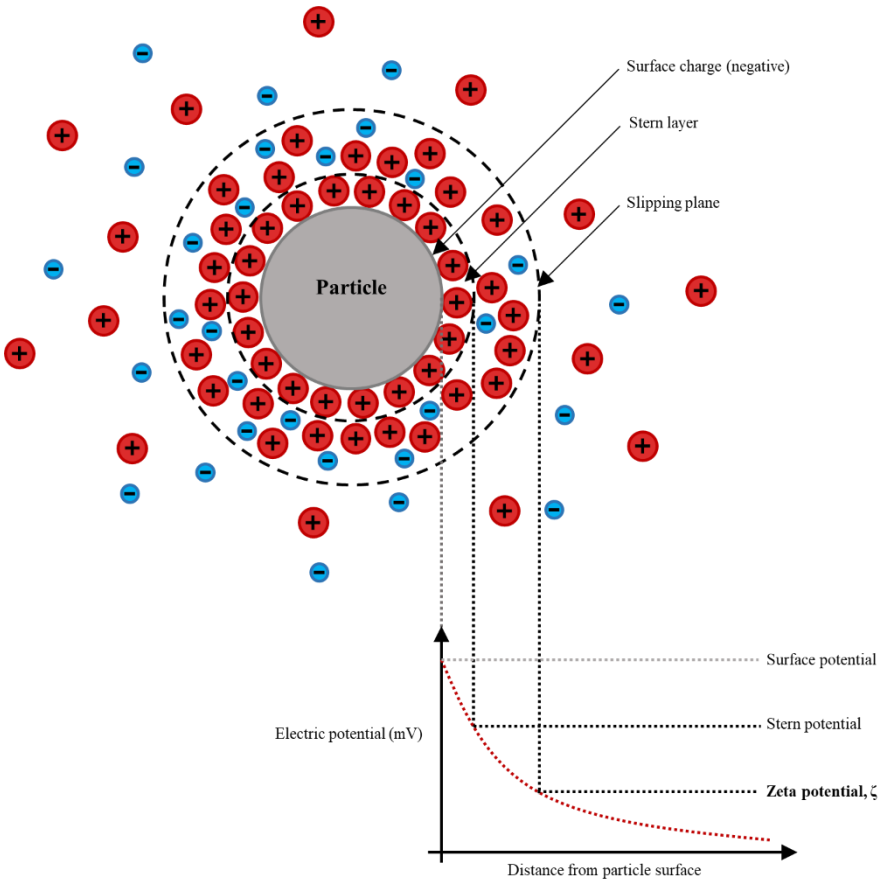


**Figure 2. Diagram to show the potential difference as a function of distance from the charged surface of a particle suspended in a dispersion medium (reproduced from** (5)**).**

The electrophoresis mechanism is made possible due to a surface charge that suspended particles exhibit due to either the dissolution or adsorption of ions. An electric field then exerts an electrostatic Coulomb force on the surface charge to promote mobility through the solution. Electrophoretic mobility can be considered positive when the particles move towards the negative electrode and negative when movement is towards the positive electrode (11). The surface charge that exists on the suspended particles also leads to the formation of a layer of counter-ions that surround the particle. This is known as the 'Stern layer' as shown in Figure 2. As the particle moves in the solution, the plane beyond which counter-ions do not migrate

along with the particle is known as the slipping plane. The electric potential at the slipping plane is known as the zeta potential, ζ (12). An increase in zeta potential leads to a subsequent increase in interparticle repulsion and electrophoretic mobility. The area contained by the slipping plane or the 'diffuse layer' of ions moves in the fluid under electric attraction but is not firmly anchored to the surface of the particle (unlike those in the Stern layer). The existence of a double layer also promotes some drag on the particle known as the electrophoretic retardation force (ERF).

The final component of EPD is the deposition of particles onto the substrate. It is necessary to establish the mechanisms that allow for particles to repel in the bulk but deposit at the electrode. The process has been applied and has shown success across many disciplines but the exact mechanisms that allow a deposit to be formed are still not entirely clear, as established by Vanderperre (13). What is known is that the production of a dense and cohesive deposit will require particles to lose their charge at the depositing electrode (2). When considering the interparticle interaction in the deposition stage, there are many different mechanisms which may occur. It is also possible that more than one of these mechanisms may occur simultaneously in a single experiment. Examples of such mechanisms are densification, deposition through direct electrostatic force, electrosedimentary deposition and bridging flocculation (9). Hamaker (5) observed that strongly adherent sediment would form when a suspension was left to stand due to gravitation. When considering the interaction between the particle and substrate/electrode, particles adhere to a surface due to the increased pressure exerted by incoming particles mobilised by the applied electric field. As noted by Vanderperre (13), as solid loading is increased, the zeta potential of the particles shifts towards the isoelectric point supporting the mechanism of charge loss at the electrode. Grillon et al. (14) would go on to theorise that particles will neutralize upon contact with the electrode or deposit and become static. This theory would explain particle charging through salt addition and initial stages of deposition but does not apply to thick deposits (more than a monolayer of particles). A more plausible explanation for the phenomenon was made by Sarkar and Nicholson (15) and referred to as the electrical double-layer distortion and thinning mechanism (Figure 3). This considers the movement of a positively charged particle towards the cathode in an EPD cell. When the diffuse double layer (Lyosphere) moves, fluid dynamics and applied electric field cause the double layer envelope to distort so that it becomes thinner ahead and wider behind the particle. The cations move with the positively charged particle towards the cathode. Thinning then occurs due to counterions in the elongated tail reacting with cations that are in high concentration surrounding the particle. The thinner head of an approaching particle may

now move close enough to the tail for the London Van der Waals (LVDW) attractive force to dominate and induce coagulation (16).

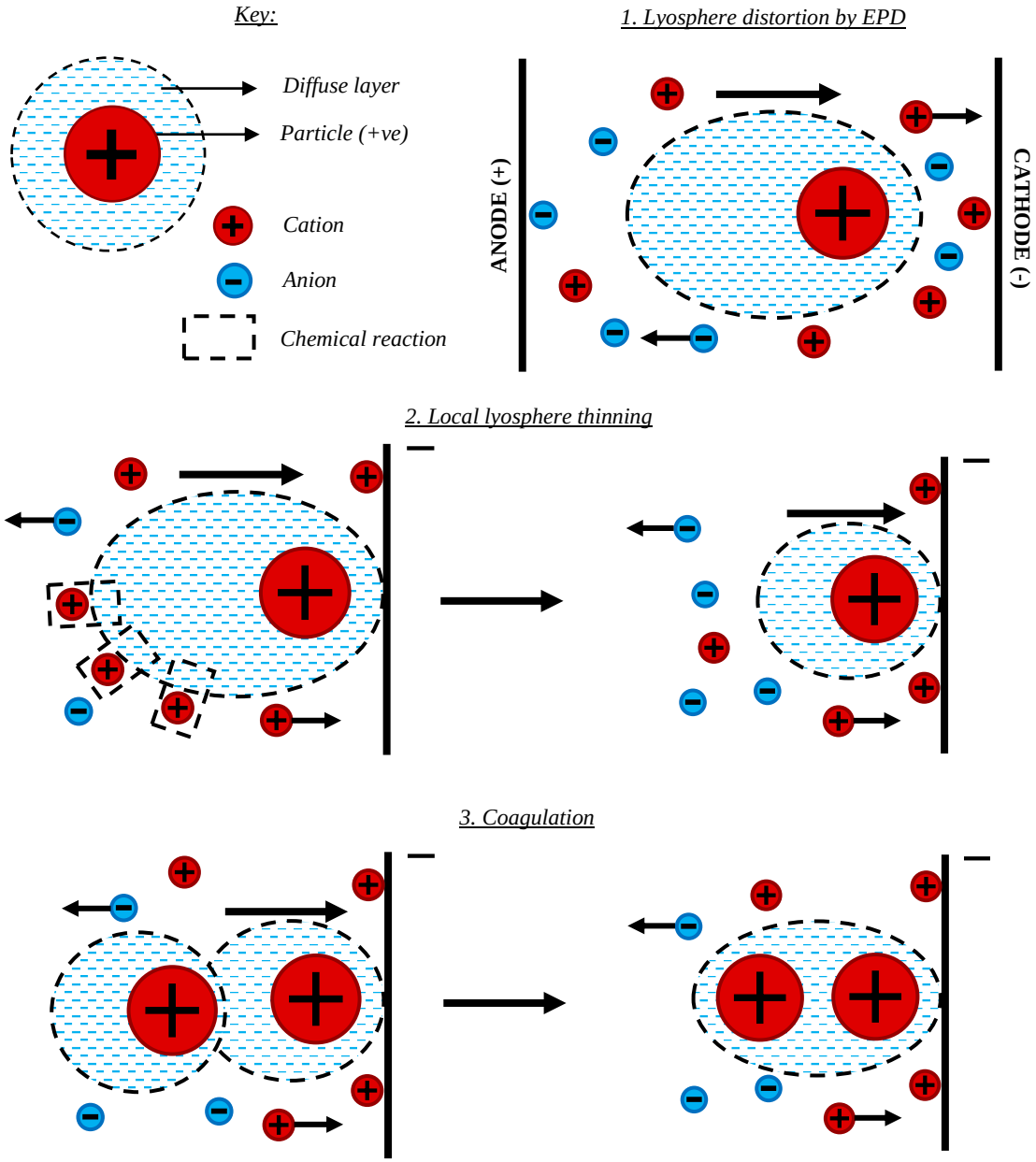


**Figure 3. Electrical double layer distortion and thinning mechanism for electrophoretic deposition** (15)**.**

In terms of drawbacks of the process, EPD is limited in how thick a layer may be deposited. The depletion and deposition of particles in the bulk leads to a decrease in the rate of deposition and, for larger layer thicknesses, a decrease in layer uniformity. Moreover, the versatility of processing parameters can also lead to a lack of control and repeatability of experiments. On a large scale, depletion of material from the bulk will not affect the formulation and material can be replenished after many experiments have been carried out. The effects of changes in molar

fraction of the suspension have a considerably larger effect when testing on a laboratory scale and may lead to inconsistencies in results. Because of this, ingredients need to be replenished more regularly which can be difficult if there is no accurate method for tracking the depletion of certain materials. There are methods to assess this through conductivity (17), pH or weight change of the suspension but adding these stages further complicates the process taking away from the supposed simplicity.

### 2.1.1. Factors affecting electrophoretic deposition.

Through the extensive experimentation of the EPD process, factors that affect the resulting deposited material become more evident. Optimal combinations of these parameters are found depending on the materials in use and are further investigated in this section. These factors can be grouped by whether they are changed through the suspension or by experimental parameters and an overview of these parameters is shown in **Table** 1.

**Table 1. The effect of EPD conditions on material deposit** (18)

| Parameter | Effect | | Desired range |
|---|---|---|---|
| Suspension parameters | | | |
| Zeta potential of bath | Low | Reduces electrophoretic mobility and dispersion stability | >±25 mV |
| | High | High deposition rate | |
| Dielectric constant of liquid | Low | Insufficient dissociation of charging salts | 12-25 F/m |
| | High | Reduces electrophoretic mobility | |
| Viscosity of liquid | Low | High deposition rate | 0.5-3 mPa s |
| | High | Low deposition rate | |
| Salt concentration in bath | Low | Low zeta potential and insufficient binder for adherence | ~$10^{-6}$-$10^{-3}$ M |
| | High | Too much binder formation | |
| Water concentration in bath | Low | Low zeta potential and inadequate binder | 1-3 vol.% |
| | High | Gas evolution due to hydrolysis at the cathode | |
| Deposition parameters | | | |
| Binder in bath | Low | Particles to do not adhere | Depends on material |
| | High | Too much binder present that diminishes luminescence | |
| Electric field strength | Low | Slow deposition rate | 3000-8000 V/m |
| | High | High deposition rate, possible non uniform deposit | |
| Deposition time | Low | Deposit too thin | 5s – 60 min |
| | High | Particles may settle out of bath | |

| | | | |
|---|---|---|---|
| Dispersant | Low | Agglomeration and settling of particles | Depends on material |
| | High | Too much water added with glycerin (hygroscopic) | |
| Particle size | Large particles | Settle due to gravity (gradient in deposition) | Submicron – 20 µm |
| | Nano-sized particles | Tendency to agglomerate | |

Zeta potential is measured to indicate the charge of particles in the suspension and the ability of the suspension to be electrostatically dispersed (18). It may also be utilized to calculate the electrophoretic mobility following Hamaker's equation (5). This can be increased by the addition of cations and more specifically nitrate salt concentration (19)(20)(21). In a study where $Mg(NO_3)_2$ and $Al(NO_3)_3$ were used as adsorbing additives (21) increased zeta potential decreases the occurrence of agglomeration and therefore sedimentation in the suspension. Agglomeration is avoided by the use of a high electrostatic repulsion which is due to high particle charge. As the deposit forms, particles become more attracted to each other as they move closer. A high particle charge causes particles to repulse each other during deposition. They will occupy positions and lead to a higher particle packing density. It is therefore imperative that a high and uniform surface charge of the suspended particles is achieved. If there is a low particle charge, particles would coagulate even for relatively large inter-particle distances. This causes a more porous, sponge-like deposit. The addition of salts also leads to a more porous low deposit density. The addition of cations prevents or decreases the possible anchoring of the colloidal particles to the cathode and thus increases their distance from each other.

The dielectric constant is the relative permittivity of a material denoted as the ratio of its permittivity to the permittivity of a vacuum (22). An increase in the dielectric constant causes an increase in conductivity (in pure liquids). Impurities such as water within the liquid influence conductivity. Too low a dielectric constant will cause deposition to fail because the dissociative power is insufficient. On the other hand, high dielectric constant yields a high ionic concentration within the liquid which reduces the electrophoretic mobility (15). Because of this, the ionic concentration should be kept as low as possible.

Conductivity is also very important for the formation of a smooth consistent deposited layer in the EPD process. When a substance is too conductive, the particle motion is slow, therefore the rate of deposition is vastly decreased. When a substance is too resistive**,** particles charge electronically, and their stability is lost (2). Resistance has also been shown to increase through

experimentation which also decreases the rate of deposition with an increase in deposition time (15). Another reason may be due to the formation of ion depletion layers in the deposit (23), or mass transport limitations through the growing deposit layer (24). This change in resistance is also found to be related to layer uniformity (17). For certain suspensions, deposit resistance increases dramatically during EPD which therefore causes the potential drop over the suspension to decrease. This then leads to a smaller driving force for electrophoretic deposition. Conductivity does not change by more than 10% during experimentation (17) so the drop in electric field strength is down to the deposit causing extra resistance.

Deposition is also affected by the electrolytic bath pH value. The acidity of a bath can be increased or decreased by the addition of acidic or alkaline substances, respectively. An increase in the acidity of an electroplating bath results in an increase in the concentration of dissociated ions in the aqueous solution. Due to the increased ionic concentration, the deposition current density increases until it stabilises or continues to increase, depending on the composition of the solution. Changing pH has also been shown to cause alteration of the characteristic properties (adhesion and roughness) of the deposited layers, elemental/compound precipitation and an increase in deposition current density (25).

Particle size has also proved to be a crucial factor that influences the EPD process. It is reported that the most suited particle size for the deposition of ceramic and clay systems is within the range of 1-20μm (26). For homogeneous and smooth deposition results through EPD, it is of utmost importance that particles remain completely dispersed and stable. Larger particles tend to settle so are avoided as the mobility of particles due to electrophoresis should be higher than that of gravity. Heavier particles start to cause a settling suspension. This leads to a gradient in deposition – thinner above and a thicker deposit at the bottom with a vertical electrode. For EPD to occur with larger particles, one would require an extraordinarily strong surface charge. Smaller particle size prevents the formation of cracks after heat treatment due to a more even distribution of stresses in the deposited layer (2).

The effect of deposition current density relates to Faraday's law of electrolysis (27). The deposition current density is related to the thickness of the deposited layer. Therefore, the deposition current density is dependent on factors affecting the energizing of inherent ions in the electrolyte such as stirring rate, bath temperature, the concentration of constituent and electrical conductivity of the substrate. Literature also proves that altering the current density will influence the morphological, compositional, and structural properties of the deposited layer (28)(29).

The drying process has also been shown to influence the morphology of the deposited layer and should be closely considered in the post-processing of an EPD deposited layer. During drying and/or sintering, a coating densifies and as a result, shrinks. In the majority of EPD experiments, however, the substrate will not change in dimension so stress will be built up in the coating. The easiest way for this stress to be relieved is through the formation and propagation of cracks in the deposit. There is also the possibility that the opposite will occur. The substrate may expand more than the coating in the drying process, therefore generating compressive stresses in the coating. Sarkar (30) found that cracking in a coating can be minimized by choosing a solvent with low surface tension. Low surface tension in a solvent can be associated with high evaporation rates which will also promote cracking. To combat this, a solvent with a low surface tension (acetone) may be mixed with a solvent with a slower evaporation rate (ethanol) to reduce cracking. This technique was tested by Peng and Liu (31). Following the mechanisms explained in **Section 2.1**, it is important to recognise that aside from effective solvent selection, stirring also contributes to good particle stabilization so must be carefully selected. Stirring of colloidal particles should not be the overriding factor to good dispersion within the solvent and can be carried out through peristaltic pumping, magnetic stirring, or ultrasonic vibration. Selection can be made due to particle size, solvent viscosity, or solvent volume. Magnetic stirring has the drawback of convection forces which can become greater than the force experienced through electrophoresis. This can be solved by changing the dimensions of the stirrer bar used and adjustment in the rpm of stirring. Ultrasonic agitation has a limitation on the size of the container used for the EPD process but gives a much more even dispersion of particles.

### 2.1.2. Alternative methods of material deposition.

It is important to consider alternatives to the electrophoretic deposition process to understand why it is a preferred method. The benefits of using EPD for the deposition of semiconductors onto metal substrates have been demonstrated in **Section 2.1**. Advantages of the process include its simplicity of apparatus, the versatility of processing parameters and good layer uniformity of deposited layers. Chemical Vapour Deposition (CVD) is a process used to deposit a wide range of thin film materials including semiconductors, insulators, metals, and superconductors. These materials are used in the fabrication of optical, protective, and protective coatings (32). The essential mechanisms of the CVD processes are chemical reactions in the gas phase and on surfaces, under the influence of momentum, energy, and mass transport (33).

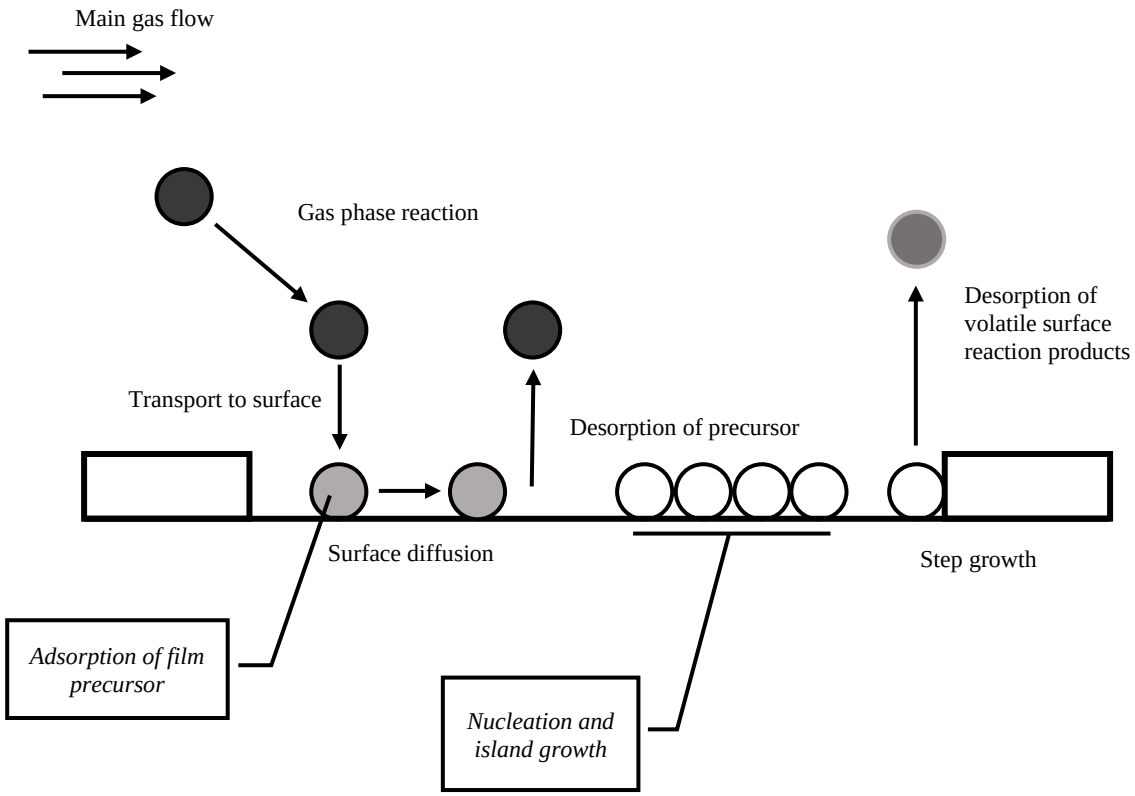


**Figure 4. Precursor transport and reaction processes in CVD (reproduced from** (34)**).**

As shown in Figure 4, the key steps in the overall CVD reaction are the evaporation and transport of precursors in the bulk gas flow region into the reactor [1], gas phase reactions of precursors in the reaction zone [2], mass transport of reactants to the substrate surface [3], adsorption of reactants on the substrate surface [4], surface diffusion to growth sites and chemical reactions leading to film formation [5] and finally desorption and mass transport of remaining fragments away from the reaction zone [6]. The rate of growth is determined by the temperature of the substrate, the operating pressure of the reactor and the composition/chemistry of the gas phase (34). CVD is a highly accurate and well-controlled process that allows for high reproducibility of deposited thin films over large surface areas. Although it has its benefits, the process does have very high equipment costs and high-temperature requirements (35). Compared with EPD, CVD is less suited for rapid prototyping but has the advantage of very high-quality coatings. For the early stages of research, EPD allows for experiments to be carried out in a lab with simple apparatus to test and validate layer chemistry and performance whilst CVD incurs a considerable cost so may not be worth investment at the early stages of research.

Electroplating is a process that is very similar to electrophoretic deposition and the two are often confused. The key difference between the two processes is the mechanism for material deposition. As previously established, in the EPD process, particles are suspended in a fluid

and migrate to the depositing electrode under an electric field. Electroplating involves depositing metals or semiconductors onto a conducting substrate by passing an electric current through an ionic electrolyte in which metal or semiconductor ions are present (25). Positively charged cations are attracted towards the cathode whilst negatively charged anions to the anode. They are then neutralised by gaining electrons through reduction or losing electrons through oxidation and are deposited onto the working electrode (36). A schematic for small-scale electroplating is shown in Figure 5.

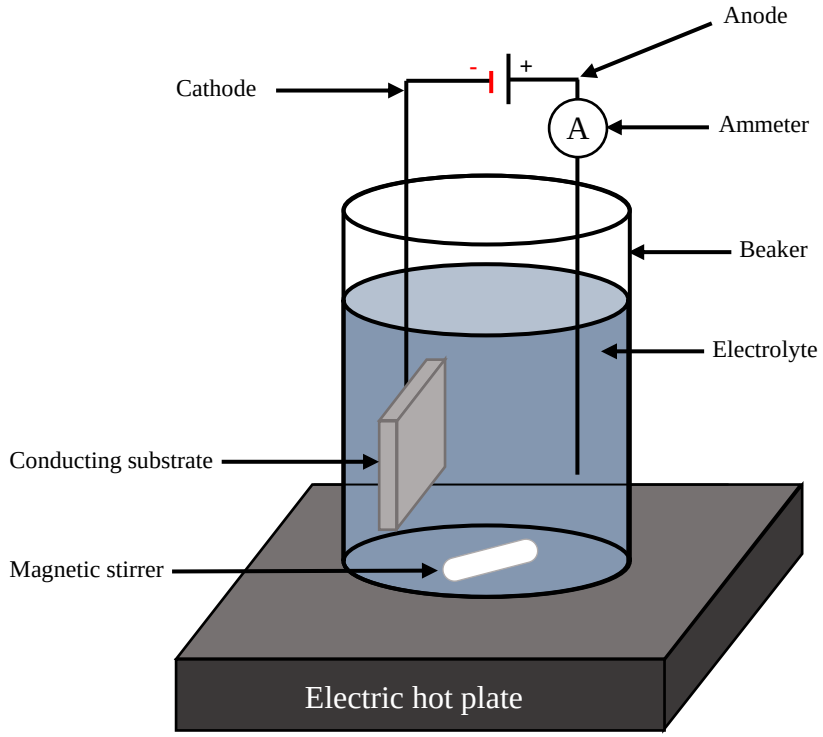


**Figure 5. Typical two-electrode electroplating setup** (25)**.**

Electroplating provides a precise and controllable method for depositing coatings onto a conducting substrate, it allows for a high-quality and smooth surface finish and can be carried out with a wide range of materials (25,37). The limitations of electroplating come from its inability to produce thicker films and incompatibility with non-conductive substrates and particles that are used in EPD.

### 2.1.3. Coating methods for complex geometries.

As will be expanded upon in the following section, the use of electrophoretic deposition for the coating of complex 3D geometries is yet to have considerable published research. There are, however, alternative methods that can coat complex substrates and have been applied in industry for many years. Atomic layer deposition (ALD) is a thin-film deposition technique

based on the sequential exposure of precursors and reactants in the vapour phase. The precursors are supplied into the reaction chamber and a thin film is formed as they react with each other (38). In comparison to CVD, ALD has the superior qualities of angstrom-level thickness control, higher uniformity and excellent conformality and has become one of the most reliable techniques in depositing a wide range of materials. The process is composed of four stages: precursor exposure, precursor purge, reactant exposure and reactant purge. Due to these stages being self-limiting at the surface, the film thickness is controlled precisely by the number of ALD cycles (39). The main limitation of the process is its high cost and the complexity of the equipment. The equipment for ALD is extremely specialized which causes it to become difficult to set up and maintain. The high levels of accuracy cause the deposition rate to be very low when compared to other techniques so is not preferable for rapid prototyping or testing.

Spray coating is another technique that has been used to coat more complex 3D geometries but is a relatively simple method that does not coat as uniformly or precisely as techniques like ALD. Spray coating does not require a smooth or planar surface (40) and is easily scalable when compared to other processes. Although some methods have seen a drawback in poor layer uniformity (41) and inability to coat with larger particles, there is promise in the emergence of the high-velocity air-fuel (HVAF) spray technique which has provided highly adherent coatings with negligible porosity (40).

### 2.2.Coating complex geometries using EPD.

As demonstrated in **Section 2.1.1**, there is a wide variety of parameters and factors that will affect the final deposit through the EPD process, but these are heavily tested onto 2D substrates (5,7,13,14,20,21,42). Suggestions and conditions may be taken from these notes but for this project, it is important to understand how these factors may be optimised for a 3D substrate. EPD onto a 3D substrate is not well documented but several sources may assist in establishing a suitable design for experiments. A major change that a design of experiments must undergo is the design of the counter electrode. For 3D substrates, it is demonstrated that a uniform deposition on all sides of the sample is achieved using a concentric, stainless steel foil cylinder placed inside of a beaker (43). For this, the electrode spacing was set at 15 mm with a counter electrode height three times that of the scaffold sample. Deposition in this process was successful but there was an issue with coating the inner surfaces of the scaffold. This is due to the uneven nature of the electric field which may be fixed by a much more complex counter-

electrode design. This design of experiments in Figure 5 highlights the simplicity of the EPD process and how complex apparatus is not required for effective experimentation.

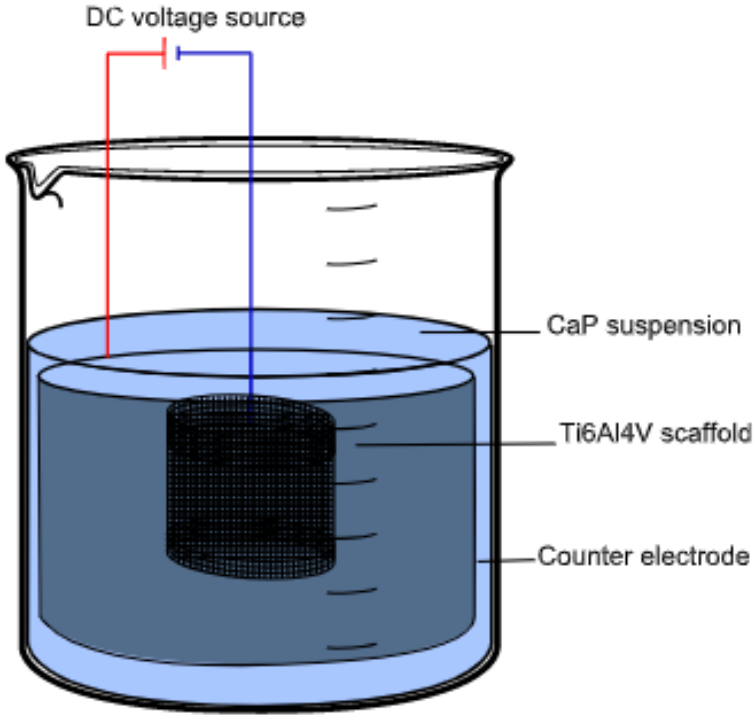


**Figure 6. Schematic representation of EPD cell used in** (43)

Another variation of experimentation onto a 3D substrate is shown in Figure 7. Here, selective electroplating is used which is slightly different to the design used in this thesis. The same concept of coating a 3D concept is used through rotation of the substrate. When plating the solenoid inductor, a motor was used to rotate the solenoid to produce an even coating around the whole piece (44). To avoid twisting the wires, the motor oscillated back and forth with an AC input from a function generator. This produced an almost equal electrical field around the component and gave successful results for the deposited layer. Experimental design as shown through these two sources gives a general idea of the build that may be used for this study. With the importance of the counter electrode design being made more obvious, an efficient

experimental set-up may be established and used throughout.

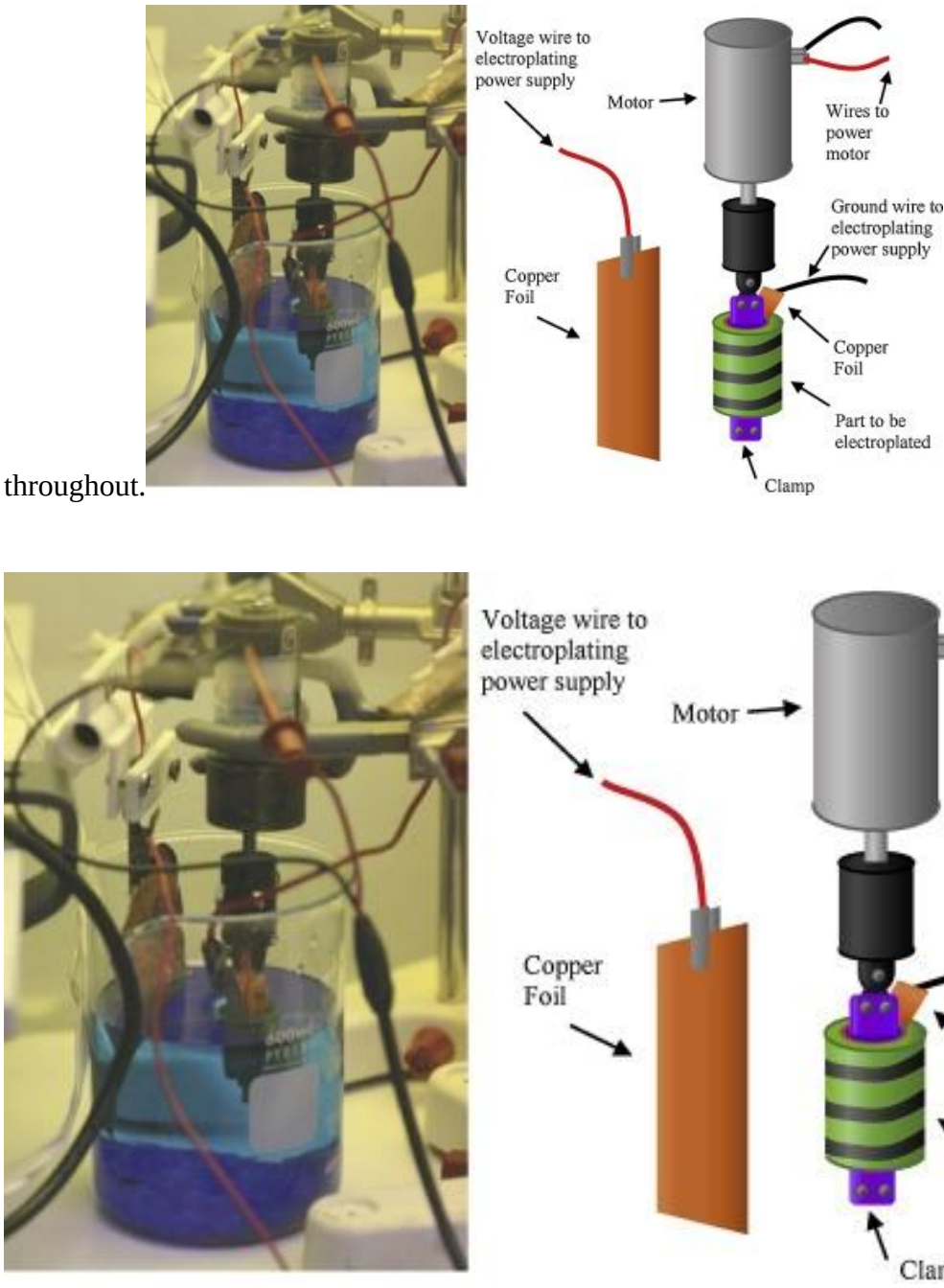


**Figure 7. Selective electroplating onto a 3D component** (44)

### 2.3.Alternating current electroluminescent (ACEL) technology

Alternating current electroluminescence (ACEL) devices have progressively gained more attention in recent years due to their preferable properties and have proved to be a viable substitute for their direct-current counterparts (DCEL (Direct Current Electroluminescence)). For example, charge accumulation in ACEL devices can be avoided due to the frequent changes in the direction of the applied electric field (45). ACEL devices operate by the introduction of

an alternating current and sinewave frequency to trigger the recombination mechanism. This introduction excites the light-emitting phosphors, raising them to a higher energy state. As these electrons fall to a lower energy state through electron-hole radiative recombination and annihilation, photons are emitted (46). AC-driven EL devices can be classified into three categories: (1) thin-film electroluminescent devices; (2) light-emitting diodes; and (3) light-emitting field effect transistors (47). Here, there is the focus on thin-film electroluminescent devices with a build that consists of the following layers: transparent electrode (ITO film), emitter (phosphor), dielectric and a metal electrode (Ag) (45). Compared to organic EL, AC-driven inorganic phosphor powders EL devices are more appealing. This is due to their wider viewing angle, fast response time, low power consumption, obvious contrast, simple manufacture, and cost-effectiveness (48). The luminance of inorganic phosphor powder EL devices is generally lower than that of OLEDs and PLEDs. Despite this, their levels are usually regarded as sufficient for applications such as panel lighting and device screens (49).

Original designs of the ACEL device were an emissive layer sandwiched between dielectric and electrode layers on either side with one electrode/dielectric being transparent. This was developed to overcome breakdown and stability issues. The change into the single dielectric layer would now allow for a thinner device whilst retaining its original luminance properties (50). The dielectric layer is incorporated for its contribution to the protection against charge transport, charge storing, protection against leakage-bound charges, stability in high electric fields, and stability against atmospheric conditions like humidity. There has been a history of either inorganic or organic dielectric materials. Inorganics have extremely high dielectric constants but are crystalline in nature. Organic have a lower dielectric constant but allow for more flexible devices (51). Insulating dielectric offers preferable properties for EL devices. The dielectric layer prevents electrochemical reactions between the emissive layer and the electrodes whilst stopping the deterioration of the emissive layer by external moisture and oxygen in the atmosphere (49).

With an expanding necessity for high-performance and efficient screens, there is the requirement for phosphors in use to keep to the same performance. Phosphor layer thickness is required to stay around 3 particle diameters. This ensures that the deposited layer has pinhole-free coverage but is not so thick that light emission is reduced. The amount of non-luminescent material should be minimized where possible. The deposited layer should have maximised layer uniformity to ensure consistent optical performance and luminance. The deposit should also have sufficient adhesion strength to withstand handling during use and manufacture (42).

### 2.3.1. Light-emitting diode (LED) technology

Light-emitting diodes (LEDs) use electroluminescent technology by way of DCEL. In LEDs, the emitted light is blue at the source (InGaN -Indium Gallium Nitride) and to emit white light, a yellow phosphor (rare earth YAG:Ce) is required to be placed over the top of the blue-emitting InGaN LED (Light emitting diodes). This will absorb and emit longer wavelength green and red light and down-convert the high energy blue wavelength output via Stokes Shift (52). This process brings evidence of both heat losses and the issue of 'Blue light.' Heat losses occur via the generation of non-radiative phonon vibrations rather than photons, causing LEDs to suffer from elevated levels of heat dissipation. Due to the addition of yellow phosphors and given the high energy blue output, LEDs produce a 'faux' white light which, when used for extended periods, has proved to be detrimental to sleep patterns and subsequent health. Electric field strength on the phosphor determines luminance, current density does not. Conversely, OLED and LEDs are current-driven devices and luminance, therefore, depends on the input current density (49).

When compared with LEDs, EL devices require extremely low current densities and extremely low power requirements as well. The benefit of ACEL devices as opposed to alternatives is that charge accumulation is avoided because of the frequent overturning of the applied electric field. This, in turn, improves the operational lifetime of the device and its power efficiency (49). Polarization current in EL devices means that they are tolerant to defects and are fabricated without the need for costly clean room facilities. Conversely, defects in OLEDs and LEDs trap free charges and reduce current density leading to a decrease in luminance. ACEL devices are surface light sources where the emission is uniform across the whole surface area. In comparison, LED is usually used as more of a point light source. ACEL devices also do not rely on environmental temperatures so have a wide operating window from -60 to 95ºC. Although their operational window is broad; humidity has been reported as a limiting environmental effect due to its ability to accelerate the ageing process. Condensation on the surface of the LED also becomes an issue as it causes light to be scattered and brightness to decrease (49).

### 2.3.2. Material selection of ACEL layers

One of the first successful examples of an ACEL device was by Tiwari et al (53) who prepared an ACEL device with manganese-doped zinc sulphide (ZnS:Mn) as the phosphor material. In this experimentation, a thin film device was investigated which takes the structure of a

phosphor emissive layer between two insulators, which was in this case $MgF_2$. This design used electron beam evaporation to deposit allowing for much thinner layers to be formed. Doping and co-doping the host matrix with different transition metals are key approaches to fabricating inorganic phosphor materials. For the emissive layer, one of the major requirements of choosing a host matrix is its band gap. ZnS is the most used host material due to its chemical stability. There is evidence of ZnSe, CdS, ZnGaS and as an alternative to traditional sulphides, GaAs, GaN (Gallium Nitride) may be used for some devices. The most used doping agent in ACEL technology is copper which has shown evidence of both blue and green emission. Blue is emitted when Cu ions are at interstitial sites in the ZnS whereas green is emitted when Cu ions replace Zn from a ZnS lattice (54). The use of ZnS is widely documented and has shown the most success across all literature (55–57), the one limitation is the inability to reach all colours of the visible spectrum.

For the dielectric layer, barium titanate ($BaTiO_3$) has been the most popular choice among several groups. The extremely high dielectric constant (in the range of 2000–3000 at room temperature) is the main reason for being so popular. Examples of its use are evident through multiple studies(55–57). By adding barium titanate particles to the composite, the electric field is focused on the EL particles which leads to higher light emission. Few alternatives have been identified for the dielectric layer, but notable findings have come using silicon dioxide ($SiO_2$), aluminium oxide ($Al_2O_3$), tantalum oxide ($TaO_x$) and hafnium oxide. Gupta et al (58) made use of hexagonal exfoliated boron nitride (h-BN) for the dielectric material in this study. It was documented to have provided more stability against catastrophic dielectric breakdown at higher applied voltages compared to the commonly used $SiO_2$ and $BaTiO_3$. The other advantage of using h-BN layer in place of $SiO_2$ is that the former is thermally more stable compared to the latter. A study by Stauffer and Tybrandt et al (57) used an alternative technique in the production of their device through the mixing of the phosphor and dielectric into an individual layer. The theory here is that the matrix with a high dielectric constant will instead focus the electric field on the EL particles, which will increase the charge separation within the EL particles and thus the light emission. They covered the phosphor particles effectively so that, upon application of driving voltage, phosphor particles were subjected to an extremely high electric field. They reported an impressive 700% improvement in ACEL brightness after their approach.

Consideration must also be made for materials used in the outer electrode for an ACEL device. This comes with its challenges due to the necessity to have a layer that is partially transparent with some element of conductivity. This is usually done through nanowires that run through a

transparent polymer (Polyethylene terephthalate, PET). Silver nanowires (AgNWs) have attracted attention to many applications around optoelectronics and microelectronics because of their low sheet resistance (10 Ω/sq.) and high flexibility (59). Park et al (55) makes use of an AgNW PET substrate which was more transparent than its indium tin oxide (ITO) counterpart at all wavelengths. Coverage of the nanowires was less than 10% such that the substrate is transparent. Testing alongside ITO, the sheet resistance of the ITO test increased by 50% when put under continuous concave-to-convex stresses. Continuous bending of ITO electrodes leads to cracking and delamination, which are limiting their flexibility (60). A carbon nanotube (CNT) electrode has been tried as an alternative to ITO electrodes. However, its high sheet resistance ( kΩ/sq) has been a major challenge for the performance of thin-film devices on it (60). Schrage and Kaskel et al (56) utilised a single-walled carbon nanotube (SWCNT) counter electrode which was spray coated directly onto the emissive layer.

### 2.3.3. ACEL device production techniques

Electrophoretic deposition is a novel way of fabricating ACEL devices and is something that is not widely documented compared to processes like metalorganic chemical vapour deposition (MOCVD), spray coating or spin coating. Sputtering, thermal evaporation and ion beam deposition have been used during pilot stages, but research has moved towards simpler methods of production (61). Spin coating is usually preferred as it decreases two coating steps into one. Through manufacture, there is the ability to also mix and coat phosphors with organic binders simultaneously. The downfalls in this process come with the inability to control desired patterns (62). Screen printing is the most used printing method for ACEL device fabrication. Screen printing solves the issues with alternative processes and allows the coating to be prepared from small to large sizes with a smooth surface in each layer of the screen. Park et al (55) prepared ACEL devices (ACPELDs) by a screen-printing method. Screen printing consists of a printing paste containing the functional materials which are deposited through a fine screen with a rubber squeegee. This screen can be patterned. Functional materials like PEDOT: PSS, ZnS:Cu or other phosphor materials are mixed with an ink which serves as the transport medium. It is a process that provides huge variations over substrate materials like ITO, textiles, PET, and metal surfaces (61). There have also been attempts at a dispenser printing technique (63), an inkjet printing technique (64) and a pad printing with silicon transfer pads (65). Talbot et al (18) gives the most in-depth investigation into EPD for solid-state lighting technology where uniformly thin and highly packed conformal layers were achieved. This was carried out onto a flat substrate for LED devices so gives a good platform to develop from.

### 2.4.Concluding remarks

The literature on the various topics this project covers reveals that there are multiple areas in which the Luxtec Global product may challenge the current industry and address the gaps in knowledge that exist. Firstly, ACEL devices do not currently demonstrate an output or efficiency that would be sufficient for domestic lighting. ACEL technology has been designed to function as a flat plate and because of this the output is limited and the deposition techniques encourage formations of defects which in turn lower the output efficiency. The research carried out by Luxtec Global now looks to challenge this and increase the output by combining the proven layer-by-layer build with a 3D emissive source to increase the emitting surface area. Using this theory, the output will be more concentrated in a smaller area, therefore, increasing output from the device. To deposit the individual layers, a more complex technique than screen printing (traditional method for production of ACEL devices (3)) is required, and electrophoretic deposition is successful in the deposition of the required materials (20,21,42,66). As found in the literature (2), electrophoretic deposition allows the user to modify the experimental apparatus to deposit onto more complex shapes. This review has highlighted the factors which have the greatest effect on the deposit - these can be split into factors related to the suspension and those related to the process. Suspension properties include the zeta potential of particles, viscosity, and salt concentration of the fluid. Factors related to the process include applied voltage and deposition time. Optimal conditions will change with different formulations and using the literature of previous experiments these must be identified and then potentially modified for each layer. Deposition onto a 3D structure has proved to have some success (43) but there is still the ability to optimise this process in the search for more uniform and total coverage of a 3D substrate. The main issue that arises from deposition onto a 3D substrate is uniformity of the electric field, challenges in both counter electrode design and orientation with respect to the substrate, as well as managing the dispersion of particles.

Using the research that has already been carried out, the project objectives can be justified through the identification of gaps in the literature. Electrophoretic deposition of the layers of an ACEL device onto a complex 3D substrate is something yet to be experimented. This novel approach will allow potentially higher efficiency output of ACEL technology whilst also improving the uniformity of deposited layers. This work also can be transferred to new areas where deposition onto 3D shapes is required.

# 3.Methodology

### 3.1.Introduction

Through the literature review, there is the understanding that electrophoretic deposition of ACEL layers onto a 3D substrate is not documented to an extent that will assist this study. It is possible to now develop an idea for the most suited material to the process and the device. For each layer, there are several sources (55–57)to support the use of $BaTiO_3$ for the dielectric, ZnS phosphor as the host matrix for the emissive layer and AgNWs dispersed in polymer for the transparent outer electrode. To find suitable conditions for experimentation of each layer, it has been established that there are multiple parameters which will now need to be optimised through rigorous testing. Using results from 3D substrate experiments (43,44) it is demonstrated that there is a necessity to use some variation of a cylindrical electrode for a uniform coating to be achieved.

### 3.2.Proposed build sequence and geometry.

As established in the above section, the build sequence will be deposited onto an aluminium coil with a surface area of 4.71 $cm^3$ (45 mm height, 50 mm coil diameter, 3 mm wire diameter). A photo of the coil is displayed in Figure 8, this is used in place of the metallised (Aluminium) polycarbonate coils intended for the final product.


**Figure 8. 3D render of sample**

The sequence of layers will be dielectric (1), encapsulating polymer (2) followed by the phosphor emissive layer (3). Each of these layers will be evaluated individually and in sequence.

### 3.3.Materials

The following materials were used in this study based on the recommendations of the sponsoring company. Formulations for individual suspensions were revised as required based on the findings of the study.

#### 3.3.1. Dielectric layer

A provisional recipe is shown in **Table** 2. Barium Titanate ($BaTiO_3$) was obtained from US Research Nanomaterials, Inc. Product Number: US3830. The powder had an average particle size of 200 nm. The use of barium titanate as a dielectric layer for AC electroluminescent devices is widely documented in the literature (55–57). The main motivation to use this material is its exceedingly high dielectric constant which is between 2000-3000 at room temperature (3), as is the nature of inorganic dielectric materials. There is also proof of the EPD of barium titanate achieving dense, smooth layers which are of utmost importance for this layer of the device. Ethanol and acetylacetone as solvents are well-documented for the electrophoretic deposition of barium titanate. Organic solvents such as acetylacetone have been used to suppress the stress effects that occur during shrinkage in the drying and sintering stages. This is due to its low surface tension allowing an improved green density and deposit thickness. The addition of a secondary solvent such as ethanol to the suspension fluid was reported to give rise to an improved deposition efficiency (66) so is utilised for this study. Finally, polyvinyl alcohol (PVA) is added to the formulation as a dispersant to improve colloidal stability. A study has shown that incremental increases in PVA to the suspensions will cause an increase in deposition efficiency (67). PVA also aids in the particles' contact intimacy in the green body leading to higher deposit densities after sintering .

**Table 2. Provisional suspension formulation for barium titanate layer**

| *Component* | *Role* | *Concentration* | *Supplier and product details* |
|---|---|---|---|
| *Barium titanate ($BaTiO_3$)* | Active particle | 5.0 g/L | US Research Nanomaterials, US3830 |
| *Ethanol* | Solvent | 50.0% | FisherBrand, 13268633 |
| *Acetyl acetone* | Solvent | 50.0% | FisherBrand, 15650530 |
| *Polyvinyl alcohol (PVA)* | Dispersant | 1.0 ml/L | Alfa Aesar, 41241 |

### 3.3.2. Encapsulating polymer layer

To protect the dielectric layer by improving adhesion to the surface of the substrate, a polymer layer was incorporated into the build. This polymer layer would also allow for any pinholes in the previous layer to be covered and prevent the device from short-circuiting A provisional recipe was used as described in Table 3.

Table 3. Provisional formulation for polymer layer

| *Component* | *Role* | *Concentration* | *Supplier and product details* |
|---|---|---|---|
| *Poly-methylmethacrylate* | Active particle | 4.0 g/L | Sigma, 182230 |
| *Ethanol* | Solvent | 85.0% | FisherBrand, 13268633 |
| *Deionized water* | Solvent | 15.0% | - |
| *Sodium cholate hydrate* | Additive | 1.0 g/L | Sigma, 27029 |

The molecular mass of PMMA used in this investigation was 120,000. PMMA has been widely used firstly as a shell material in encapsulation due to its high chemical stability, biocompatibility, nontoxicity, and good mechanical properties (56). More specifically with use in ACEL production PMMA has good adhesion properties for both particles and electrodes, high electrical resistivity, and low water permeability so can be more effective in protection from environmental factors (57). PMMA of such molecular mass cannot be dissolved in water or ethanol alone but can be dissolved in ethanol-water solvent (15 % water) at 55ºC. A concentration of 4 g/L of PMMA was selected by the sponsoring company. The use of 1 g/L Sodium Cholate Hydrate (NaCH) additive allowed for PMMA solubilization not only at 55ºC but also after cooling to room temperature.

### 3.3.3. Phosphor emissive layer

A provisional recipe for the emissive layer was used as described in Table 4.

**Table 4. Provisional formulation for phosphor layer**

| *Component* | *Role* | *Concentration* | *Supplier and product details* |
|---|---|---|---|
| *RGB phosphor trimix* | Active particle | 5.0 g/L | See Table 5 |
| *Magnesium nitrate* | Additive | 0.1944 g/L | Sigma, 237175 |
| *Isopropyl alcohol* | Solvent | 98.0% | FisherBrand, 10306390 |
| *Deionized water* | Solvent | 2.0% | - |
| *Glycerin* | Additive | 2.0% (Additional) | FisherBrand, 10579570 |

A combination of red, blue, and green phosphors (CaS:Eu, ZnS:Cu,Al and ZnS:Ag respectively) will be used for the emissive layer to give a white light with an appropriate colour temperature. Through preliminary research, the sponsoring company were able to establish how the percentage distribution of the phosphors in the deposited layers would affect the warmth of the resulting emitted light. The percentage distribution estimated to achieve a warmth of 6200 K is shown in **Table** 5.

**Table 5. Phosphor trimix percentage mass distribution.**

| *Phosphor* | *6200k concentration* | *3200k concentration* | *Product code** |
|---|---|---|---|
| *CaS:Eu* | 26.8% | 22.0% | FL63/ |
| *ZnS: Cu,Al* | 35.0% | 15.0% | GL29A/ |
| *ZnS:Ag* | 38.2% | 63.0% | GL47/ |

**Supplier: Phosphor Technology Ltd.*

ZnS is the most widely used host matrix and is doped with transition metals for all colours across the visible spectrum to be achieved. ZnS exhibits a favourable band gap and has good chemical stability for these applications. As magnesium nitrate ($Mg(NO_3)_2$) is added to the suspension it will dissociate slightly, providing ions to positively charge the phosphor particles. This reaction also forms hydroxides and alkoxides which will act as the binder materials for this layer (3). Adhesion of this layer is of utmost importance hence the necessity for these binders. Water is added to the formulation due to the high purity of the Isopropyl Alcohol ( IPA) in use. Small quantities of glycerol will ensure the fluid becomes slightly more viscous to assist in particle suspension. This will also be added as a rheology modifier for the formulation. The sponsor also wanted to explore the use of sieving to standardise the particle size of the phosphors. The sieving process will be further explained later in **Section 3.5** but will aim for particle size to be reduced to the range of 11 – 4 µm. The median estimate for PSD (Particle Size Distribution) of the phosphors is 4.9 – 13.6 µm, therefore particles may range from <1 – 30 µm. This broad range in particle size is what leads to substantial issues in the uniformity of screen-printed emissive layers along with input energy wasted due to attenuation from a dense phosphor layer of different particle sizes.

### 3.3.4. Additional chemicals used in this study.

As a result of the experimentation, it was necessary to modify the initial recipes to improve the deposition or adhesion of the various layers. The added chemicals are listed below to simplify the subsequent account of the layer deposition.  accounts for these materials.

**Table 6. Additional chemicals used in the study.**

| *Component* | *Layer* | *Role* | *Supplier and product details* |
|---|---|---|---|
| *Polyvinylpyrrolidone (PVP)* | Dielectric | Improve adhesion | Alfa Aesar, A14315 |
| *Acetone* | Encapsulating polymer | Solvent for dip coating | FisherBrand, 10779874 |
| *Hexadecyltrimethylammonium bromide (HTAB)* | Encapsulating polymer | Improve zeta potential | Alfa Aesar, A15235 |
| *Sodium hydrogen phosphate* | Encapsulating polymer | Improve ionic strength | Laboratory Chemicals, A11817 |
| *Citric acid* | Encapsulating polymer | pH stabiliser | Laboratory Chemicals, J64322 |

### 3.4.Preparation methods for experimental suspensions

Larger amounts of powders and liquids were weighed using a 10 mg resolution mass balance with smaller amounts of additives using a 0.1 mg resolution balance. By using the density of the liquid, the required volume was converted to mass and measured out on the balance. Mixing of solvents and powders was carried out in glass bottles using magnetic stirring. A heated stirrer was used to make up some of the polymer suspensions that did not disperse at laboratory temperature.

### 3.5.Sieving of phosphors

The sieving process was incorporated into experiments to get a uniform particle size distribution among the three different phosphors. Wet sieving was carried out using an AS 200 basic Vibratory Shaker from Retsch GmbH paired with two stacked sieves of mesh sizes 4 µm and 11 µm. These were then secured with the supplied fixing nuts, “standard” lid and O-rings to ensure no liquid/ material escaped. Amplitude was set at 60% (arbitrary units on device) for 40 minutes in 10-minute intervals. Phosphors were wet-sieved separately in batches of 10 g with 200 ml of deionized water. Once the process was completed, the remaining material was washed from the surface of the sieves and collected in separate glass beakers. Once this material had settled, water was siphoned off and particles in the 11 – 4 µm range were cleaned with IPA. These were then left in the fume cupboard to dry and could then be used for

experiments. As to control any spillages all stages of the sieving process were carried out in a fume hood with the sash lowered when machinery was initiated. The collected phosphors were analysed using a Morphologi 4 by Malvern Panalytical. This allowed for the measurement of particle size, shape and characterization. Sieves were cleaned through sonication in a water bath and dried in air. Cleaning would ensure consecutive processes would not be contaminated by the previous phosphor.

### 3.6.Electrodeposition equipment

The electrodeposition experiments used an EPS-601 electrophoresis power supply produced by Amersham Pharmacia. This device is primarily intended for clinical applications requiring electrophoresis. Electrophoresis separations can be controlled by voltage, current or power. The EPS-601 automatically switches over the controlling parameter according to programmed limits and conductivity variations in the system. Typically, the device was run with a prescribed voltage, and limits were set for current and power. Table 7 gives ranges for each parameter on the power supply. With the voltage being set before experiments, the current of the system would be displayed on the device and was taken note of every 5-10 seconds.

Table 7. Parameter ranges for electrophoresis power supply**.**

| *Parameter* | *Output range* | *Programming resolution* |
|---|---|---|
| *Voltage* | 0 – 600 VDC | 1 V |
| *Current* | 0 – 400 mA | 1 mA |
| *Power* | 0 – 100 W | 1 W |
| *Time* | 0:01 – 500 h | 1 min |

### 3.7.Drying of samples

Samples were dried in an oven for 10 minutes at 120ºC. This temperature was selected as an appropriate upper limit to prevent distortion of the metallised polycarbonate coils that would be used in production. Sintering was not used in this study as the plastic coils would not be able to withstand the hot temperatures that would promote the formation of a solid film.

### 3.8.Evaluation of deposit weight and adhesion.

The primary means of evaluating the deposit was by weighing coated samples. This enabled rapid feedback when adjusting the process variables. Samples were weighed before and after EPD experiments using a 0.1 mg resolution mass balance to assess the mass of the coating. As

requested by the sponsoring company, the adhesion of the deposit was initially tested through a crude method of attempting to scrape material from the surface of the substrate. This gave no quantitative analysis of the deposited layer so was not a reliable method to assess adhesion. With this and other methods of analysis selected by the sponsoring company, there is the ability to achieve rapid feedback but a lack of reproducibility. The addition of further elements of repeatable analysis is something that should be considered in future experiments. Alternative methods for testing adhesion are explored in **Section 6.2** With all layers the aim is to achieve a deposited layer in which no material can be removed so if the material is easily removed through these techniques, some change would be made to the deposition process.

### 3.8.1. Optical analysis of deposits.

Images of the deposited layers were taken using 3D microscopy (Alicona Infinite Focus, Alicona Imaging GmbH). After experimentation, individual substrates are set up in various orientations to analyse each face (top/bottom/outside/inside). The photos and renders generated allow for coverage, thickness, and roughness to be analysed and compared. Altering processing parameters and electrolyte composition influences how the material is deposited on different areas of the substrate. Analysis of each face reveals which parameters would give the most even, high-quality coverage of the entire coil and would therefore be experimented with further. To find the thickness of poorly deposited layers, the depth of the ‘gaps’ can be measured which gives an approximate measure of the thickness of deposited material. For substrates with better coverage, a thin strip of Polyvinyl Chloride (PVC) insulating tape was wrapped around several different points of the substrate before experimentation to act as a mask. After the coating is deposited, the tape is removed to reveal an area of zero deposit in which layer thickness can be measured (Shown in Figure 9). When being assessed under the microscope, a contour or area thickness may be calculated by drawing a line or rectangular area respectively. Layer thickness over an area would be possible over a flat surface but as the substrate has a circular cross-section, a contour along a line was used (represented by a red line in Figure 34). An average layer thickness can be calculated from this contour by identifying the average distance between peaks and troughs of the contour. The microscope would not physically allow for certain areas of the substrate to be measured so the collected values for layer thickness were not true for the entire deposited layer.

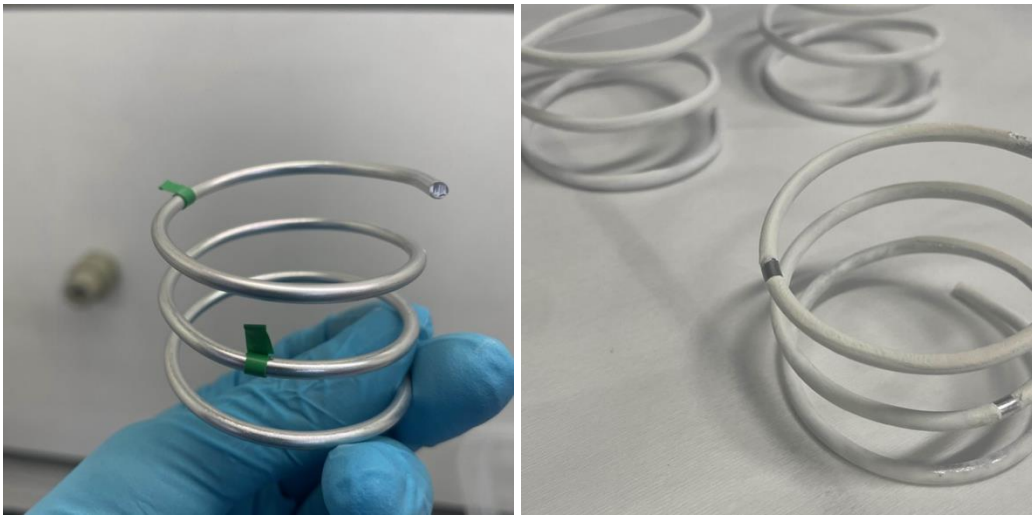

**Figure 9. Taping of coils before experiments and the resulting deposit.**

This measure would cause the value for layer weight to be slightly skewed so this method of analysis would only be used on repeat experiments where parameters had given a layer weight close to the target. Surface roughness is also assessed on both clean and deposited coils.

### 3.9.Concluding remarks

This chapter has outlined the materials and methodologies used in the experimental programme. Additives were selected for the process due to experimental data shown through literature that would allow for the suspension to successfully carry out the 4 components of EPD: particle dispersion, particle charging, electrophoretic migration, and deposition. Analysis of samples after experimentation ensures that the deposited layer can be assessed in terms of the deposited mass, substrate coverage and layer thickness. These can be compared against targets set by the sponsoring company with adjustments being made to processing parameters accordingly. With there being the requirement to first verify experimental techniques due to a novel apparatus design, each layer can first be deposited and assessed separately. It is important to also consider the particle sizing and how this will affect their response to an applied electric field.

**Table 8. Particle size of colloidal particles**

| *Material* | | *Median particle size (µm)** |
|---|---|---|
| *Barium titanate ($BaTiO_3$)* | | 0.2 |
| *Phosphor* | *CaS:Eu* | 5.0 |
| | *ZnS: Cu,Al* | 8.0 |
| | *ZnS:Ag* | 6.5 |

*****As reported by supplier websites*

This is an important factor in making adjustments to processing parameters and is a major reason as to why layers may not have a consistent deposit. Success of these individually will allow for sequenced deposition of the layers and subsequent analysis against the same targets. Following chapter will look to optimise both the processing conditions and the apparatus.

# 4.Development of suitable tank and electrode geometry for EPD

## 4.1.Introduction

This chapter details the development of the apparatus for electrophoretic deposition, focussing on the size of the vessel for housing the EPD solutions as well as the geometry. The focus of this work was on reducing the inventory of solvent required for the process as well as reducing the distance between the sample and counter electrode so that the voltages used could be minimised. Both these approaches were necessary to improve the safety of the process so that it could be safely carried out in the laboratory. At the start of the project, a series of deposition tanks were provided by Luxtec and intended for use in the project, but these were not found to be suitable. The mounting frame also supplied would prove to be unnecessary through experimentation due to the required wiring in the tank. The numerous obstructions would complicate the loading and unloading of the substrate. Although the tank was designed to assist in controlling certain parameters, it would prove detrimental to experiments once the process is initiated. The loose connection of the counter electrodes would allow for the stirring to rotate components connected to the frame and render certain experiments invalid. There proved to be a host of parameters that would affect deposition, so the process eventually underwent numerous changes.

## 4.2.Tank assembly supplied at the start of the project.

Initially, it was proposed by the sponsor that 5L capacity tanks were to be used. The tanks for this study used components from the Hoefer SE600 Standard Dual Cooled Electrophoresis Unit **Appendix 7.1**. These tanks are constructed from acrylic and are intended for protein and nucleic acid electrophoresis. From there, the lower buffer chamber and safety lid were used to fashion the main tank. The sponsoring company then incorporated their purpose-built mounting frame used to hold both the sample and two aluminium counter electrodes. The adjustment for this study into electrophoresis onto a metallic 3D substrate is shown schematically in **Appendix 7.2**. The tank dimensions are 320 x 290 x 140 mm, and material is kept suspended through magnetic stirring using a 60mm stirrer bar. As suggested by the sponsoring company, the arbitrary stirrer setting number is set to be 2.8/2.9 on the dial of the magnetic stirrer (390-

410 rpm). This will be related to a speed in rpm later in the study. There are a few notable observations to take from this tank design.

The mounting frame will first ensure that the counter electrodes and the substrate are at a consistent distance apart throughout experiments. This acts as a control, allowing for tests to be repeatable with fewer moving parts. The sample is attached through a concealed connection that will ensure the sample is the only component of the build that is deposited onto it. The arms which attach the counter electrode to the frame have multiple slots which allow for electrode spacing to be increased/decreased. This adds the possibility to assess the effect of electrode spacing on material deposition. The frame will also remove the need for human interaction with the sample when moving from the tank to the oven. Any external contact with the experimented sample will cause the material to be removed from the surface giving a false result for layer weight and uniformity.

The counter electrode design is two rectangular plates of Al 5083 alloy suspended 5 cm away from the sample. Unlike traditional methods of electrophoretic deposition, this 3D sample requires coating in more than one plane. The theory of the sponsoring company for this experimental design is that there is now an electric field that surrounds the whole sample so material will be deposited on all surfaces. This is a novel approach so adjustments to experimental design were anticipated from the initial stages. Through their research, the sponsoring company had a set of parameters that would be used for each layer, and these are shown in Table 9**.**

Table 9. Parameters for individual layers

| *Parameter* | *Dielectric* | *Encapsulating Polymer* | *Phosphor* |
|---|---|---|---|
| *Deposition type* | Cathodic | Anodic | Cathodic |
| *Applied voltage (V)* | 500 | 400 | 450 |
| *Processing time (s)* | 36 | 45 | 233 |
| *Stirrer setting* | 2.8/2.9 | 2.8/2.9 | 2.8/2.9 |

Based on a review of the chemicals required for the process, it was determined that the tanks were not suitable due to the incompatibility of some of the solvents with acrylic. Because of this, the change was made to a tank of the same dimensions but fabricated out of glass. This consisted of 5 glass panels that were fixed by solvent-resistant epoxy (3M Scotch-Weld Structural Adhesive DP 100) in simple T-joints at the edges of the panels. Should there be any degradation in the epoxy, Dowsil sealant was used on the interior edges to prevent leakage. A

6th panel, or lid, can then be placed atop the 5 other panels during experimentation as a safety measure and has the necessary cut-outs so wiring may be passed through. The tank can be seen schematically in **Appendix 7.3** with the real-life build shown in Figure 10.

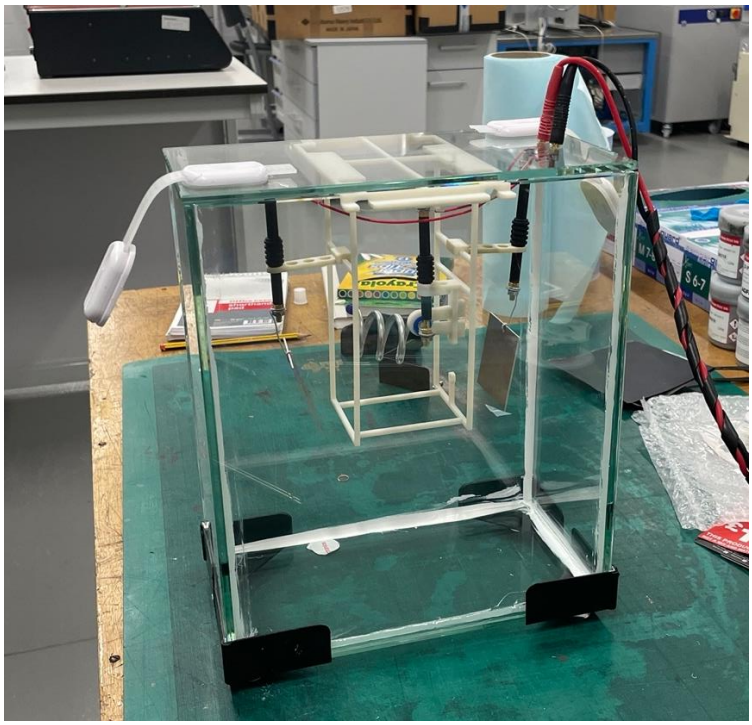

**Figure 10. 5L glass tank build**

The proposed glass tank still presented several issues. Firstly, the solvent inventory in the tank of 5L presented a significant hazard were the tank to break, leak or catch fire. The inventory posed problems with storage and disposal as there was still room for optimisation of original recipes which would cause previous formulations to be left as waste. Another issue that rose was the selected voltage for electrophoresis. Voltages upwards of 400 V, dictated by the proposed gaps between the samples and the counter electrode, presented a higher risk so had to be decreased to a more sensible value. risks associated with high volume prevented any experimentation using the larger glass tanks in the university labs. With these limitations, the tank had to be downsized to a more manageable volume. The tank would now be housed in a metallic casing as a safety measure. The panels for the now smaller tank were designed so that the frame could still be used for experiments. The results from experiments using the rectangular tank with square electrodes are documented in **Section 4.3** with an explanation for the necessity to further alter the experimental set-up to that investigated in **Section 4.4**.

### 4.3.Testing in small format rectangular glass tank.

### 4.3.1. Experimental set-up.

The tank ingredients for the experiments in this section for a 1 L suspension are shown in Table 10**.** Tank panels and wiring for this build were supplied by the sponsoring company due to the issues identified in the previous section. As this experiment would establish the proof of principle, with the plan to optimise further, only the red phosphor (CaS:Eu) was used in suspension. The layer would also be easier to assess once deposited due to its bright colour. Using a single colloidal particle means the experiment can be treated like those carried out through literature. Once a sound set of conditions and parameters could be established through testing like this, other phosphors may then be incorporated.

Table 10. Tank formulation for initial EPD testing

| *Ingredient* | *Quantity* |
|---|---|
| *Isopropyl alcohol* | 980 ml |
| *Deionized Water* | 20 ml |
| *CaS:Eu phosphor* | 5 g |
| *Magnesium Nitrate* | 0.1944 g |
| *Glycerol* | 20 ml |

A 60 mm stirrer bar was used with the same magnetic stirring equipment and kept at a steady 118-120 rev/min. The mounting frame with the substrate connected was then lowered into the tank. The experimental set-up can be seen in Figure 11**.**

**(a)** 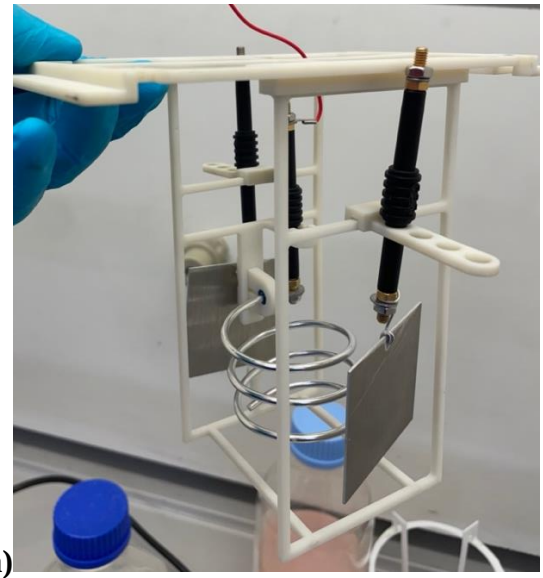 **(b)** 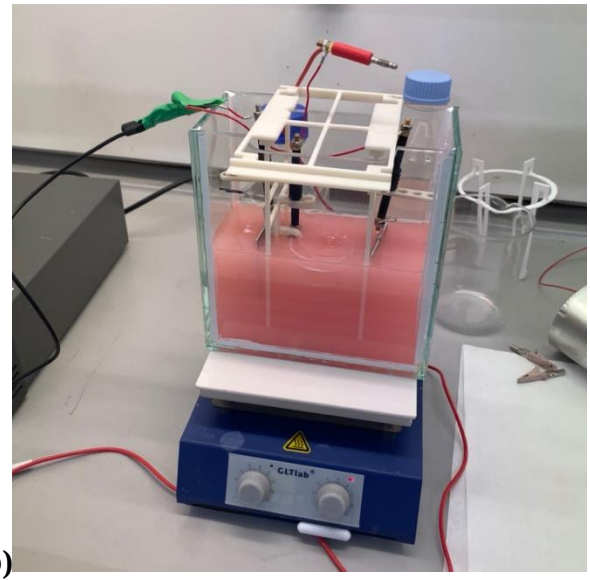

**Figure 11. Experimental set-up of small glass tank a) mounting frame supplied by sponsoring company and b) fully assembled build.**

The metal casing was briefly removed so the interior of the tank was more visible, and the placement of electrodes could be better assessed. It was then replaced upon starting the experiment. Following the safety issues met in 4.2 the processing parameters were all stepped down to safer values for these tests. With electrode spacing at 50 mm, parameters were set at 280 V applied voltage, 100 mA current limit and a processing time of 180 s. Once set up, the power source was initiated for the specified time and observations were made.

### 4.3.2. Effect of stirring through experimentation.

Seconds into the initiation of the magnetic stirrer, the fluid would form a vortex, lowering the level of liquid below the top of the substrate. Relatively intense stirring inside the tank is necessary to ensure that the phosphor particles are kept in suspension and, due to being heavier than other colloidal particles, the phosphor required higher stirring than anticipated. The basis for the prescribed agitation speed was unclear so it was understood that some adjustments would have to be made. Through literature, it was assumed that sharp interior edges would encourage self-baffling within the tank, but the speed was too high. This swirling effect also forced the counter electrodes to move out of position (not parallel to the tank end face). This was down to the frame and its design to allow for electrode spacing to be decreased. As these attachments were not permanent there was some movement in the counter electrodes. The wires connecting to the counter electrodes also proved to be too flexible for the parameters used. It would take minimal force to bend the wires suspending the counter electrodes and this was demonstrated when the stirring was increased. The aluminium plates would collide with the coil or twist to face the wrong direction as the wiring could not withstand the force induced by stirring. This would change the electric field through the experiment which is a parameter that is required to be kept constant through experiments.

### 4.3.3. Analysis of deposited material.

There were plenty of drawbacks that would need improvement before further experiments were carried out. The benefit of this test was that material had deposited onto the substrate as shown in Figure 12**.**

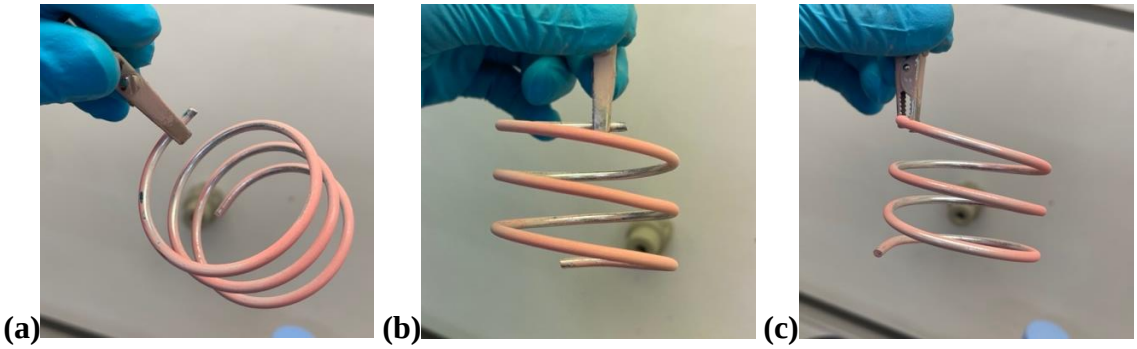


**Figure 12. Resulting deposit of experiments showing (a) interior surfaces, (b) face of the coil facing the counter electrode and (c) face of the coil 90º to the counter electrode.**

As this was an initial test, weights were not recorded, and the analysis was solely by eye. There was an inconsistency in the material deposit, but the results verify that the materials used in suspension and for the substrate can successfully perform cathodic deposition. Success at such an early stage of experimentation came through the validation that the formulations and processing conditions had the capacity to deposit material onto the substrate. There is room for refinement of the process through altering processing parameters and engineering the apparatus to achieve a more uniform coating.

As stated, deposition onto the substrate was successful in certain areas of the coil but there were obvious spaces in the deposit where there was little-to-no deposited material (Shown in Figure 12a and **c**). To understand this, the mobility of the colloidal particles and the alignment of the counter electrodes must be assessed. Figure 13 demonstrates the difference in electric field strength between the front and the side face of the substrate.

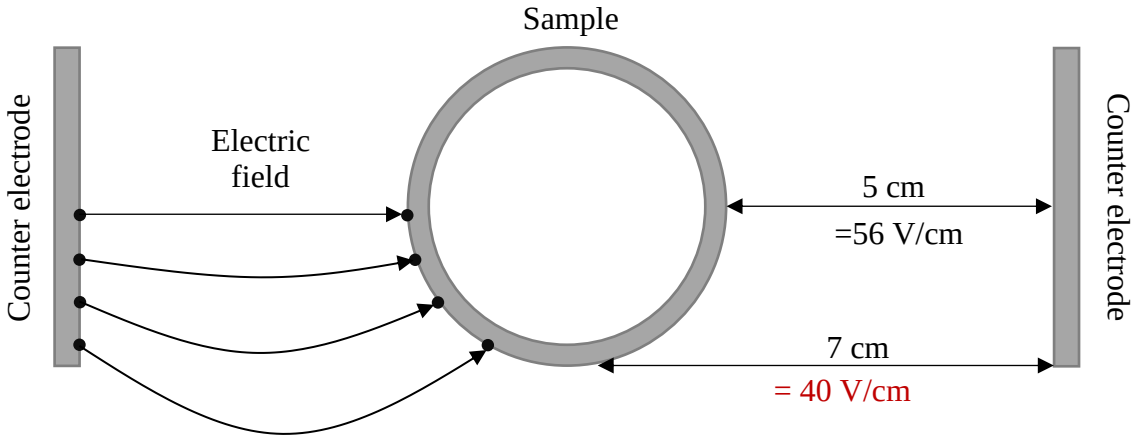


**Figure 13. Schematic representation of effective electric field and electric field strength due to counter electrode dimensions**

This can be used to explain the lack of coverage on the sides of the substrate as particles here will have much lower electrophoretic mobility and are more likely to be influenced by either

gravitational forces or movement due to stirring. Poor deposition, more evident on the interior faces, can also be due to shadowing. The shadowing effect occurs when there is an object or part of the substrate which obstructs particle movement away from one electrode to the other. Examples of obstructions that cause shadowing in these experiments are the frame but also the substrate itself. Components of the mounting frame in most cases are small in dimensions so will not have an outstanding shadowing effect but are still an obstruction. The substrate itself prevents particles that are migrating from a counter electrode from reaching the inner surface of the opposite side of the coil. This is an issue that will occur with most counter-electrode designs that are solely facing the exterior of the substrate.

Another complication that developed through this experiment is the exposed charged material incorporated into the mounting frame.

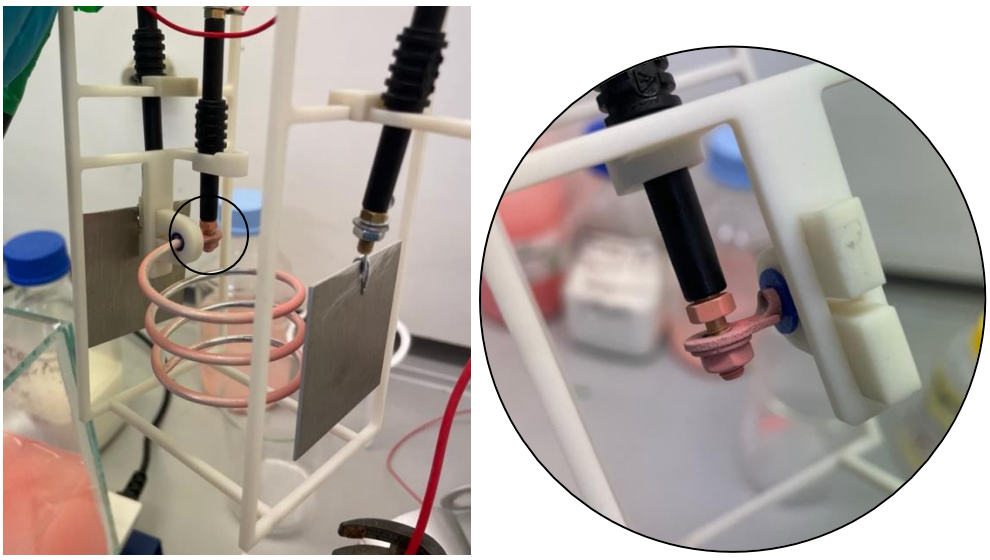

**Figure 14. Material deposit onto mounting frame component.**

As is shown in Figure 14**,** certain areas of the frame are deposited onto through the process. Over time, the reactions taking place on the surface of this material will cause it to degrade and reduce electrical contact between the frame and sample. A simple solution for this would be to ensure components that are not to be deposited on to are coated in a polymer or some non-reactive material. Unintentional coating of these parts also means that material is being wasted in the tank as phosphor is now being deposited elsewhere.

The final drawback of the experimental design was the complexity of the mounting frame. Dismantling the frame for the annealing stage proved very time-consuming, navigating through the different scaffolds and wires. The wires had to be individually unscrewed from the frame whilst ensuring no contact was made with the substrate. With efficiency and speed of

production being of utmost importance for this build, the time taken here seemed unnecessary and that simplification of the design would remove these issues faced. Once disconnected from the wiring, the whole frame was supposed to be placed in the oven for annealing. This theory was slightly flawed as there were now other components attached that would not withstand the temperatures selected. Because of this, the substrate was carefully removed from the frame and placed in the oven by hand. At this stage, there was the issue of the wiring. The process of removing the sample from the frame was not as simple as previously anticipated due to the wires being tangled in the vicinity. This made what was meant to be an efficient procedure much more complex and proved to be counterintuitive and caused damage to the coating.

## 4.4.Development of an axially symmetrical EPD system

### 4.4.1. Design objectives

With the results of previous experimentation, it was evident that there was room for improvement in experimental procedures but there were techniques that may be brought forward. For example, the formulation for the phosphor seemed suitable for experiments so needed truly little adjustment besides the addition of the other two phosphors. This section describes the redesign of the apparatus to address the following issues:

- Asymmetry of the sample with respect to counter electrodes.
- Inconsistent voltage gradient.
- Efficiency and practicality of sample loading/unloading.
- Solvent volume.
- Safety of the tank assembly.
- Reduction of voltage.

The sponsoring company also aim to reduce processing times of this process where possible so that production of the final device is quick and efficient. Following this, smaller adjustments in processing parameters and adjustments can be made, and a full study into the electrophoretic deposition of the individual layers will be investigated.

### 4.4.2. Electrode placement

The previous tests on the 1 L rectangular tank revealed several drawbacks in the design of the experimental set-up. The most obvious was the counter electrode design and how it would not allow for the entirety of the sample to be coated as shown in Figure 12. This, therefore, required a change in the design of the counter electrode to ensure that the electric field strength was

equal around the entire sample. Like the experiments in (43,68), the approach selected was for a concentric cylindrical aluminium foil counter electrode (70 mm width, 0.05 mm thickness). This would ensure a constant electric field surrounding all faces of the coil once connected to the power supply. Negishi et al (68) made use of a stainless-steel wire mesh which is something that may be considered were these experiments not to work.

The large tank dimensions used in the previous study proved to be unnecessary for electrophoretic deposition on this scale. Firstly, the electrophoretic deposition process only concerns particles suspended between the substrate and the counter electrode. A larger tank or a larger inter-electrode distance allows for particles to be dispersed further from the substrate and decrease the likeliness of deposition. The formation of a vortex was unexpected for these experiments as a rectangular tank with sharper interior edges was assumed to 'self-baffle' and decrease the effect of swirling. Swirling encourages poor particle dispersion in the suspension fluid, again decreasing the deposition rate. Stirring also caused counter electrodes to move throughout the experiment but this is a parameter that must be controlled for future experiments. Looking to eradicate these issues for future experiments, the new tank and counter electrode build was established.

To ensure the counter electrode was rigidly held in place, the tank size was reduced to a 600 ml beaker (FisherBrand FB33114) with a 500 ml operating volume. This would allow for the foil to be placed flush with the inner walls of the beaker and then be connected to the power source from a single point. Through measurement of the inner diameter of the beaker (87 mm), the dimensions of the counter electrode were now measured to be 70.00 x 273.32 mm and therefore a surface area of 0.0191 $m^2$. The change in tank size decreases the electrode-to-sample spacing to 10 mm which allows for the voltage to be lowered for experiments. This, along with a smaller quantity of required solvent, becomes safer and is a technique that is established through the mentioned literature. As most figures for tank formulation have been selected on a concentration basis, recipes can be scaled down easily for future experiments.

A change in the counter electrode design would also remove the necessity for the mounting frame suggested for experiments. As it showed to have some shadowing effect on the substrate and made removal of the sample more time-consuming, it was removed from experiments from this point. Instead, the samples would be connected by a crocodile clip and held in suspension with a clamp stand as shown in Figure 15. This design would still mean that samples are rigidly held at a constant distance through experiments and contact was not made with the samples after deposition. Once the deposition is complete, samples can be raised out of the suspension by holding the clamp stand.

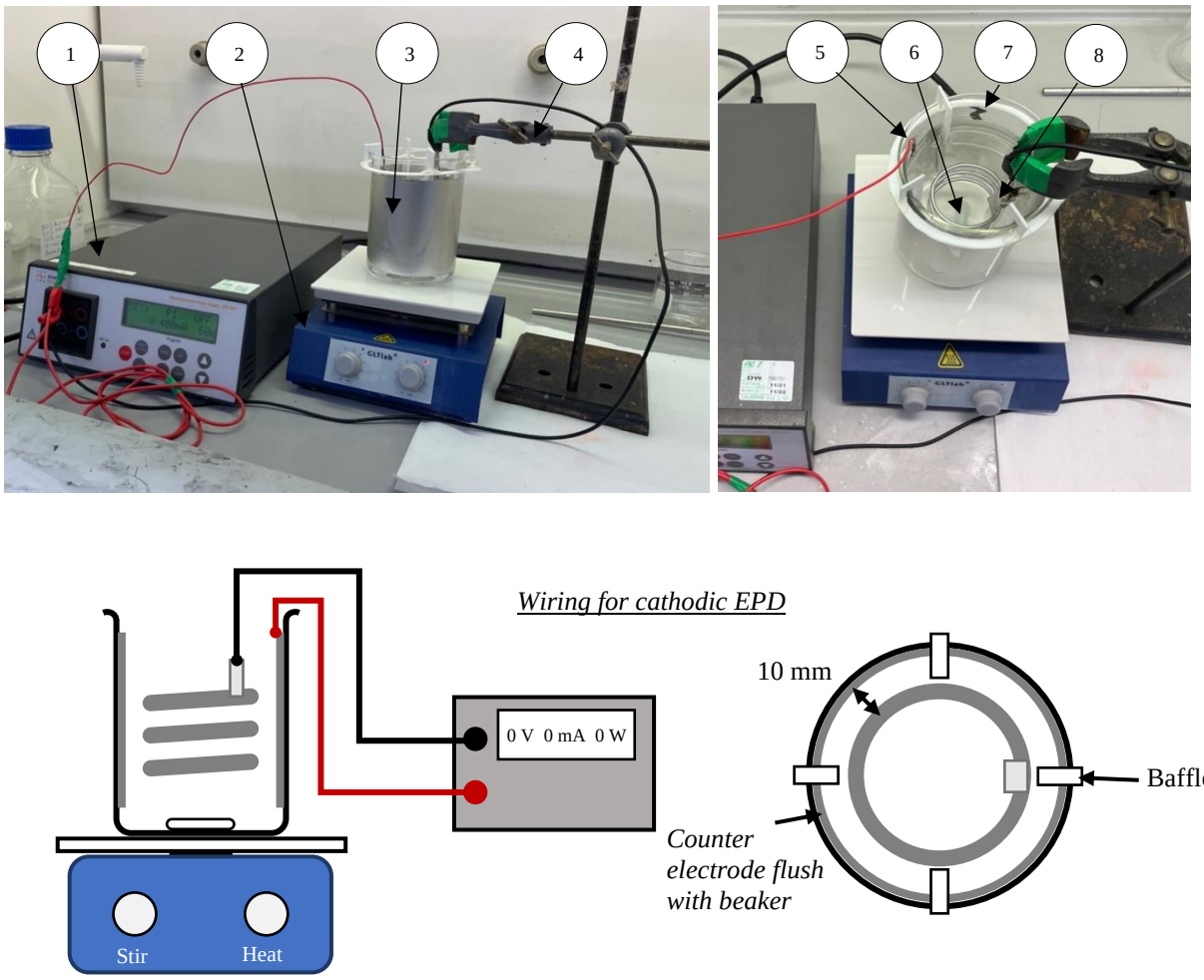


**Figure 15. Experimental set-up for axially symmetrical EPD.**

The one drawback of this design would be that the electrode spacing was not as accurately measured. The sample would be lowered into the suspension, and the centre of the beaker would be established by eye. This is a parameter with room for improvement and is assessed later in the study. The new tank design is a much simpler approach that prevents the wiring from obstructing the efficiency of experiments.

The final experimental setup should resemble the images in Figure 15. The power supply (1) should be placed in the fume cupboard adjacent to the GLTlab hotplate/magnetic stirrer (2). These should not be plugged in or turned on until all other components of the set-up are in place. The beaker (3) is then placed on the magnetic stirrer and a 35 mm stirrer bar (6) is placed inside. The foil counter electrode (5) should be cut 5 mm longer than the circumference of the inner face of the beaker. This will give a slight overlap that will allow for a crimp connector to be wired to the counter electrode. Whilst disconnected from the power supply, the foil counter electrode is lowered into the beaker so that it is flush with the interior surface. The baffle

structure intended to reduce vortexing (7) can then also be lowered into the beaker. Any exposed wiring should be covered with electrical tape and following this, the counter electrode should be wired to the positive terminal. To set up the sample, a crocodile clip (8) should be wired to the negative terminal and tightly held in the clamp stand (4). The sample may then be placed in the clip. The height of the clamp should then be adjusted so that the sample is in the vertical centre of the counter electrode. This can be done on the outside of the beaker with the sample placed up against the edge of the beaker. This way, vertical distance is easier to see ad therefore measure. Electrical components may now be turned on in preparation for deposition.

### 4.4.3. Counter electrode dimensions

The previous section highlighted the move from rectangular counter electrodes to a cylindrical shape due to the requirement of a uniform electric field surrounding the coil. This would ensure that firstly the outermost faces of the coil would all experience a uniform deposit. The theory is that the rest of the substrate would also achieve a uniform deposit, but this was highlighted not to be true after initial validation experiments. There was a consistent lack of deposition on the bottom and interior faces of the coil throughout. Steps may be made to alter particle size, and viscosity of the fluid or stirring but here the problem is partially solved by increasing the width of the counter electrode. Increasing the width from 70 mm to 95 mm drastically improved the coverage of the samples through testing of the phosphor layer. This is explained schematically in Figure 16 where there is a favourable electric field being formed that will increase the force on particles acting against gravity to coat the underside of the coil.

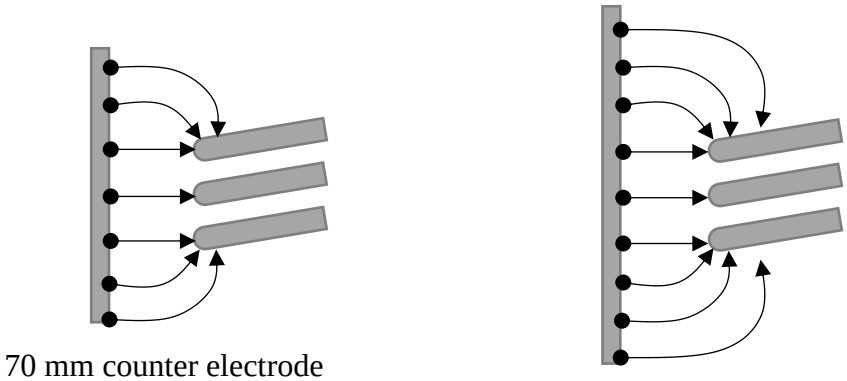

70 mm counter electrode

90 mm counter electrode

**Figure 16. Schematic representation of electric field exhibited in 70 mm and 90 mm counter electrodes.**

A larger counter electrode will also improve the mobility of particles to the inner faces of the coil. There is still a lower coverage on the inner faces of the substrate, but this is anticipated as is seen in the results in (43). In areas closer to the centre of the 3D scaffolds there is a lower

amount of deposited material which may only be solved by more complex counter-electrode geometry. A more complex geometry for these experiments is suggested in **Section 6.2** but here it is demonstrated that deposition can be improved by an increase in the width of the counter electrode.

### 4.4.4. Stirring

The supplied magnetic stirrer allowed for a change of stirring intensity by a dial on the front face of the device. This used a scale from 0-10. As this was more of an arbitrary scale to measure stirring intensity, experiments were first carried out to assess the relation of the stirrer setting to the actual rpm. The method of this was to set up a beaker filled with water on the magnetic stirrer and place a 60 mm stirrer bar inside. A larger stirrer bar would allow for the rpm to be assessed much easier. Once set up, stirring was set at a certain value and was initiated. The stirrer bar was then video recorded for 10 seconds and the footage slowed to count the number of total revolutions in that amount of time. This could then be multiplied by 6 to find the revolutions per minute. It is evident that there is ample room for human error in this process but with the rpm of the stirrer not being displayed by the manufacturer, this was the best alternative found. This was carried out at several different values on the dial and inputted into a spreadsheet. This would reveal the linear relation rpm had to the stirrer setting and meant an equation for rpm could be established. This equation could now be used to find the rpm from the value set on the stirrer dial. The collected data and resulting equation are shown in Figure 17.

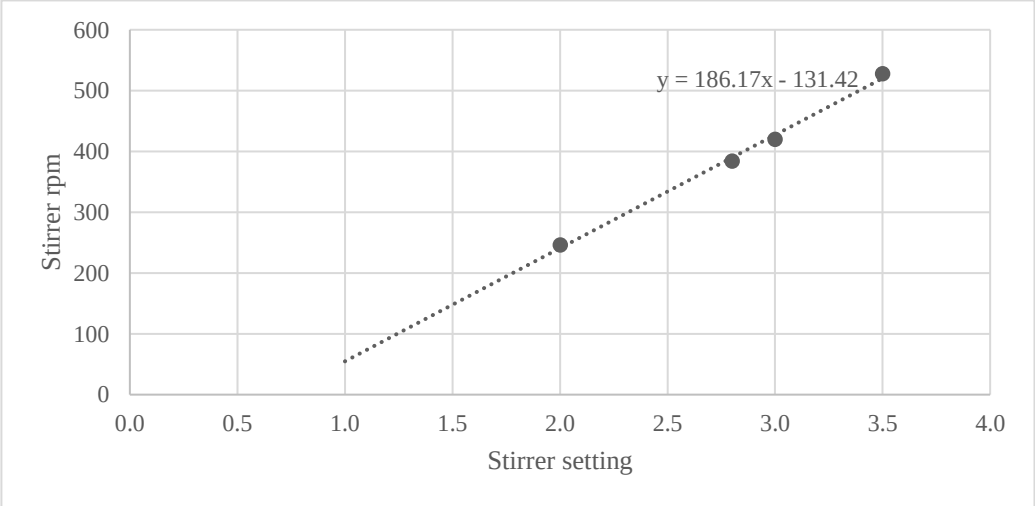


**Figure 17. Graph to calculate rpm from the equivalent stirrer setting.**

### 4.4.5. Use off baffles to prevent vortexing.

The particles used in the previous experiment were heavy so required substantial stirring to counteract the settling of the material. This intense agitation comes with the expense of adding turbulence to the tank. Swirling and the formation of a vortex with stirring during experiments are detrimental to the resulting material deposits. Considerable forced convection may prevent deposition by inducing a washing-off effect of the material. Stirring is a parameter that is important to ensure particles are suspended in the solvent so is not something that may be removed. Tests both with and without stirring at 180 V and a processing time of 233 s were carried out. As is shown in Figure 18, it is visible how impactful the effect of gravity is with these materials.

(a)

(b)

**Figure 18. Consecutive EPD tests with (right) and without (left) stirring. (a) top face and (b) underside of samples**

To maximise stirring without introducing the negative effect of swirling, the theory of baffles was introduced to this study. Through literature, it is understood that central mixing gives an inefficient flow pattern and the tangential velocities developed to cause the fluid mass to spin (69). Particles then swirl around the container and settle at the bottom of the tank as there is nothing to promote axial flow. This can be solved by offsetting the mixing angle, changing the vertical mounting of the mixing device or by baffles. Baffles prevent the swirling motion by impeding rotational flow without interfering with the radial or longitudinal flow (70). They will also promote a top-to-bottom fluid movement preventing any settling at the bottom of the tank. With the use of baffles being well documented through literature, it was found that

optimal dimensions for the baffles were 1/12 vessel diameter and should be installed at radially, spaced at 90º. Kamla et al (71) found an optimal compromise between power consumption and swirling of the fluid was demonstrated at an angle of 70º but this was for more viscous fluids, so the 'standard' measurements were used. As some harsh solvents are used through experimentation, polytetrafluoroethylene (PTFE) sheets (3mm thickness) were selected to fabricate the baffles. Dimensions for the baffles are shown in Figure 19.

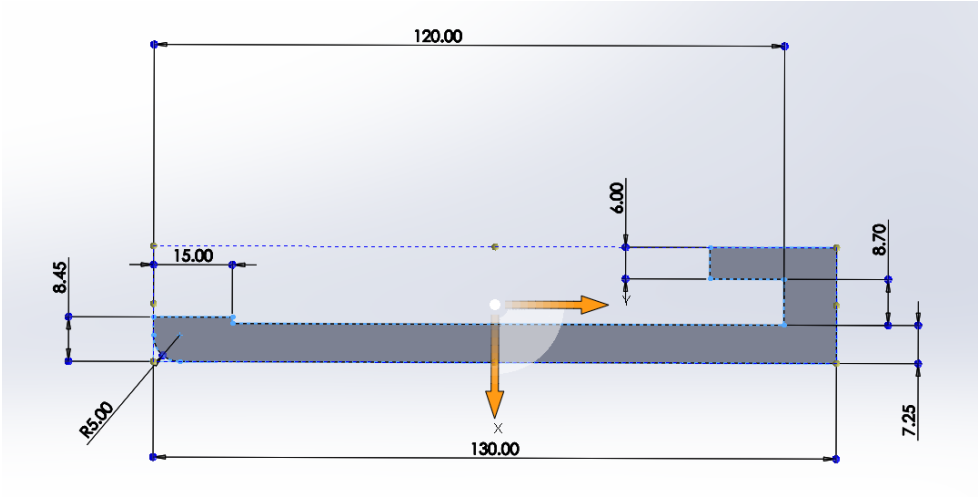


**Figure 19. Baffle dimensions (mm)**

The choice of these dimensions was made with the support of the sponsoring company along with data from the literature (69). The design would allow for the 4 baffles to be hooked over the side of the tank and lie flush with the beaker. Once fully fabricated, the baffles negated the swirling effect and would cause particles to be much better suspended in the solvent. A 'dried herbs' test is pictured in Figure 20 where particles are visibly better suspended. Herbs are of different densities to the materials that are to be used for experimentation so will not react identically but gave a good example of the effect of baffles.

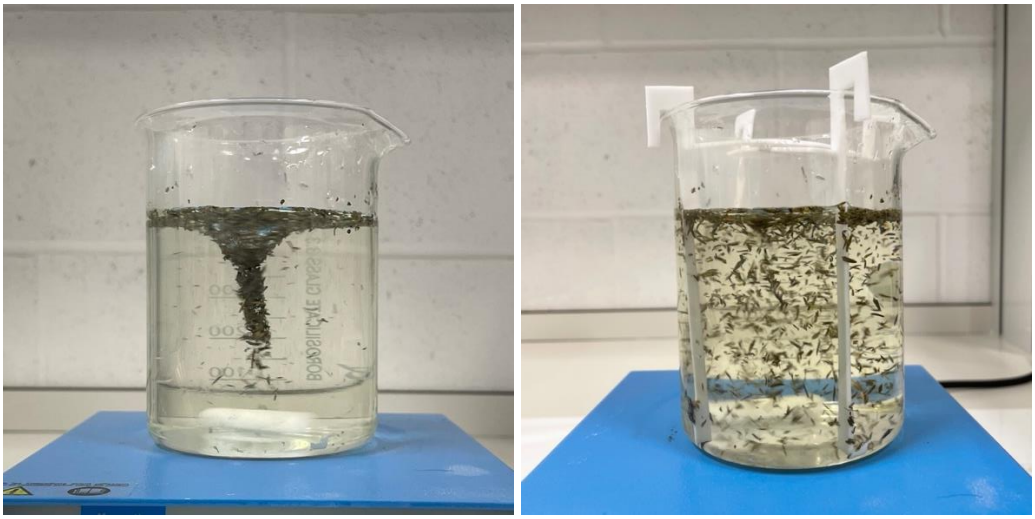

**Figure 20. Mixing pattern without (left) and with baffles (right)**

As found with components earlier in the study, the tangential velocity of the stirring motion would cause the baffles to rotate slightly and move with the liquid. To solve this, epoxy was used to join all baffles to a ring of PTFE so they would stay rigid when stirring is initiated. These changes are shown in Figure 21.

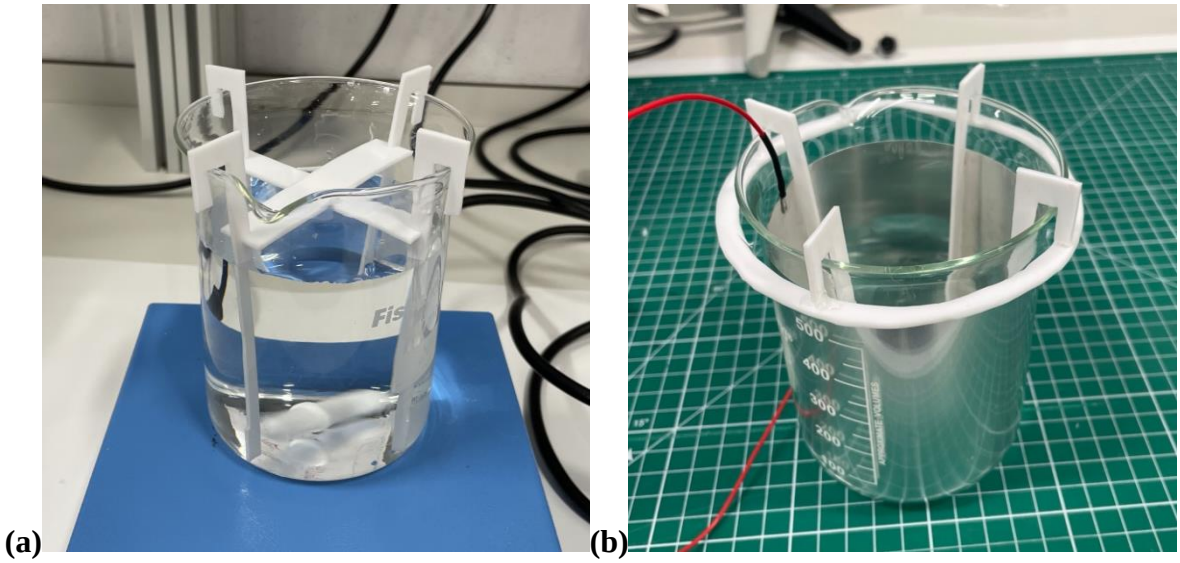

**(a)** **(b)**

**Figure 21. (a) original and (b) improved baffle design**

### 4.4.6. Additional central electrode

In **Section 4.4.3** it is documented that the design of the counter electrodes will improve the coverage of the substrates. Through validation tests, there is still an issue of deposition onto the inner face of the coil. For uniform coverage to be achieved of the entire coil, there must be equal electric field strength at every surface. With a shape as complex as a coil, it is near impossible to achieve a counter-electrode design that will incur equal field strength at every

point. Because of this, it is expected for the coating to be not entirely uniform in terms of layer thickness. In an attempt to bring the coating closer to uniform, a central counter electrode was tested to see if this would help with coating the inner face of the coil. Like the original design of experiments, the two counter electrodes were wired to the same terminal. The central counter electrode was an aluminium rod of diameter 4.7 mm and length 200 mm. The surface area of the submerged central counter electrode was 0.0014 $m^2$ (compared to 0.0191 $m^2$ for the outer counter electrode). The rod was held in place with a separate clamp (Shown in Figure 22) on the same stand as the coil. This would allow for some level of control of electrode spacing. The rod was lowered to the same depth as the foil so that some length of material was exposed outside of the fluid. Like other changes made, an experiment was carried out on the phosphor suspension to test the theory. An experiment was also attempted on the dielectric layer.

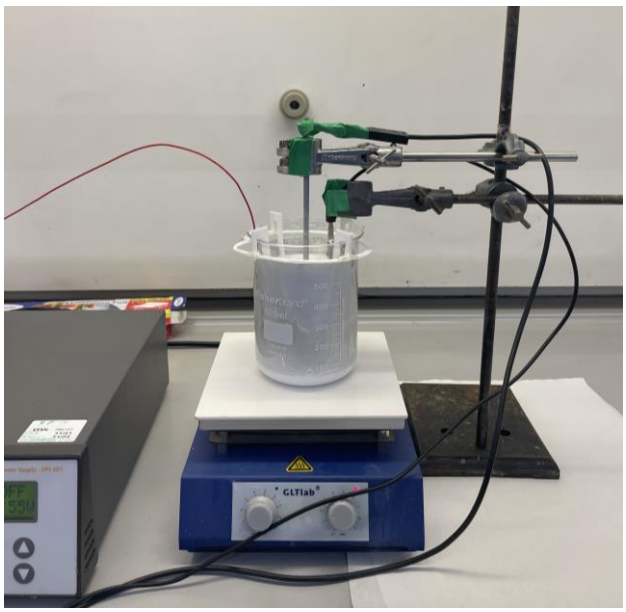


**Figure 22. Experimental set-up using a second central counter electrode.**

The theory that the inner face would be coated was proved wrong in this case with the layer either having the same or worse morphology than in other experiments. The phosphor experiments gave an almost identical layer weight with poor coverage on the inner face and the dielectric demonstrated worse layer uniformity and coverage. The central counter electrode had a much smaller surface area which equates to a much lower electrical field strength. Because of this, convection or gravitational forces would dominate the force from the central electrode leading to minimal assistance in coating the inner face of the substrates. The ‘piling’ effect witnessed through dielectric experiments is further investigated in **Chapter 5,** but results demonstrated that this became worse in experiments that used a central counter electrode. It

should be noted that separate experiments were not tested with just the central counter electrode. It is possible that if experiments with each counter electrode are carried out separately the problem of coating the inner face could be solved. This is something that will be explored in **Chapter 6** but for experiments in this study, it will cause deposition time to now double as two experiments need to be carried out for each sample. The desire for rapid production of these layers is a goal of the sponsoring company so extended amounts of time for each layer are not desirable.

### 4.5.Conclusion

This chapter allowed for the original design of experiments for this study to be optimized into a process that will be repeatable and give reasonable results. Through preliminary testing on the phosphor layer, there is evidence of a vast improvement in coil coverage due to the changes made with the build (Figure 23). As analysis of the deposited layer weight was not measured for preliminary tests, there will still be changes made to processing parameters to achieve the layer weight set by the sponsoring company.

**(a)**  **(b)** 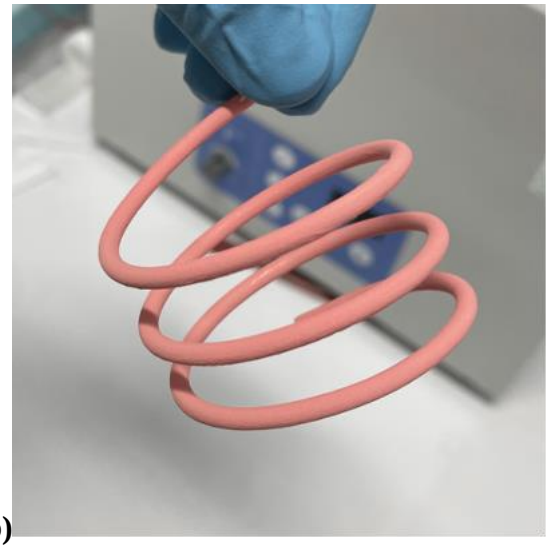

**Figure 23. Comparison of deposited layer (a) before and (b) after process optimisation**

This innovative design of experiments will now allow for a uniform voltage gradient in a circular sample. The smaller volume of the solvent decreases the number of wasted chemicals and facilitates safe operation in a laboratory environment. The redesign has sped up the optimisation process as samples can be loaded/unloaded much quicker. Some areas still have room for improvement but will require further investment in a time and financial sense. For the following chapter, experimental procedures will be carried out with apparatus as shown in

Figure 15. The changes ensure particle dispersion in the suspension is optimal whilst also promoting coverage of the whole substrate. Formulations for each individual layer are shown in Chapter 5 with justification for any changes made.

# 5.An experimental study of the deposition of dielectric, encapsulating polymer and phosphor layers for an electroluminescent build.

## 5.1.Introduction

For this experimental study, the deposition of each individual layer covered in **Chapter 4** was now carried out using revised formulations and experimental set-up. The goal of this chapter is to find the optimal parameters for deposition of the individual materials, which will then build into the sequencing of said materials for the ACEL device. The layers to be tested are phosphor (1), encapsulating polymer (2) and dielectric (3). Formulations for the layers that will follow these have been briefly covered but due to time constraints were not tested.

As stated towards the beginning of this thesis, this method of depositing material onto a 3D substrate comes with several challenges, some of which were discovered in the previous chapter. Parameters such as formulation, concentration, voltage, stirring, use of baffles and electrode dimensions may all be changed to improve the resulting deposit. With these many influential factors to the final deposit, there are several different combinations which could be tested. The approach taken for this study was to assess a single parameter or condition and attempt to correct and optimise it where possible. Once individual layers are optimised there then comes the challenge of sequencing. Due to the now different surface onto which material will be deposited, there is the possibility of material being stripped from the substrate or dissolved in the solvent. Challenges and setbacks were anticipated and any changes that negatively affected the deposit would not be carried forward onto the other layers. In the analysis stage, the mass of deposited material was measured and compared against the values set by the sponsoring company. The difference between the two values is annotated in tables using the notation +/- with positive values showing there is too high a mass deposited onto the substrate. This can be represented by the equation:

$$Mass\ difference\ (g) = Target\ (g) - Measured(g) \qquad \textbf{Equation 2}$$

Using this value, processing parameters could be adjusted to bring the value as close to zero as possible (target value achieved).

### 5.2.Deposition of the phosphor layer

The selected tank formulation for phosphor layer experiments is shown in Table 11**.** The formulation was made for a 500 ml operating volume. The experiments carried out for this layer used the experimental set-up established in **Chapter 4** and deposition of the layer was carried out onto a bare aluminium substrate. Polycarbonate samples that would eventually be used in the final device were not experimented on as they are a more expensive commodity that are not suited to extensive testing. The aluminium coils could be cleaned through sonication and reused in experiments without their structural properties being affected. As there were fewer parameters with considerable changes and no alterations required to be made to the formulation, this layer was able to be optimised much more quickly than the other two.

Table 11. Tank formulation for phosphor EPD

| *Tank ingredient* | *Quantity* |
|---|---|
| *Isopropyl alcohol* | 588 ml |
| *Deionized Water* | 12 ml |
| *RGB Phosphor Trimix* | 5 g (6200k) |
| *Magnesium Nitrate* | 0.11664 g |
| *Glycerol* | 12 ml |

Through literature, it was established that phosphor concentration would not have any effect on the adhesion of the deposited layer (42). It was however discovered that a range of 1-5 $kg/cm^3$ was optimal for the morphology of the deposited layer (72). With particle size being known and maintained, this explains how too high a concentration would exhibit poor layer uniformity whilst low concentration would lead to high deposition time allowing for settling of phosphors. Due to these findings, changing the concentration of the phosphor was not investigated and a concentration of 5 g/L was used. As to find the most optimal conditions for this layer, the effect of stirring, voltage and sieving were thoroughly investigated.

Experimentation of the phosphor layer was carried out initially with just the CaS:Eu phosphor and no sieving prior. Through research carried out by the sponsoring company, the target layer weight was set at 0.079 g. Their research into material density and features of an optimal ACEL device design would mean that a uniform material deposit of this weight would achieve a monolayer of particles. This figure was selected with the assumption particles were spherical

and all the same size. Experiments were tested parallel to those done for the barium titanate layer so notable findings could be taken and tested on the other layer. Adhesion could be assessed after drying in the oven.

### 5.2.1. Preliminary experiments (pink phosphor)

As stated, the first experiments utilised only the red CaS:Eu phosphor to assess the suitability of the new experimental design. Layer weight and current were not recorded for initial experiments. An applied voltage of 180V with a processing time of 233 s was used for the initial tests. As there had been no previous experiments carried out before this, baffles were not used in experimentation and the smaller counter electrode width of 70 mm was used. The resulting deposit is shown in Figure 24**.** It should be noted the sample in Figure 24 is held upside down.

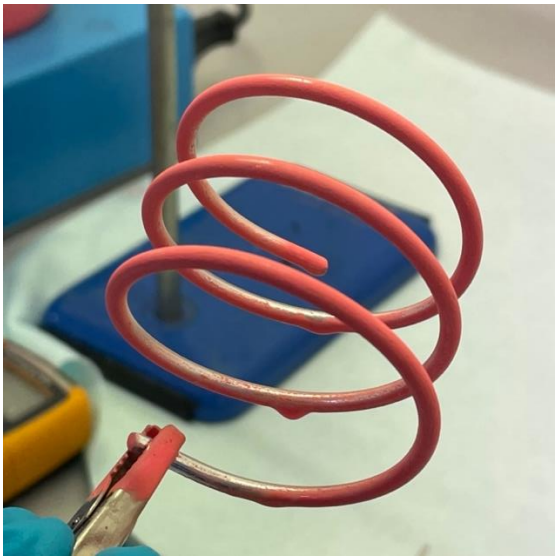

**Figure 24. Results of first EPD experiment of phosphor layer.**

As is shown in the image, there is successful deposition onto the sample with a uniform coating. The surrounding counter electrode allowed for the whole outer face to be coated to what seemed an even thickness. The upper tip of the sample had no deposited material due to this being the area that it was connected to the crocodile clip. As the image shows, in this area material is deposited onto the clip instead of the coil. Not well represented in the image is the coverage of the bottom face of the coil. The heavy particles used had low electrophoretic mobility compared to the gravitational mobility they experience. The particles would therefore be more likely to settle on the top than deposit on the bottom face. The lower tip, on the other hand, has a good deposit of material on both the internal and external face. This is an example of how shadowing affects the inner surface of the sample. The inner surfaces at the centre have

a much lower mass of deposited material than the tip as the opposite exterior face is obstructing particle mobility. This obstruction is not detrimental as such as material is being deposited on the outermost face but causes there to be a lower deposit on the interior. The tip of the coil, however, does not have any obstruction between its inner face and the counter electrode so demonstrates good coverage.

It is understood that a major factor influencing this is the stirring. The agitation forces particles away from the centre of the beaker as a vortex forms. Particles are not evenly suspended in the fluid and causing the outer face to have a better coating of material. Low processing times for this experimental set-up would give a poor deposit hence why it is kept high throughout. Due to the lack of deposition on the bottom face of the sample, an experiment was attempted which involved two depositions onto the same coil. For the first, the tip was covered (Figure 25a), and then the same parameters were repeated (180 V, 233 s) with the sample suspended upside down. The resulting deposit is shown in Figure 25b and c.

(a) 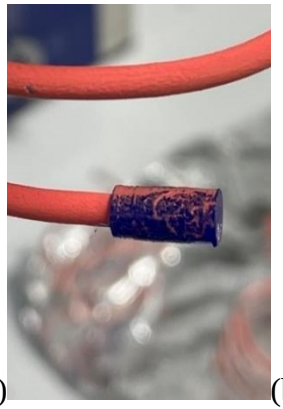 (b) 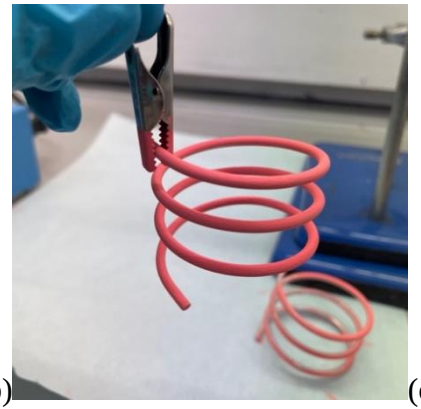 (c) 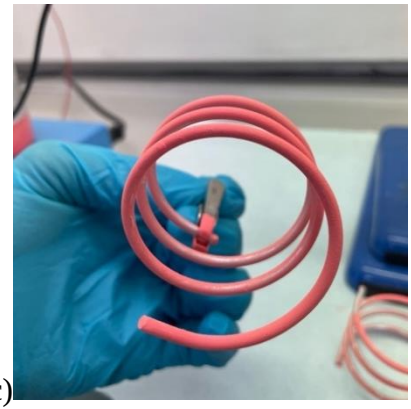

**Figure 25. (a) Component used to cover the tip of the sample before the second coating. (b) top and (c) bottom face of the sample after second deposit**

The deposit achieved from this experiment was much improved. Rotating the sample would allow for the bottom faces to now be coated to the same extent as the top. The drawback of this experiment was that the repeated deposit would cause the outermost face to now have a much thicker deposit whilst the inner face still showed some spaces in the deposit. In this way, the lack of coverage on the bottom face is solved but the inner face still has a thinner deposit. Later experiments analysing deposited weights would prove that the parameters used here (most notably processing time) would exhibit a layer weight much higher than the target value. The removal of the tip cover and rotation of the sample would also cause the material to be lost from its surface, again contributing to a less uniform coating. These experiments proved that the experimental set-up needed some changes which came with the addition of baffles and a

larger counter electrode thickness. Once these changes were brought in and validated as shown in **Chapter 4,** experiments were now carried out using all three phosphors, so a new formulation was made. Experiments would now be assessed on layer weight, rate of deposition, adhesion, and layer uniformity through microscopy.

### 5.2.2. Preliminary experiments (phosphor trimix)

Experiments with all three phosphors now bring a wider range of PSD of the colloidal particles. This difference influences how the formulation will react to the parameters used in previous tests. This change was the motivation for investigating the sieving of the phosphors and is looked at more closely in **Section 5.1.4**. The quantities of each phosphor shown in **Table** 5 were established to ensure the warmth of emitted light was to the specifications of the sponsoring company (6200 K). The initial experiments with the new formulation including the trimix of phosphors covered a large combination of parameters and are shown in Table 12**.**

Table 12. Results from initial phosphor EPD

| *Experiment number* | *Voltage (V)* | *Processing time (s)* | *Stirring rpm* | *Coil weight (g)* | *Cumulative (g)* | *Layer weight (g)* | *+/- (g)* | *+/- (%)* |
|---|---|---|---|---|---|---|---|---|
| *1* | 180 | 233 | 390 | 8.7416 | 8.9503 | 0.2087 | 0.1297 | 164.18% |
| *2* | 180 | 180 | 390 | 8.7714 | 8.9387 | 0.1676 | 0.0886 | 112.15% |
| *3* | 180 | 300 | 390 | 8.8640 | 9.1109 | 0.2469 | 0.1679 | 212.53% |
| *4* | 190 | 233 | 390 | 8.6766 | 8.8897 | 0.2133 | 0.1343 | 170.00% |
| *5* | 170 | 233 | 390 | 8.7366 | 8.9242 | 0.1876 | 0.1086 | 137.47% |
| *6* | 180 | 233 | 613 | 8.7107 | 8.8801 | 0.1694 | 0.0904 | 114.43% |

**The ‘Cumulative’ column gives the coil weight after experimentation from which the original weight can be subtracted to calculate layer weight. Mass difference is expressed in grams and as a percentage (+/- (g) and +/- (%) respectively).**

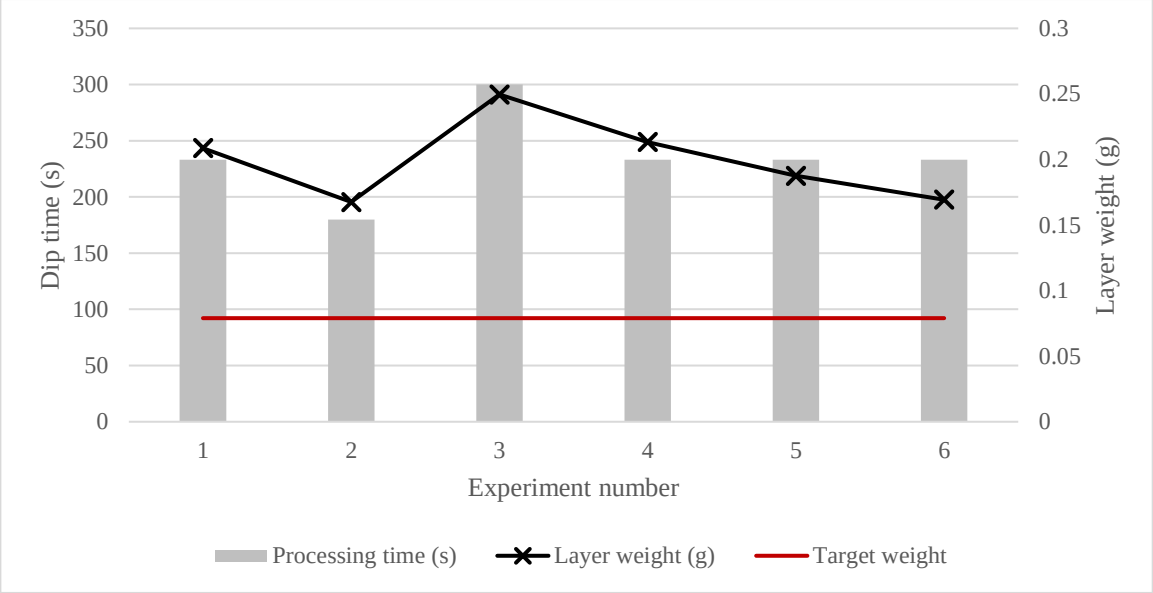


**Figure 26. The effect of changing parameters on phosphor deposited through EPD.**

These experiments allowed for a better understanding of how the trimix phosphor formulation would react to the electrophoretic deposition process. Examples of the deposited layers are given in Figure 27. From these results, evidence shows that resulting deposits are consistent across most parameter combinations. All deposited layers have almost total coverage of the sample and alterations in the processing parameters did not drastically change layer uniformity. Results from this set of experiments prove that the addition of the baffles would now improve the suspension of the colloidal particles. It is demonstrated that the stirrer setting that was used previously would not cause any wash-off in the deposited layer and particles would not experience the high velocities caused without baffles. As the baffles also promote vertical movement of the particles in the fluid, all areas of the coil will now have some level of coating. This is an improvement to the previous tests that would have zero deposit on the inner face of the coils. Measurement of the deposited layer weight would now allow for parameters to be adjusted to give the correct layer weight.

The resulting deposits and their layer weight reveal that the processing times used for experimentation were too high and needed to be decreased substantially. The final two columns of Table 12 draw a comparison between the achieved layer weight and the target set by the sponsoring company. The results also demonstrate that minor changes in processing parameters would have an insignificant effect on the deposited layer weight. For example, a decrease of 20 V in applied voltage from coil 4 to coil 6 would cause a decrease in layer weight but by only 0.0257 g. In this instance, layer weight would have to decrease by 170% to reach the target so a bigger change in processing parameters would have to be made.

(a)

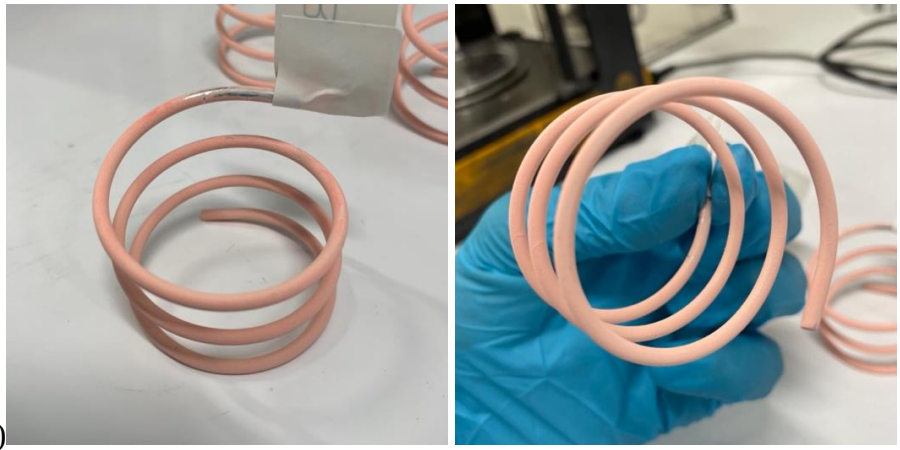

(b)


(c)

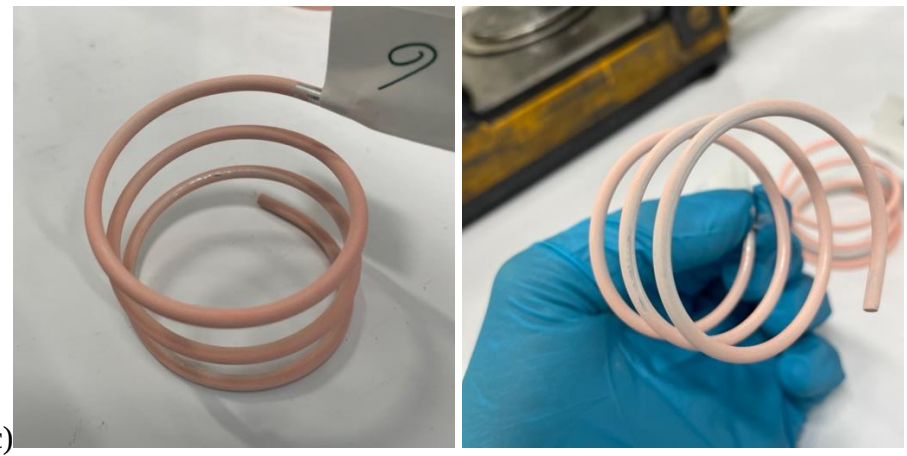


**Figure 27. Deposited layers of (a) coil 3, (b) coil 4 and (c) coil 6 from Table 12**

processing time and stirring also had a noticeable effect on deposition. An increase in processing time by 120 s from coil 2 to coil 3 caused the material deposit to increase by 0.082 g. This magnitude of change is the same as the target layer weight which would suggest a decrease by a similar amount is required to reach the target. An increase in stirrer rpm from 390 to 613 causes a decrease in layer weight by 0.0393 g. Stirring set too high will begin to affect the suspension of the particles and a less uniform layer will form as shown in Figure 27**c.** These images show that the layer begins to exhibit poor coverage on the interior and bottom

faces. The results achieved from altering the processing parameters suggest that: processing time needed to be decreased, stirring has an optimal rpm and noticeable changes to layer morphology would require a larger change in voltage.

Using the layer weight combined with the processing time, the rate of deposition in g/min can be established as shown in **Table** 13**.** The rate of deposition was calculated for a more justified adjustment to be made to processing time once an experiment had been attempted. From the rate of deposition, experiments that used different combinations of parameters could be compared against each other to understand what would increase the rate of particle migration to the substrate. As found in the literature (18), a higher rate of particle migration would encourage a less uniform deposit. From this, there was the understanding that an optimal value for the rate of deposition must be found. The rate of deposition was calculated using the following equation:

$$Rate\ of\ deposition\ (R) = \frac{layer\ weight(g)}{processing\ time\ (s)} * 60 \qquad \textbf{Equation 3}$$

**Table 13. Rate of deposition of phosphor through EPD experiments.**

| *Experiment number* | *Voltage (V)* | *Processing time (s)* | *Stirrer setting (rpm)* | *R (g/min)* |
|---|---|---|---|---|
| *1* | 180 | 233 | 390 | 0.0537 |
| *2* | 180 | 180 | 390 | 0.0559 |
| *3* | 180 | 300 | 390 | 0.0494 |
| *4* | 190 | 233 | 390 | 0.0549 |
| *5* | 170 | 233 | 390 | 0.0483 |
| *6* | 180 | 233 | 613 | 0.0436 |

The effect the parameters have on the rate of deposition can now be assessed more closely. The first observation to be made is how the rate of deposition changes over time. Each test exhibits a rate of deposition within a tight range, but a greater decrease comes with increased stirring and a voltage drop. Investigation into the effect of system resistance on the rate of deposition is carried out in the later stages of the thesis. The rate of deposition may now be used to correctly adjust processing time. With an average rate of deposition of 0.0524 at an rpm of 390, the target layer weight of 0.079 should theoretically be achieved at a processing time of 90 seconds. There are slight differences in voltage through these experiments, but this calculation gives a sensible range to now test the deposition of phosphors.

### 5.2.3. The effect of stirring on phosphor deposition

The particles used for this layer are heavier so tend to settle in the fluid if not correctly agitated. It was necessary to find the stirring conditions that would give the best particle suspension whilst also allowing for a uniformly deposited layer. **Chapter 4** demonstrated that baffles were beneficial to particle suspension. They allow for a higher magnitude of stirring without the formation of a vortex so were used throughout experiments for this layer. For these experiments, controlled parameters were set at 180 V and 85 s due to the calculation of appropriate stirring for this voltage. Experiments to assess the effect of stirring speed on phosphor trimix deposition were carried out and can be seen in Table 14.

Table 14. Results from experiments investigat**ing** the effect of stirring on deposition.

| *Experiment number* | *Stirrer setting (rpm)* | *Layer weight (g)* | *+/- (g)* | *R (g/min)* |
|---|---|---|---|---|
| *1* | 520 | 0.0671 | -0.0119 | 0.0474 |
| *2* | 427 | 0.0761 | -0.0029 | 0.0537 |
| *3* | 390 | 0.0871 | 0.0081 | 0.0592 |
| *4* | 315 | 0.0638 | -0.0152 | 0.0647 |
| *5* | 241 | 0.0917 | 0.0127 | 0.0615 |
| *6* | 148 | 0.0671 | -0.0119 | 0.045 |

This displays how the rate of deposition changes with increasing stir speed and is represented graphically in Figure 28.

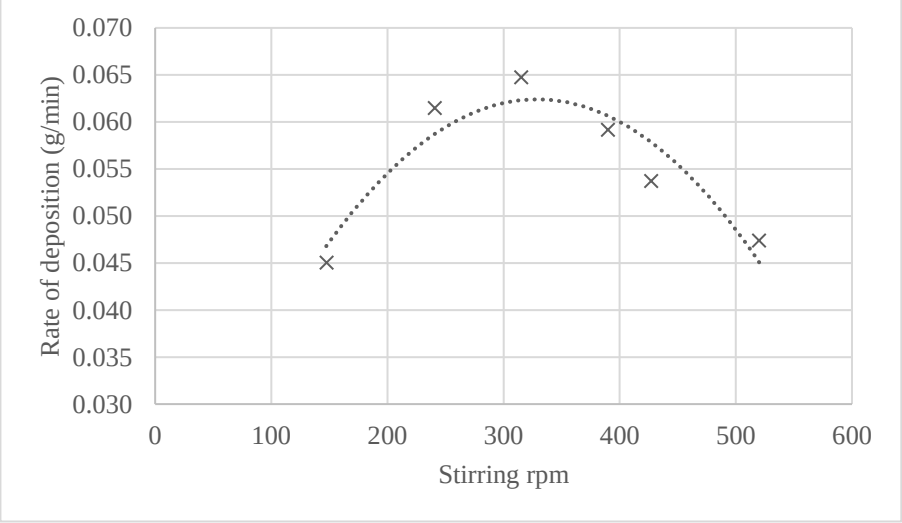


**Figure 28. Effect of stirring on the rate of deposition**

As the rpm of the stirrer increases there is a peak rate of deposition. It should also be added that the stirring speed heavily affects the layer uniformity. From the photos in Figure 29 stir

speeds at the extremities give a poor deposition. Although the rate of deposition is quite high when rpm is at 241 and 427, a favourable deposit would be observed in the 315-390 range. This process, due to the small volume, is overly sensitive to adjustments in stir speed as a subtle change from 241 to 390 improves a very inconsistent layer to a deposit with almost total coverage (Figure 29). With colloidal particles being heavier for phosphor experiments, the effect of stirring becomes more prevalent as the particles are quicker to settle. The effect of settling is shown in Figure 29, where stirring is too low, heavy particles settle on the top of the sample but not the underside. This is due to the lack of agitation at the bottom of the beaker leading to poor suspension. At higher rpm, the particles are better suspended and improve coverage of all faces of the sample. Baffles are used through all phosphor experiments as larger particles would not be suspended as well as the barium titanate. The optimised stir speed used in tandem with the baffles would allow for a deposit that reached all areas of the substrate.

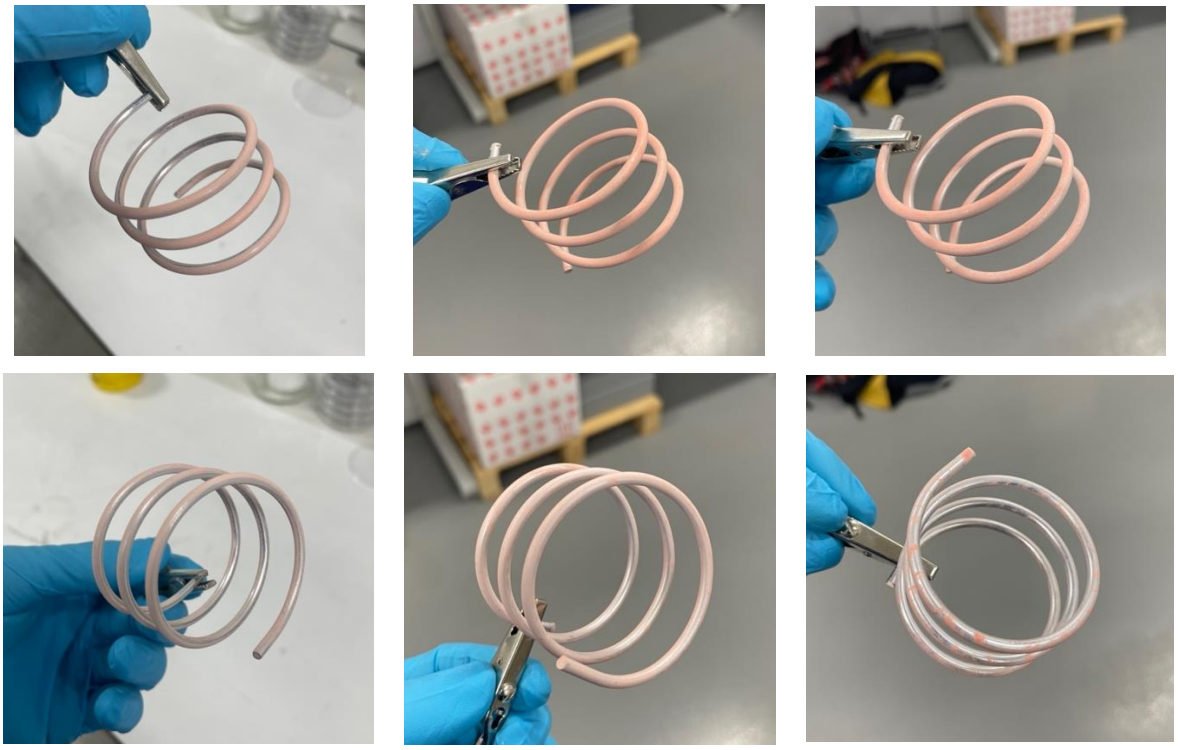

520 rpm 390 rpm 241 rpm

**Figure 29. Effect of stirring speed on layer deposit**

This set of experiments would display an optimal condition for stirring for this layer in the 315-390 range that gives good layer uniformity and rate of deposition. This condition was therefore set as a constant for the following experiments in this study.

### 5.2.4. Sieving of phosphors

Larger particles that are suspended in the bath used in electrophoretic deposition come with the risk of settling due to gravity. This gravitational mobility acts against the electrophoretic and may cause several results with the deposited material. Firstly, particles can settle on the top face of the substrate as seen in previous experiments. Electrophoretic deposition due to a settling suspension causes a gradient in the deposited material. In this instance, the layer thickness will be greater towards the bottom of the substrate as this is the direction the particles are moving. Aside from these two resulting deposits, particles may also settle at the bottom of the beaker and there is no material deposited. As established in previous experiments this can be solved by a combination of other parameters which each have to be optimised. The sponsoring company look to investigate the effect of sieving to lower the range of particle sizes in suspension whilst optimising the deposited layer. Particles that are all a similar PSD become more predictable as they will react in the same way to the EPD process and therefore make the formation of a monolayer a more feasible prospect.

Through literature, there is conflicting evidence on the topic of particle sizing as different processes and products require specific morphologies of a deposited layer. For example, Sato et al (72) discovered that smaller particles used in the EPD process (0.06 µm as opposed to 3 µm) would exhibit fewer cracks in the deposited layer during drying which is majorly important in most deposited layers. This evidence forms the theory that a deposited layer with smaller particles allows for stresses to be well distributed which prevents areas of localized stress and therefore crack formation. The requirement for a uniform, smooth deposit is seen across most literature and for this to occur, a wide range of PSD is preferred. As in (17,42), results have shown that larger particles assist in achieving a uniform deposit. In these studies, a higher volume of larger particles decreases the porosity in the deposited layer. This is due to smaller particles having the ability to fit between larger particles, filling the interstitial space more efficiently. With the requirement for a monolayer for the phosphor, sieving ensures that particles exhibit similar electrophoretic mobility when in an electric field allowing for easier optimisation of other parameters.

Sieving followed the process set out in **Section 3.5** with each phosphor being sieved separately. Particles in the range of 4-11 µm were collected after being cleaned and dried out so they may be used in experimentation. Due to their decrease in size and therefore mass, the sieved phosphor particles were now slightly better suspended in the solvent and gave a marginally improved deposited layer. The change to the sieved phosphors did not offer any noticeable improvements in adhesion as this was already a strength of the phosphor layer before sieving. A higher concentration of smaller particles also leads to lower processing times as their

electrophoretic mobility is much higher (5). The sponsoring company developed the theory that sieving the phosphors would increase the likeliness of a monolayer, but this was with the assumption all particles are perfectly spherical and of identical size. The theories developed by the sponsoring company would make an incorrect assumption that colloidal phosphor particles are somewhat spherical and similar in size. From this, it can be established that a uniform monolayer would become much more difficult to achieve in this application. Combining this with other challenges met throughout meant that the main objective of the research evolved to achieving total coverage (both inner and outer faces) of the substrate whilst maintaining the targeted layer weight.

### 5.2.5. Effect of applied voltage on deposition

Through literature (2,5,73) and previous experiments, it has been established that the electric field (V/cm) has a major effect on the deposited material. Applied voltage (V) is proportional to the strength of the electric field so can be incrementally altered to assess its effect on these experiments. Electric field strength was first demonstrated to change through the alteration of the counter electrode dimensions in **Section 4.4**. The changes made here from a two-electrode set-up proved that areas of weaker electrical field strength (perpendicular faces of the sample) have a lower mass of deposited material. The progression to a cylindrical counter electrode would now make the field strength equal around the outer face of the coil and therefore improve material deposit. Although layer uniformity can be heavily influenced by further optimisation of counter electrode design, the voltage should also be investigated.

In their study of the electrophoretic deposition of ZnS phosphors, Talbot et al (18) would suggest that maximising the applied voltage and therefore electrical field strength is not necessarily beneficial to the process. If the electrical field strength is too high, the rate of deposition increases to a point where the deposited layer is no longer uniform. For dense coatings, this would be preferable but not for the thin uniform coating which is the aim of this study. In contrast, too low an electric field strength will exhibit a much lower rate of deposition which requires an increase in processing time. Thus, Basu et al (73) found that electrophoretic deposition would achieve more uniform films at moderate applied fields (25-100 V/cm) as opposed to higher applied fields (>100 V/cm). Lower applied fields would simply not offer sufficient mobility, whilst higher fields do not allow for particles to find the optimal position to achieve a closely packed coating. This study looks to find a rapid and efficient process that will achieve a uniform deposited layer so an optimal V/cm for this process would have to be established through rigorous testing. The experiments will be carried out in a potentiostatic

fashion where voltage is also to be kept constant. This is due to the evidence that galvanostatic deposition (constant current) has difficulty in exercising a uniform deposit across a depositing cathode (74).

As to assess the effect of voltage on material deposit for the phosphor layer, a range of higher voltages was selected and tested for this layer. Experiments were carried out in the same fashion as previously shown in **Section 5.1.2** but with the wider counter electrode (95 mm) incorporated. Data was now also collected for conductance, pH and current through experiments. Conductance was measured in µS using a Fisherbrand Traceable Conductivity Meter Pen (product code: 11714226) and the current was displayed on the power source. Conductance and pH for the formulation used in experiments were constant at 6 µS and 5.5, respectively.

Initial experiments used results from the previous section to begin experimentation with the parameters shown in **Table** 15**.**

**Table 15. Primary EPD experiments of sieved phosphor trimix.**

| ***Experiment number*** | ***Voltage (V)*** | ***Processing time (s)*** | ***Layer weight (g)*** | ***+/- (g)*** | ***Phosphor concentration (g/L)*** |
|---|---|---|---|---|---|
| *1* | 180 | 105 | 0.0239 | -0.0551 | 4.5796 |
| *2* | 260 | 180 | 0.0881 | 0.0091 | 4.5557 |
| *3* | 260 | 175 | 0.1293 | 0.0503 | 4.4676 |
| *4* | 260 | 160 | 0.1148 | 0.0358 | 4.3383 |
| *5* | 260 | 140 | 0.1081 | 0.0291 | 4.2235 |
| *6* | 260 | 133 | 0.1146 | 0.0356 | 4.1154 |
| *7* | 280 | 130 | 0.1134 | 0.0344 | 4.0008 |
| *8* | 280 | 105 | 0.1001 | 0.0211 | 3.8874 |

As is shown in Table 15, phosphor concentration was now also tracked by the quantity of material deposited onto the sample. This is not exact due to some material being deposited onto the crocodile clips and possible loss through oven placement. The concentration was regularly replenished to 5 g/L, but this would prove to be another parameter that affects the deposition of material. This is covered later in the study.

The first observation to be made is the low deposit exhibited by the test on coil 1. The sieved phosphors react very differently to phosphors that are not sieved in the experiments in **5.1.2** and **5.1.3**. This is due to the particles being overall lighter in weight. Although the PSD is

decreased so that mobility is increased, the mass of deposited material takes more time or force to reach the same mass. This was reasoning for the initial increase to 260 V which would now increase the deposited layer weight by over 0.06 g. The comparison between these two experiments is shown in Figure 30.

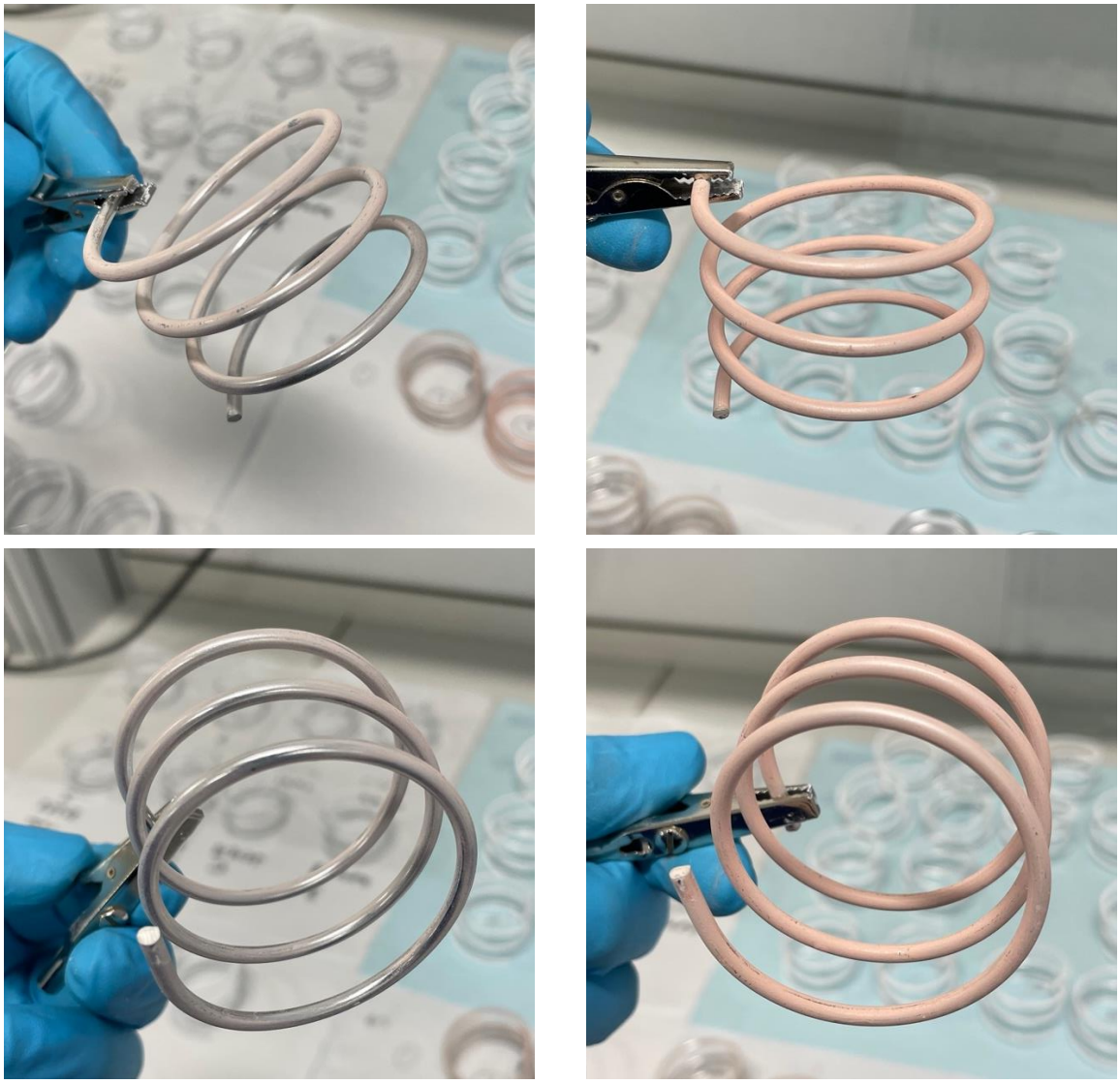

Coil 1 Coil 2

**Figure 30. Comparison between experiments at 180 V(1) and 260 V(2)**

These results demonstrate the effect of voltage on deposition. The following experiments aimed to repeat at different parameters to lower the layer weight to the target of 0.079 g. Coil 3 onwards demonstrated a sharp increase in the deposited layer weight with parameters being lowered which was unexpected for these experiments. Using the results in (42) there is the understanding that the conductivity of the bath will increase with every deposit due to an increasing ionic content. This combined with the knowledge that higher conductivity promotes

a higher throwing power can be the explanation for this increase in the deposited material. Throwing power is a measure of the ability of the suspension to coat a cathode of irregular dimensions (17) so an increase will improve the coating of the sample. The later experiments in this set show that there is an operational limit to the voltage of the system. Although this may be partly the result of a decreasing concentration, the is a truly modest increase in the deposited layer from coil 6 to coil 7. These experiments are also an example of the trade-off between voltage and processing time. A decrease in voltage and an increase in processing time (and vice versa) causes minimal change to the mass and morphology of material deposited.
As to assess voltages between 180 and 260 and bring the layer weight closer to the target, the experiments shown in **Table** 16 show the resulting figures when tested at 200-220 V.

**Table 16. EPD experiments of sieved phosphor trimix (lowered voltage).**

| ***Experiment number*** | ***Voltage (V)*** | ***Processing time (s)*** | ***Layer weight (g)*** | ***+/- (g)*** | ***Phosphor concentration (g/L)*** |
|---|---|---|---|---|---|
| *1* | 220 | 105 | 0.1446 | 0.0656 | 4.8613 |
| *2* | 200 | 126 | 0.1213 | 0.0423 | 4.7167 |
| *3* | 200 | 110 | 0.1099 | 0.0309 | 4.5954 |
| *4* | 200 | 115 | 0.1060 | 0.0270 | 4.4855 |
| *5* | 200 | 80 | 0.0931 | 0.0141 | 5.0000 |
| *6* | 200 | 80 | 0.0795 | 0.0005 | 4.9069 |
| *7* | 200 | 80 | 0.0856 | 0.0066 | 4.8274 |
| *8* | 200 | 80 | 0.0931 | 0.0141 | 4.7418 |

For the above experiments, EPD was carried out for coils 1-4 before the rate of deposition was assessed and used to calculate deposition time for the remaining experiments. It should be noted that before experiments on coils 5-8 deposited phosphor was accounted for and replenished. Using the average rate of deposition for coil 1-4 (0.0639 g/min), the processing time that would theoretically demonstrate the target layer weight was 74.17 s. To account for any losses and any error in measurements, the processing time was set at 80 s and results were documented. These results would allow for a near-optimal set of parameters to be reached. With much smaller adjustments that may need to be made in future studies. The resulting deposit from these parameters is shown in Figure 31**.** There is still room for improvement in this layer, but the deposit achieved demonstrated good adhesion and uniformity with reasonable coverage. With optimal results being achieved at a low processing time and low

voltage of 200 V, it is evident that a higher voltage does not have a major benefit for this application. As the layer weight and thickness are targeted to be lower than those seen across the literature, medium values for voltage and processing time are suited to these experiments.

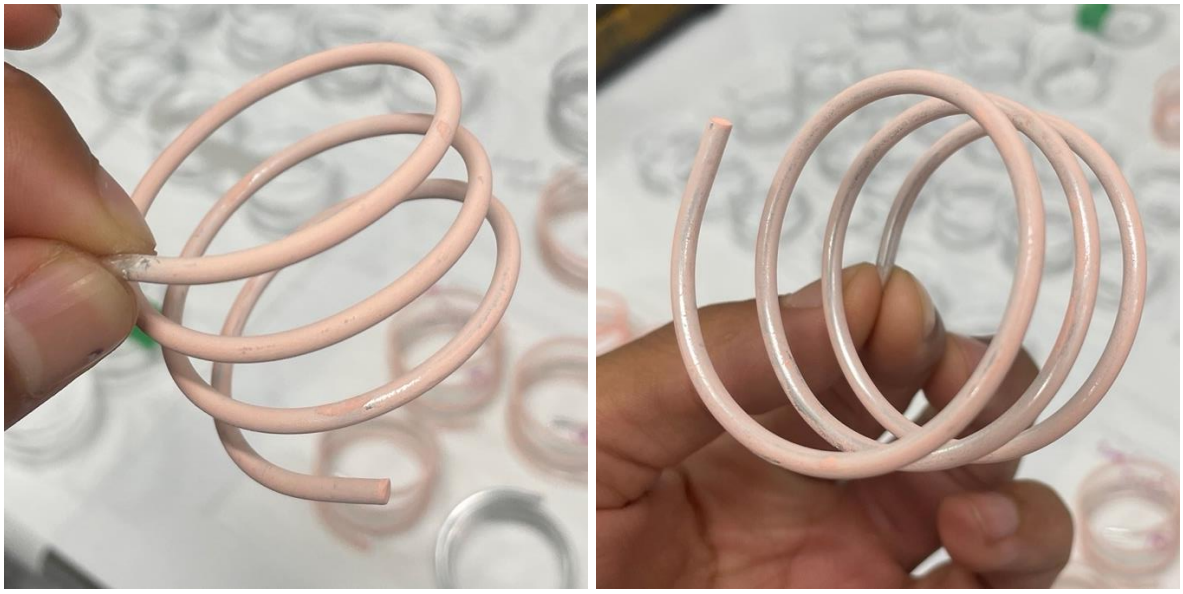

**Figure 31. Resulting deposit from optimal processing parameters**

To conclude this section **Table** 17 shows selected experiments through testing and their resulting rate of deposition.

**Table 17. Results showing the effect of voltage on the rate of deposition.**

| *Experiment number* | *Voltage (V)* | *Processing time (s)* | *Layer weight (g)* | *+/- (g)* | *R (g/min)* | *Phosphor concentration (g/L)* |
|---|---|---|---|---|---|---|
| *1* | 180 | 105 | 0.0239 | -0.0551 | 0.0137 | 4.6122 |
| *2* | 200 | 105 | 0.0654 | -0.0136 | 0.0374 | 3.7873 |
| *4* | 240 | 105 | 0.0787 | -0.0003 | 0.0450 | 3.7219 |
| *6* | 280 | 105 | 0.1001 | 0.0211 | 0.0572 | 3.8874 |

From this and the graphical representation in Figure 32**,** these results demonstrate both the importance of finding optimal voltage and how the rate of deposition changes through experiments. The results show that there is a positive correlation between voltage and rate of deposition.

As previously mentioned, there are areas in experimentation that can be affected by error (human and machine). For EPD, there is the issue of falling concentration with material deposit. In these experiments, material lost through deposition was replenished after each round

of experiments. The effect of concentration on deposition is more closely examined in **5.2.2.** As found in the literature, slight changes in the concentration of phosphor would not have a major effect on the adhesion (42) of the deposited layer but it does add an element of unpredictability to experiments. The constant changing of concentration means that, unless a small quantity is replenished after every experiment, it was hard to exactly replicate an experiment. With this, there is the issue of placement of the sample in the exact centre of the counter electrode. This is made difficult by the opacity of the suspension fluid and the clamp stand not being a fixed entity. Incorrect placement of the coil can lead to uneven electrical field strength around the sample leading to an uneven deposited layer. Methods to solve this are investigated in **Chapter 6**.

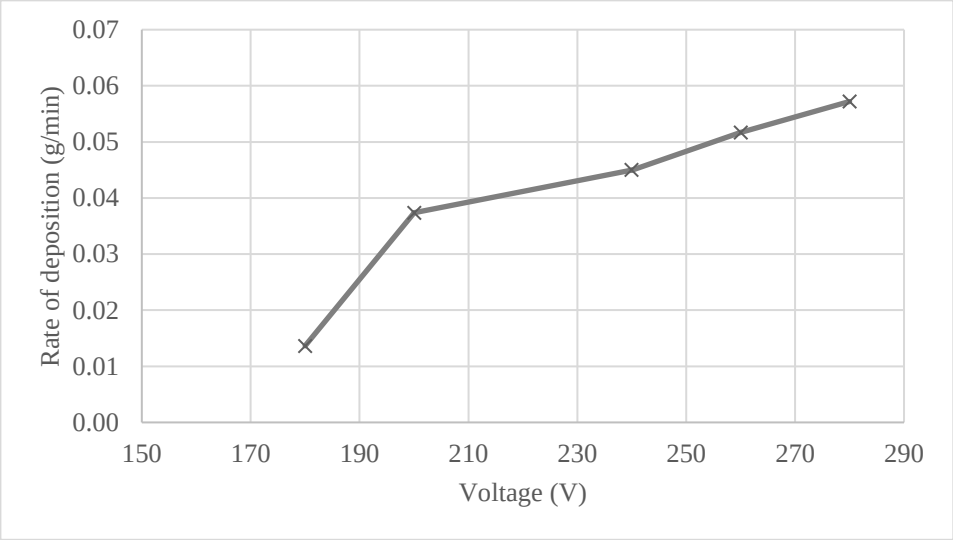


**Figure 32. Graphical representation of the effect of voltage on the rate of deposition**

### 5.3.Deposition of barium titanate layer

Both the electrophoretic deposition of barium titanate and its use as a dielectric material in ACEL devices are widely documented in the literature (3,7,50,55,66). For the dielectric layer, experiments were carried out with a similar procedure to that of the phosphor. A major difference between the two layers is the size of colloidal particles and therefore their zeta potential. The heavier nature of the phosphors and how this affects particle suspension is covered in **Section 5.1**. As the $BaTiO_3$ particles have a much lower mass and particle size, effective dispersion of particles is much easier. Investigation into the effect of concentration of material on mass deposit was necessary for this layer as the upper limit of the power source would not exhibit sufficient deposited material when compared to the target layer weight...

This will be the first layer of the final product, so deposited layers mustn't crack or rupture. Regular production techniques for ACEL devices such as screen printing, spray coating and spin coating come with a limitation on layer thickness. For example, screen printing carried out by Park et al (55) may only achieve a layer thickness of 20µm. The sponsoring company looks to build a dielectric layer with the highest capacitance possible, therefore decreasing the layer thickness to below 5µm. The benefit of electrophoretic deposition is its ability to deposit layers this thin and so the dielectric layer was set to a target layer weight of 0.1547 g. This was calculated by the sponsoring company to deposit 3.7 mg/cm$^2$ of material onto the samples. Tank formulation for dielectric experiments is shown in Table 18**.**

Table 18. Tank formulation for dielectric EPD

| ***Tank ingredient*** | ***Quantity*** |
|---|---|
| *Barium titanate ($BaTiO_3$)* | 3 g |
| *Ethanol* | 300 ml |
| *Acetyl acetone* | 300 ml |

For dielectric experiments, baffles would increase layer weight and rate of deposition but would not always be successful in improving layer uniformity. Because of this, experiments with and without baffles were carried out.

### 5.3.1. Effect of voltage on deposited material

Like phosphor testing, there was an element of experimentation that had to be carried out for optimal conditions for this layer. As this was a novel approach to electrophoretic deposition onto a 3D substrate, the effect of voltage on deposition was examined. From the literature, it is demonstrated that even vast changes in voltage in a system have an insignificant effect on the deposited mass of barium titanate (67). There is evidence of the changing voltage not having a considerable effect on the mass of the deposited layer, but it is demonstrated that layer weight has a positive correlation to processing time (7). Moreover, higher voltages will be detrimental to the layer uniformity of the deposit. To assess its reaction to the experimental design used in this study, a range of 180 – 330 V was tested with varying processing times. Using this data, a further parameter could be controlled in later experiments. The concentration for preliminary experiments was 5 g/L as this was the quantity suggested by the sponsoring company. The data for the range of tested voltages are shown in **Table** 19 alongside the deposited layer weight and the rate of deposition. Voltage would again be altered in **Section 5.2.2** where a range of concentrations is investigated.

**Table 19. Preliminary EPD experiments depositing barium titanate (formulation solid concentration of 5 g/L).**

| *Experiment number* | *Voltage (V)* | *Processing time (s)* | *Layer weight (g)* | *+/- (g)* | *Baffles (Y/N)* | *R (g/min)* | *Phosphor concentration (g/L)* |
|---|---|---|---|---|---|---|---|
| *1* | 200 | 120 | 0.0331 | -0.1216 | N | 0.0166 | 5.0000 |
| *2* | 200 | 120 | 0.02 | -0.1263 | N | 0.0142 | 4.96 |

| | | | | | | | |
|---|---|---|---|---|---|---|---|
| | | | 84 | | | | 69 |
| *3* | 200 | 240 | 0.042 | -0.1127 | N | 0.0105 | 4.9385 |
| *4* | 250 | 240 | 0.1122 | -0.0425 | Y | 0.0280 | 4.8233 |
| *5* | 260 | 240 | 0.0954 | -0.0593 | Y | 0.0238 | 4.7111 |
| *6* | 270 | 240 | 0.1001 | -0.0546 | Y | 0.0250 | 4.5145 |
| *7* | 300 | 240 | 0.1293 | -0.0254 | Y | 0.0323 | 4.8903 |

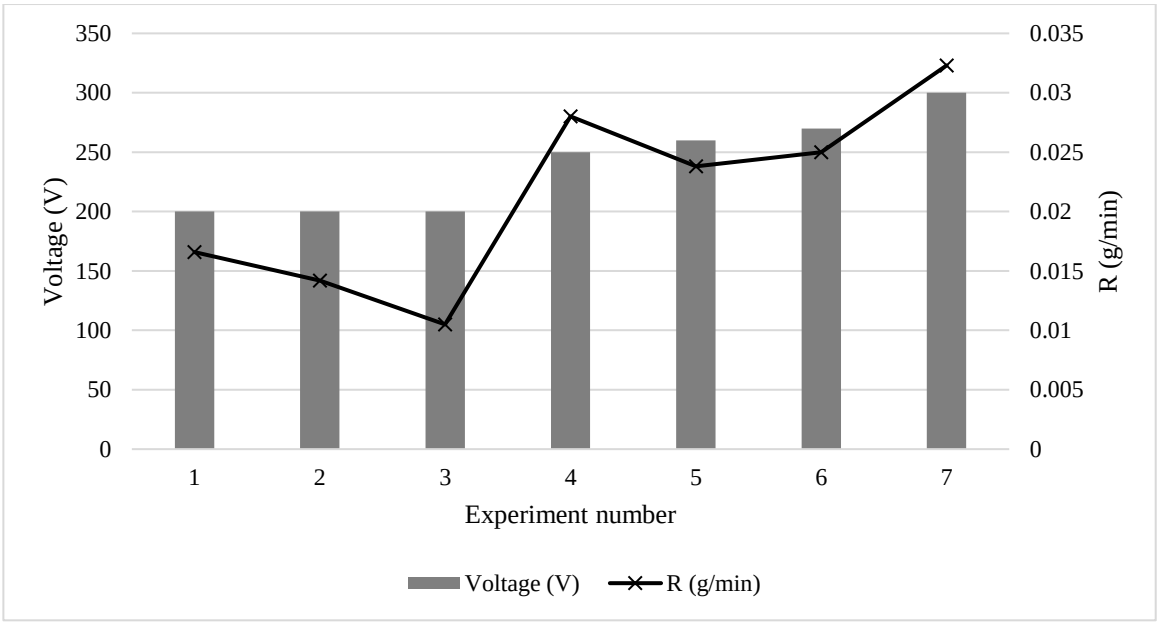


**Figure 33. The effect of applied voltage on the rate of deposition of barium titanate.**

As stated previously, there is a slight difference in the rate of deposition between experiments using baffles and those that did not. No combination of parameters in this set would suggest that 5 g/L would achieve a sufficient mass of deposited material unless processing time was increased. Some of the deposition tests were analysed under the 3D microscope to assess the coverage and uniformity of the deposited layer. Estimates of layer thickness on the top and side faces could be made through the use of the Alicona software. Microscopy images are shown in Figure 34. Images were taken at 10x magnification.

The deposits achieved from these tests were an early indication of how the process might be optimised. The images show that the target layer weight, thickness and total uniform coverage cannot be achieved simultaneously. Analysing with the naked eye and through the microscope revealed inconsistencies in layer thicknesses and gaps that were left in the deposit. In deposits with total and uniform coverage, layer weight was much higher than the target. The deposited layer of coil 1 is 0.1216 g below the target however the layer thickness is already measured at over 10 µm. This demonstrates the requirement for a wider range of higher accuracy analysis in place of the methods the sponsoring company suggested. Layer thickness would continue to increase with layer weight as is shown in the images of coil 6. Layer thickness is measured in a somewhat crude manner as it is over an exceedingly small area and along a single line, however, the deposit for coil 1 is relatively uniform. As expected from the literature, an increase in voltage hurts the layer uniformity as there is a difference in thickness between the outer face and the top face. The imagery of the top face of coil 6 also shows how layer thickness decreases towards the inner face of the coil where there is less material deposited. This is

something that was witnessed throughout phosphor experiments and suggested a need for better particle suspension.

| *Experiment number* | *Top face* | *Side face* |
|---|---|---|
| *1* | 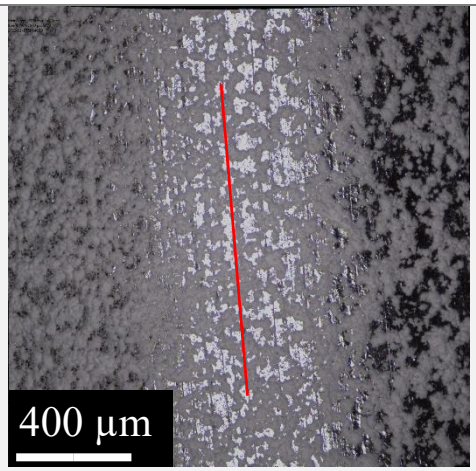 | 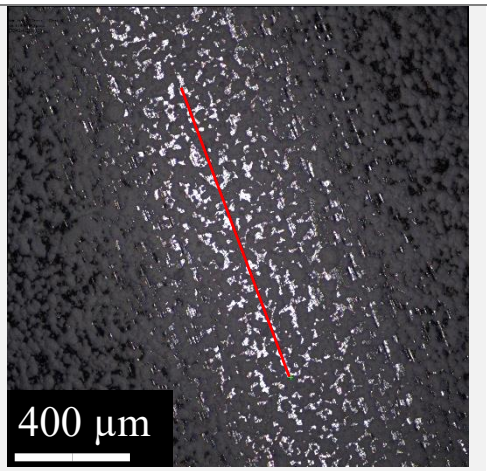 |
| *Layer thickness* | *10.2 µm* | *10.4 µm* |
| *6* | 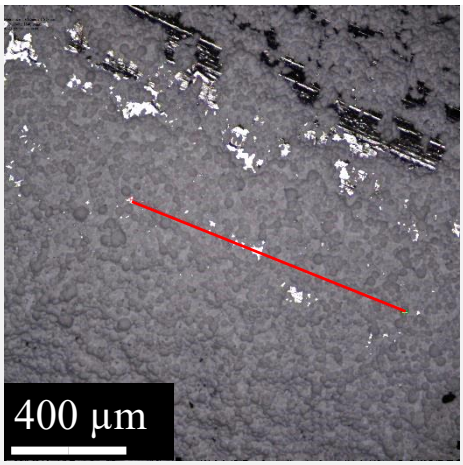 | 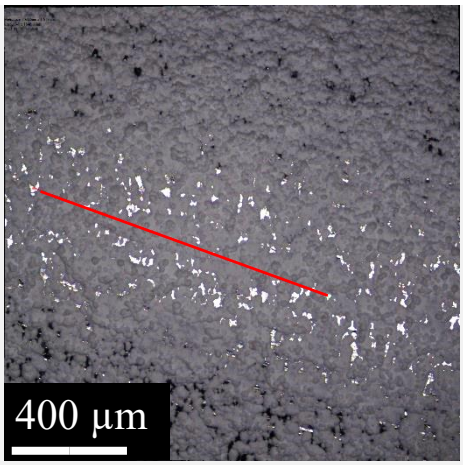 |
| *Layer thickness* | *37.5 µm* | *25.0 µm* |

**Figure 34. Alicona imagery of dielectric deposits**

As voltage cannot be raised much higher than 300 V for safety and limitations of the power source a different parameter is required to be elevated. The optimal voltage for a concentration of 5 g/L seems to be at 200 V due to the uniformity of deposited material but the spaces in the coat suggested that there needs to be a further increase in parameters or adjustments to tank ingredients. The follow-up for these experiments will be into the increase in material concentration so a greater material deposit can be achieved. Optimal voltage is a parameter that can change for different concentrations so a range of voltages will again be tested.

To summarise experiments on voltage and the preliminary experiments with 5 g/L particle concentration, voltage alone would not solve the issue of requiring a higher layer weight. The

concentration of 5 g/L was suited to the phosphor experiments as the target layer weight was almost half of the target for the dielectric layer. This along with the evidence through literature that concentration did not benefit the phosphor deposit (42) is the reason why the concentration was not sufficient for this material. The next section will discuss testing a range of concentrations to find optimal conditions for both sample coverage and conditions that will allow for target layer weight to be met in a decreased amount of time.

### 5.3.2. Effect of suspension solid concentration on the deposited layer

Prior results indicated a lower-than-required deposit thickness despite higher voltages being used. To improve this, the concentration of $BaTiO_3$ was investigated for its effect on coating weight. The concentration of 5 g/L was tested as this was the concentration used for the previous layer. The required layer weight for barium titanate is almost double that of the phosphor so it was therefore evident that a major change in some parameters was necessary. With efficiency in mind, processing time was required to stay as low as possible so doubling the processing time at the same concentration would not be a suitable solution for this issue.

Through literature, there is evidence of the benefit of increasing concentration to increase the mass of deposited barium titanate. Louh et al (66,67) experimented with barium titanate at concentrations starting at 33 g/L which is higher than the concentration used in this study for preliminary experiments. Here, specific film weight increases with increasing concentration. Further confirmation of this comes from (75) where it is stated that the volume fraction of solid majorly affects the deposited layer. At a low volume fraction of solid, particles deposit at a rate proportional to their electrophoretic mobility but a high volume fraction allows for particles to deposit at an equal rate. Using this information from the literature, a range of concentrations were selected and tested.

Bulk concentrations were set at 5, 20, 25 and 30 g/L. Like phosphor experiments, the concentration of the suspension decreased with every deposition as the material moved from suspension to deposit. To solve this, the material was readded to the solvents to replenish what was lost. This would be carried out when deposited material surpassed 15% of the originally added amount. The rate of deposition also decreases with decreasing concentration and so material concentration was regularly returned to the chosen bulk value. A decrease in the rate of deposition required an increase in processing time to achieve the same, or similar, layer weight. Experiments were carried out at each concentration with results collected and documented. A particle concentration of 5 g/L was the initial choice and experiments for this

are shown in the previous section**.** Figure 35 shows the resulting deposit that was constant across tests at 5 g/L.

**Figure 35. The deposited layer at 5 g/L**

Results from the experiments carried out at 5 g/L demonstrated that further experiments were not required at this concentration. The layer weight firstly was much lower than the target and total coverage of the coil was not achieved. Spaces in the deposit of the dielectric layer for an ACEL device would cause a decrease in efficiency so the higher concentrations were investigated. The following experiments were carried out to achieve a deposit that would exhibit total coverage of the sample but also good adhesion. Poor adhesion at the base level of this device would hinder the future layers making them much more delicate. The highest concentration tested was 30 g/L.

Experiments at this concentration all displayed a considerable increase in layer weight. The high concentration of well-suspended material also allowed for almost total coverage of the coils. The lighter weight of these colloidal particles would promote better suspension and therefore uniformity in the deposit. This combined with a now increased concentration increases layer weight considerably. The drawback of increasing concentration by this amount proved to be the uniformity and adhesion of the layer. Deposited layers are shown in Figure 36 with numerical results in Table 20**.**

**Figure 36. Deposited layer of barium titanate at 30 g/L (coil 1)**

**Table 20. EPD experiments depositing barium titanate (solid concentration in suspension raised to 30 g/L)**

| *Experiment number* | *Voltage (V)* | *Processing time (s)* | *Layer weight (g)* | *+/- (g)* | *R (g/min)* | *Suspension concentration (g/L)* |
|---|---|---|---|---|---|---|
| *1* | 300 | 160 | 0.9856 | 0.8309 | 0.3696 | 30.0000 |
| *2* | 300 | 90 | 0.2812 | 0.1265 | 0.1875 | 29.0144 |
| *3* | 300 | 125 | 0.4660 | 0.3113 | 0.2237 | 28.7332 |
| *4* | 300 | 65 | 0.3022 | 0.1475 | 0.2790 | 27.1600 |
| *5* | 330 | 70 | 0.3533 | 0.1986 | 0.3028 | 26.5802 |
| *6* | 330 | 70 | 0.4101 | 0.2554 | 0.3515 | 26.2269 |
| *7* | 330 | 70 | 0.3335 | 0.1788 | 0.2859 | 25.8168 |

As previously stated, the increase in concentration caused a definite increase in the mass of deposited material. This was anticipated through the result shown in the literature (66), but the resulting layer had some unexpected properties. Here it demonstrated that a high concentration only benefits the value for layer weight but has adverse results on layer uniformity. Through the pictures in Figure 36, it is visible the piles of material that begin to form on the top face and the protruding areas of deposit on the outer face. The high concentration does mostly solve the problem of coating the inner face of the coil. In comparison to the external faces, the inner has good uniformity. The shorter processing times with substantial amounts of material depositing rapidly do not allow for initial particles to develop a firm deposit to the cathode. This poor adhesion of the first layer of material causes a domino effect on the remaining material that is being deposited over time causing overall adhesion to be extremely poor. This

can be seen in Figure 36 where, with minimal force, the coatings on the substrate were prone to delamination.

This poor adhesion of the material was first addressed by employing a new additive to the formulation. Due to the insolubility of PVA, it was discarded from experiments. Attempts to dissolve the polymer in the formulation were made (**Appendix 7.4**) but any attempt made was unsuccessful. PVP was tested at small volumes to first analyse its solubility in the solvents. With the polymer readily dissolving in the formulation, it was added to suspensions at a concentration of 4 g/L and its results were assessed.

At an increased solid concentration of 30 g/L, there was the issue of material piling on the top surface of the coil. With concentration now being too high, particles would settle on the top face of the coil with all combinations of processing parameters. Baffles were also removed for some experiments with the theory that swirling would promote the wash-off of material. Even with these changes, particles would still form the piles shown in Figure 37**.** A decrease in voltage was also tested, but as earlier established, would have minimal effect on this material and piles would still form. Attempting to overcompensate other parameters to decrease the effect of piling would only negatively affect the deposition of material onto surrounding areas of the coil so suggested that this concentration was not suited to a substrate of these dimensions. This is shown in Figure 37 where in some deposits the only deposited material is on the top face of the coil.

Aside from the explanation of piling being due to a high concentration or settling, there is not yet a reason for this reaction to occur. Eventually, with a decrease in concentration, this would decrease to zero but is something that should be further investigated to gain a better understanding. The adhesion of material at this concentration was difficult to assess. Raw data from experiments at 30 g/L bulk concentration are shown in **Appendix 7.5.**

**Figure 37. Examples of dielectric deposits at 30 g/L bulk concentration**

**Table 21. EPD experiments depositing barium titanate (20 g/L bulk concentration).**

| *Experiment number* | *Voltage (V)* | *Processing time (s)* | *Layer weight (g)* | *+/- (g)* | *R (g/min)* | *Suspension concentration (g/L)* |
|---|---|---|---|---|---|---|
| *1* | 200 | 120 | 0.0450 | -0.1097 | 0.0225 | 20.0000 |
| *2* | 220 | 120 | 0.0549 | -0.0998 | 0.0275 | 19.9550 |
| *3* | 240 | 120 | 0.0346 | -0.1201 | 0.0173 | 19.9001 |
| *4* | 260 | 120 | 0.0485 | -0.1062 | 0.0243 | 19.8655 |
| *5* | 280 | 120 | 0.0414 | -0.1133 | 0.0207 | 19.8170 |
| *6* | 300 | 120 | 0.0423 | -0.1124 | 0.0212 | 19.7756 |
| *7* | 220 | 240 | 0.0772 | -0.0775 | 0.0193 | 19.7333 |
| *8* | 220 | 480 | 0.0725 | -0.0822 | 0.0091 | 19.6561 |

Experiments carried out at 20-25 g/L bulk concentration gave much improved results to those seen at 30 g/L with resulting layers weighing much closer to the target. The results from experiments at 20 g/L are shown in Table 21 with examples of layer uniformity shown in Figure 38.

**Figure 38. Dielectric layer deposited at 20 g/L bulk concentration.**

Results for this concentration were much more consistent in depositing a uniform and resilient coating. All deposits formed similar layers all within a tight range of layer weight. The results show that the deposit mass is too low but does suggest that the addition of PVP has improved the adhesion of the deposit. Material is no longer wiped or knocked off and can withstand some level of abrasive contact. Discovering that deposition at this bulk concentration dramatically decreases layer weight and removes the effect of piling suggests that a bulk concentration is marginally higher than necessary. Any concentration close to 30 g/L would give a deposit which exhibits piling so an optimal medium is required.

In an attempt to meet this optimal medium, the concentration of bulk concentration 25 g/L was investigated. Preliminary experiments at this concentration would exhibit small levels of piling but as concentration decreased with further tests, improved deposits were achieved. Figure 39 shows the layer deposited with parameters of 260 V and 45 s.

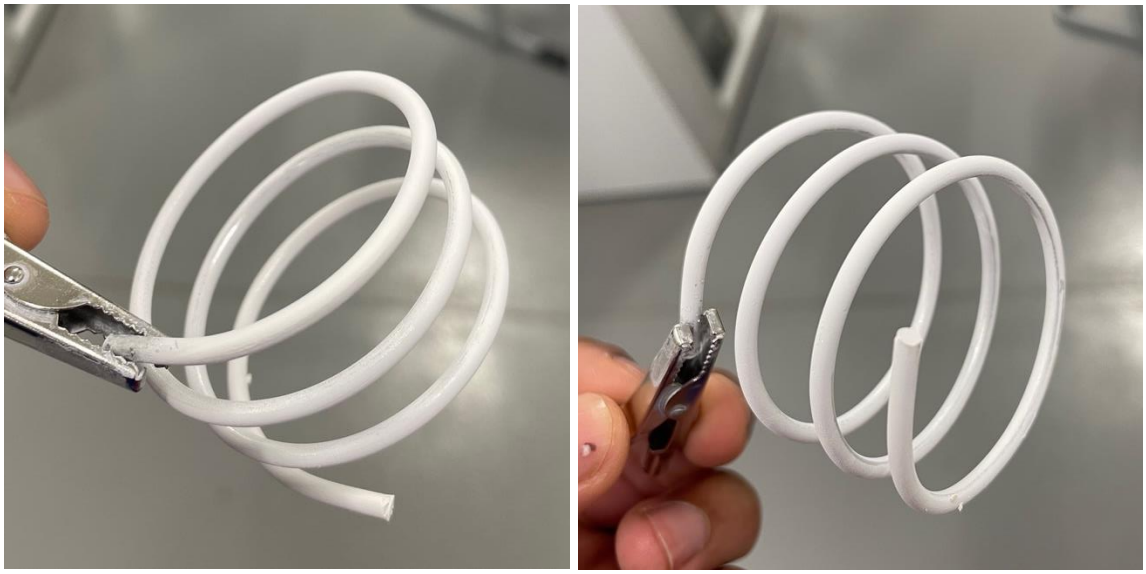

**Figure 39. Dielectric deposit at 25 g/L bulk concentration**

This deposit still exhibits some areas of the coil that are not as well deposited onto but overall gave a resilient coating with good coverage of the coil. As was found in the phosphor, counter electrodes not allowing for completely equal electric field strength do not allow for a completely uniform layer, but better particle suspension and a higher layer weight allow for a better coating to be deposited for this layer.

Along with the adjustment in bulk concentration, the influence of continuous changes to the formulation concentration should also be addressed. With every experiment that demonstrates a successful deposit, there is a slight decrease in the concentration of the system. This increases the difficulty of achieving repeatable experiments. Many distinct factors influence the material deposit and, even with constant processing parameters, there will be a difference in concentration, electrode spacing etc. In an attempt to solve this, barium titanate is replenished after a set of experiments, but it is difficult to measure this exactly. The deposition that is visible onto the crocodile clips that hold the sample in place makes it difficult to find the exact concentration within the beaker. This along with losses during the drying stage and general accidental contact will mean that a more general number of bulk concentrations is more suited to electrodeposition on this scale exhibiting several uncontrollable parameters. The effect of decreasing concentration through a set of experiments is visible in the graphical representation of results at 20 g/L (Figure 40**)**.

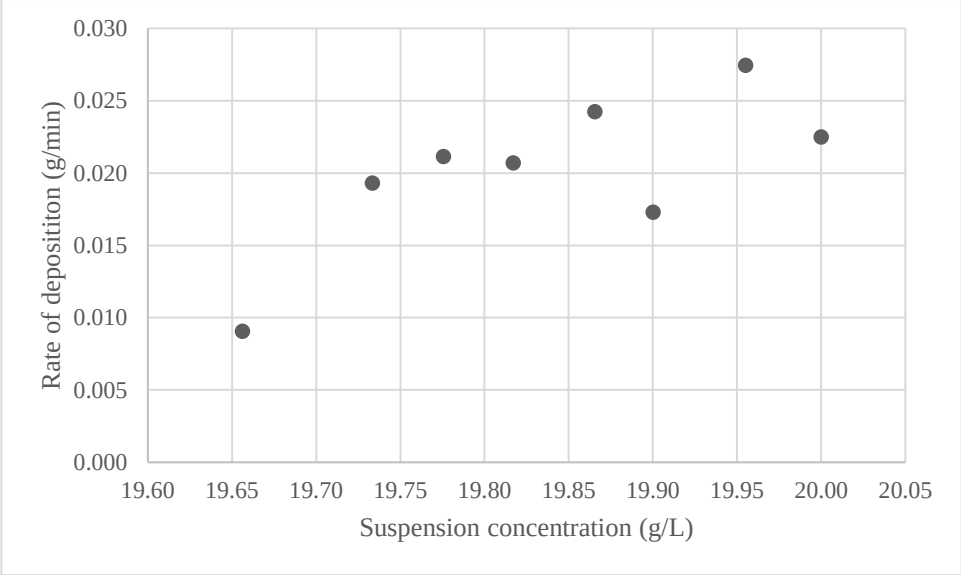


**Figure 40. The effect of dielectric concentration on the rate of deposition**

The graph shows that a continuous decrease in concentration also increases the rate of deposition. In some cases, this is not always detrimental to the results but makes results less repeatable. As shown by the bulk concentration values, a decrease eventually benefits the deposit, but an optimal set of parameters now becomes harder to achieve.

The decrease in the formulation concentration leads to an increase in system resistance due to the layer thickness of the deposit gradually increasing. This causes the rate of deposition to fall over time. This effect is more visible in the phosphor experiments where current drops through experiments, therefore, suggesting an increase in resistance (V=IR). For the dielectric experiments current remains constant suggesting that deposit resistance has less of an effect. The increase in resistance over time demonstrates that, eventually, there will be a stage where material ceases to deposit on the coil and the rate of deposition becomes zero. With this knowledge, it can be stated that with changing processing times it is unreliable to base corrected processing times on the rate of deposition. A decrease in processing time must account for the change in the rate of deposition. The rate of deposition may also be skewed by the onset of piling as this material is not depositing due to electrophoresis but due to gravity. The calculated layer weight is therefore not reflective of the process.

### 5.4.Deposition of encapsulating polymer

Originally, the aim set by Luxtec was for the layers of the emissive sources to be fabricated through electrophoretic deposition with this being a more efficient process of production. To meet this aim, a process for electrophoretic deposition of PMMA was established.

### 5.4.1. Anodic deposition of PMMA

This procedure would be different to the other layers as the material was dissolved in the solvent. This would mean that the need for stirring, and therefore baffles, was less as they were not required to suspend the polymer. Another difference would be in the deposited layer. For this layer, it would be completely invisible to the naked eye so adjustments to processing parameters would be based primarily on the layer weight. To assess the samples at a higher magnification, they would be analysed under the 3D microscope to understand the layer uniformity and coverage of material. This would reveal the requirements for alterations to the design of experiments.

The experimental setup for anodic deposition was identical to the cathodic experiments. The difference here is the electrode configuration with the sample not being connected to the positive terminal and the counter electrode connected to the negative. The formulation for the anodic deposition of PMMA is shown in Table 22. As covered in **Chapter 3**, the formulation must first be heated to 55ºC and cooled to room temperature before experimentation.

**Table 22. Formulation for anodic deposition of PMMA**

| ***Ingredient*** | ***Quantity*** |
|---|---|
| *Ethanol* | 510 ml |
| *Deionized Water* | 90 ml |
| *PMMA* | 2.4 g |
| *Sodium cholate hydrate* | 0.6 g |

Electrophoretic deposition was carried out at parameters suggested by the sponsoring company (**Section 3.3.2**) with slight adjustments made where necessary. The layer weight of 0.0038 g calculated by the sponsoring company reflected the required mass of deposit that would sufficiently coat the previous dielectric layer and fill any spaces that may have formed through the deposition. Experiments were first carried out on a bare aluminium coil to find optimal parameters and to test the validity of the research done by the sponsoring company. Prior to documented results, the necessity for new or cleaned crocodile clips between tests was identified. The results of the experimentation of this layer are shown in Table 23.

**Table 23. Anodic deposition of PMMA results**

| ***Experiment number*** | ***Voltage (V)*** | ***Processing time (s)*** | ***Layer weight (g)*** | ***+/- (g)*** | ***R (g/min)*** |
|---|---|---|---|---|---|

| | | | | | |
|---|---|---|---|---|---|
| *1* | 160 | 105 | 0.0032 | -0.0010 | 0.00182 |
| *2* | 160 | 135 | 0.0025 | -0.0010 | 0.00111 |
| *3* | 180 | 135 | 0.0039 | -0.0003 | 0.00173 |
| *4* | 160 | 30 | 0.0015 | -0.0023 | 0.00300 |
| *5* | 160 | 105 | 0.0033 | -0.0005 | 0.00188 |
| *6* | 160 | 105 | 0.0024 | -0.0014 | 0.00137 |
| *7* | 160 | 130 | 0.0036 | -0.0002 | 0.00166 |
| *8* | 160 | 140 | 0.0036 | -0.0002 | 0.00154 |

Through testing at a range of parameters, experiments eventually came to within a few percent of the target layer weight. This was done by utilising the rate of deposition to find optimal processing times at the listed voltages. The increase in voltage did offer an increase in the mass of deposit but an increase in processing time seemed to easier control the result. Through experiments, there was noticeable bubbling around the electrodes. In anodic deposition, material that is being deposited will contain negatively charged anions that react with positively charged hydrogen ions or protons. These are formed by the electrolysis of water (8). Assessing the deposit under the Alicona microscope would prove extremely important in understanding deposit composition. The photographs allowed for the layer to be seen in a way not possible with the naked eye. On the first evaluation, there seemed to be considerable spaces in an opaque deposit. This was a trend that was visible across all experimental results. Figure 41 displays the images collected from microscopy comparing the bare coil to the PMMA deposit. The areas of PMMA are darker in colour whilst holes where aluminium is visible are shiny.

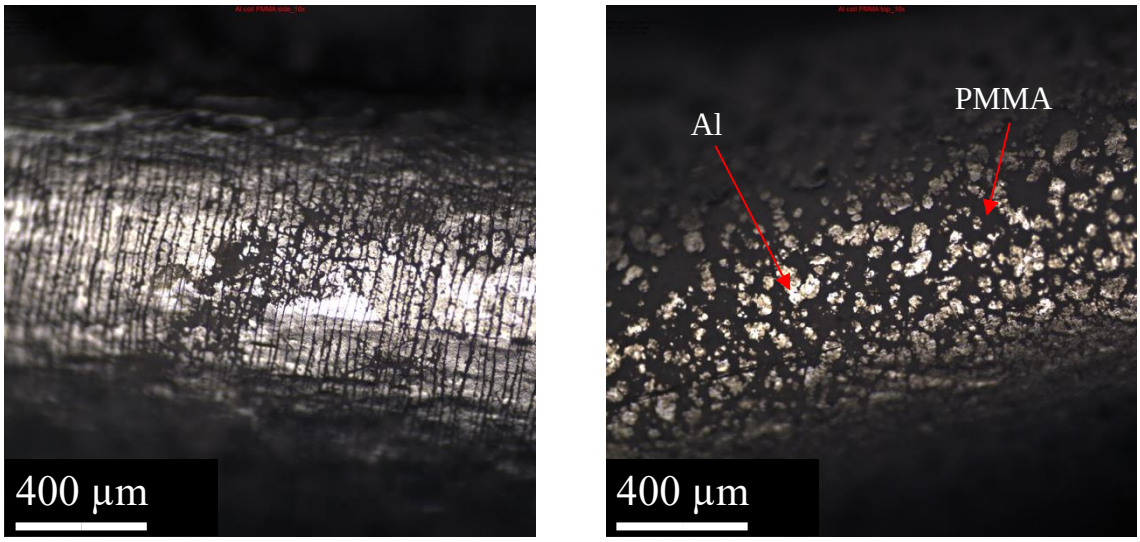


Bare aluminium sample PMMA coated sample

**Figure 41. Comparison of bare and PMMA-coated aluminium coils.**

Following these discoveries, in early tests for sequencing layers, it was found that anodic deposition would strip the previous layer deposited through cathodic deposition. This occurred due to the polarity difference in the particles which would now draw them to the counter electrode instead. Figure 42 shows a sequenced experiment before and after anodic deposition.

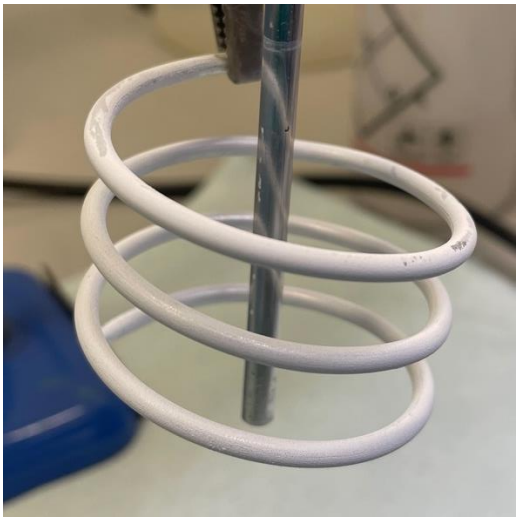

Sample before anodic deposition

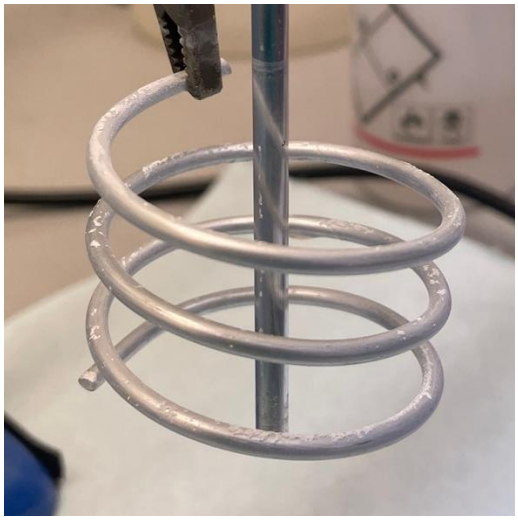

Sample post-anodic deposition

**Figure 42. Effect of subsequent anodic deposition on a deposited dielectric.**

Anodic deposition would therefore not assist in the build of these layers so was rejected from the study. Cathodic deposition of the PMMA was now attempted. with particles now exhibiting the same polarity there would not be the issue of material being stripped from the surface of the sample.

### 5.4.2. Evaluation of cathodic deposition of PMMA

The adjustment to cathodic deposition was made with the formulation shown in Table 24 for an operational volume of 500 ml. The concentration of each additive was suggested by the sponsoring company.

**Table 24. Formulation for cathodic deposition of PMMA**

| ***Ingredient*** | ***Quantity*** |
|---|---|
| *Deionized water* | 600 ml |
| *PMMA* | 2.4 g |
| *HTAB* | 10.932 g |
| *Sodium hydrogen phosphate* | 8.688 g |
| *Citric acid* | 5.763 |

The novel approach for deposition of the encapsulating layer now utilised insoluble PMMA particles with additives that would favour cathodic deposition. Sodium hydrogen phosphate was now added to improve electrophoretic mobility, hexadecyltrimethylammonium bromide (HTAB) to, in theory, increase zeta potential and ionic strength and citric acid to stabilise pH. Deionized water was originally the only liquid chosen for the suspension with small additions of ethanol to increase resistance. With conductivity now being too high, this eventually evolved into a total ethanol suspension. The key barrier to this approach was the high ionic conductivity of the solution that was brought about by the additives for increasing zeta potential, pH, and electrophoretic mobility. Conductance measurements for each of these additives are shown in Table 25.

**Table 25. Conductance readings for additives to formulation**

| | ***Conductance (µS)*** |
|---|---|
| ***Premix 1*** | - |
| *Ethanol (30 ml)* | 3 |
| *+ HTAB (1.822 g)* | 1960 |
| ***Premix 2*** | - |
| *Deionized water (20 ml)* | 3 |
| *+ Sodium hydrogen phosphate (0.724 g)* | *Error – value too high* |
| *+ Citric acid (0.48 g)* | *Error – value too high* |
| ***Premix 1 + premix 2*** | 4720 |

Due to the high ionic conductivity in the bath, the current limit was met instantly and the voltage only reached a maximum of 4 V. In an attempt to solve the issue of high current, the sodium hydrogen phosphate and citric acid quantities were first halved then totally removed with little-to-no improvement. The HTAB concentration was then lowered to 0.01 M but still gave a high conductance reading, an incredibly low voltage of 6 V and a maximum current limit reached. With the lowered quantities, the coated samples which have a now higher system resistance were tested to see if a more beneficial result was achieved. These tests were unsuccessful with the ethanol and water readily dissolving the PVP in the barium titanate layer and stripping the substrate of the deposited material. The unsuccessful results of electrophoretic deposition of the PMMA layer forced a shift in research from this electrophoretic deposition off PMMA to deposition through dip coating.

### 5.4.3. Dip coating of PMMA

Through literature research (76), sensible parameters for a dip coating process could be established and tested for the PMMA layer. A level of experimentation was carried out to understand how well the material would deposit and to find optimal parameters for the process. These parameters would then be carried forward to be tested on coils coated in barium titanate. As to not waste coils with higher quality deposits, glass slides were used for preliminary tests of the dip coating process. The solution for experiments consisted of 4 g of PMMA dispersed in 200 ml of acetone along with a small amount of crystal violet dye. Acetone was used for experiments due to its ability to readily dissolve PMMA and not PVP as seen with ethanol/water. The target weight for this layer was 0.0042g. Dye would help visualise deposition and allow for the coating to be readily evaluated by eye for consistency and density. The substrate would then be mounted into a Hounsfield Tensile tester (Figure 43**)** and lowered into the solution at a speed of 150 mm/min.

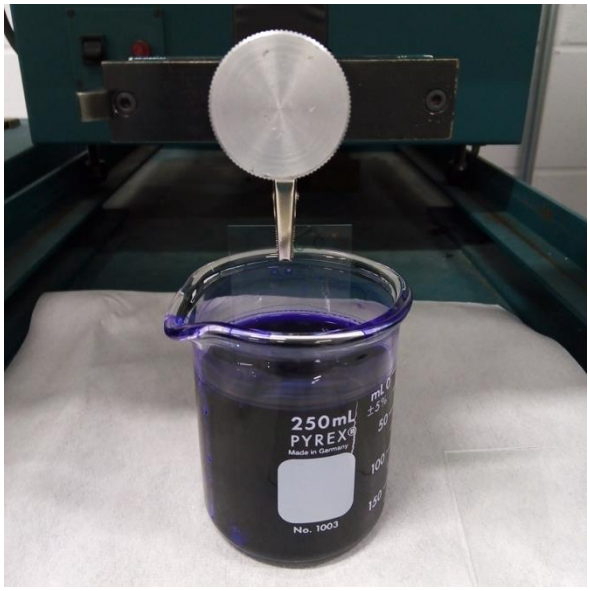


**Figure 43. Experimental set-up for dip coating**

**Table 26. Withdrawal speeds tested for dip coating to prove optimal conditions.**

***Sample withdrawal speed***

| ***mm/s*** | **mm/min** |
|---|---|
| *1* | 60 |
| *2* | 120 |
| *4* | 240 |
| *6* | 360 |
| *10* | 600 |

Once fully submerged the substrate was immediately removed at a controlled speed. It is documented through literature that an increase in withdrawal speed increases deposit thickness (76), so this is assessed here. The speeds at which the substrate (in this case glass slides) is withdrawn are shown in Table 26 and Figure 44 shows the resulting deposits.

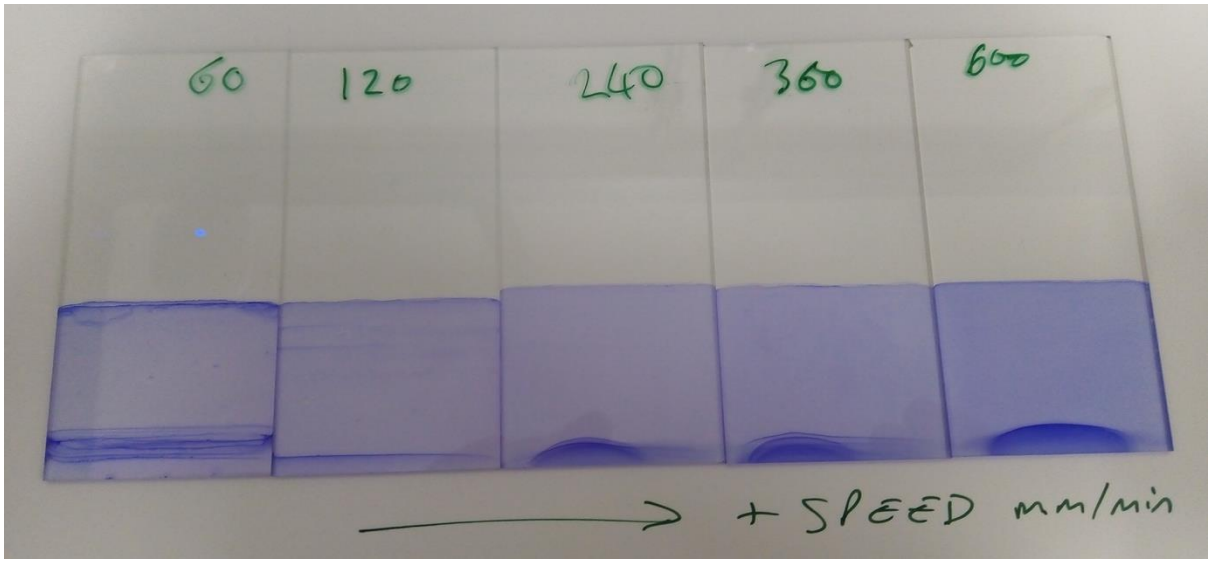


**Figure 44. Resulting deposits from stir speeds in Table 26.**

Through visual examination, consistency and amount of coverage of the slides improved with an increase in removal speed. On initial visual assessment, the process produced a consistent and tough coating that would dry quickly in ambient conditions due to the volatility of the solvent. Speeds higher than 600 mm/min gave indistinguishable results so the optimal removal speed was found to be 600 mm/min. The tester could not reach speeds above this due to mechanical limits and safety. Figure 45 shows the effect of repeating the dip coat 3 times and how the layer is denser. This set of results would verify the necessary parameters and standard of procedure that should be used for coils coated in barium titanate.

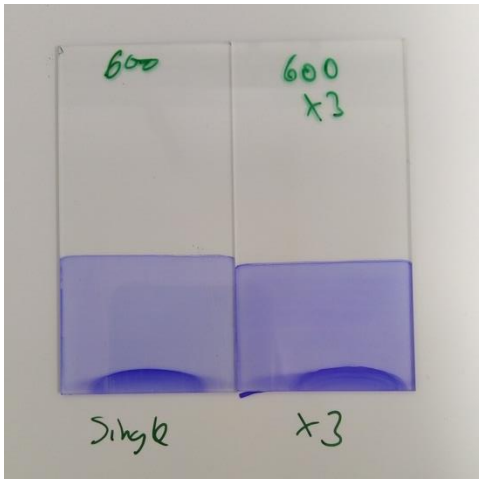


**Figure 45. Resulting deposit of multiple dip coats**

### 5.5.Sequencing of dielectric, encapsulating polymer and phosphor layer.

Documented well throughout this study, this project aims to establish a layer-by-layer deposition process to fabricate emissive sources for an ACEL device. Once extensive testing on each layer was carried out, the focus could be moved on to the sequenced deposition of these layers to build the emissive source. Optimal figures for each layer were met to within a few percent of the targets so the next stages could commence. There was the expectation that sequenced layers would react to the process differently as there is now a different surface to deposit onto. An important property of a well-functioning ACEL device is the smoothness of the layers, so deposits were assessed and chosen to be taken forward for sequenced deposition. The sequence was carried out as follows: dielectric, PMMA, and phosphor.

#### 5.5.1. Dielectric-PMMA sequenced deposition.

As established in **Section 5.3**, a process for dip coating PMMA had been formed and now could be used on coils coated in barium titanate. 600 mm/min was the removal speed that gave the best coverage of the substrate, so this was again used for the coils. Like the tests on the glass slides, the dye was used for a pilot test on a barium titanate-coated coil to again visualise the deposited layer and assess its coverage. Layer weight was not measured for the pilot. Figure 46 displays the results of this test.


**Figure 46. Resulting deposit of pilot dip coating test onto dielectric.**

The PMMA/dye coating was evident (from the purple colouring) throughout the entirety of the coil. Some areas of the coil displayed a slightly heavier coating, but this was down to localised thicker coating deposited in the barium titanate layer. The effect of 'piling' would now cause a larger deposit of PMMA in that area. After the dip coating with the dyed solution had shown some success, a new solution was made up without the dye and used to dip coat other barium titanate-coated coils. Testing was now performed gravimetrically with layer weight being recorded similarly to the other layers. Again, using the removal speed of 600 mm/min, several substrates were tested, and the results were recorded (Table 27).

**Table** 27**. Dielectric-PMMA sequencing results**

| ***Experiment*** | ***Removal time (mm/min)*** | ***Layer weight (g)*** | ***+/- (g)*** |
|---|---|---|---|
| ***1*** | 600 | 0.0036 | -0.0006 |
| ***3*** | 600 | 0.0037 | -0.0005 |
| ***4*** | 600 | 0.0024 | -0.0018 |
| ***5*** | 600 | 0.0030 | -0.0012 |
| *6* | 600 | 0.0020 | -0.0022 |
| *7* | 600 | 0.0019 | -0.0023 |
| *8* | 600 | 0.0043 | 0.0001 |
| *9* | 600 | 0.0031 | -0.0011 |

Coils used for dip coating were selected by both their proximity to the target layer weight and an evaluation by eye on the uniformity of the deposit. The target for this layer is small and may need to be adjusted as the processing technique has changed. A larger layer weight would allow for a more viscous solution for dip coating which in turn ensures that a more film-like layer

can be deposited. With the knowledge that the selected removal speed would give the largest amount of deposited material with good coverage, it was the only parameter tested. The substrates all had different morphologies of the previous deposit so would not react to the dip coating process in the same way with every test.

**Figure 47. Material stripped through dip coating due to piling.**

As found with the pilot study for dip coating, piling of material harmed the PMMA layer. An example of this is shown in Figure 47 where the material is stripped from the surface of the substrate due to its poor adhesion. This would then render the coil useless for further layers with such a large space in the dielectric layer. With substrates that exhibited deposition of barium titanate with total coverage and good adhesion, there was a further improvement in the adhesion of the layer. Material that would previously be knocked off or wiped from the surface by hand would have to be removed with sandpaper or something similar. This suggests that the PMMA dip coat was successful and beneficial.

These results show that dip coating is a preferable alternative to electrophoretic deposition and makes the deposition of PMMA much simpler and more efficient. Dip coats could be carried out in seconds and the drying process was much quicker due to the volatility of the acetone.

### 5.5.2. Dielectric-PMMA-Phosphor sequenced deposition

The next stage of experimentation was to combine the researched layers and sequence the emissive phosphor layer atop the barium titanate and PMMA. It was expected that the added layers between the substrate and the phosphor would exhibit an increase in system resistance. An increase in system resistance was demonstrated during experiments of the individual layers,

the difference here is that system resistance begins greater than what it would with bare samples. To assess this for the phosphor layer, the preliminary test was carried out at previous parameters of 75 s processing time, 2.8 stirrer setting at 200 V applied voltage. The resulting current through this experiment is compared to previous depositions of just the phosphor in Table 28 and Figure 48.

**Table 28. Phosphor and sequenced deposition tests**

| *Experiment number* | *Voltage (V)* | *Processing time (s)* | *Layer weight (g)* | *+/- (g)* | *R (g/min)* |
|---|---|---|---|---|---|
| *1* | 200 | 75 | 0.0849 | 0.0059 | 0.0679 |
| *2* | 200 | 75 | 0.1138 | 0.0348 | 0.0910 |
| *3* | 200 | 75 | 0.0941 | 0.0151 | 0.0753 |
| *4* | 200 | 75 | 0.1061 | 0.0271 | 0.0849 |
| *Sequenced* | 200 | 80 | 0.1003 | 0.0213 | 0.0752 |

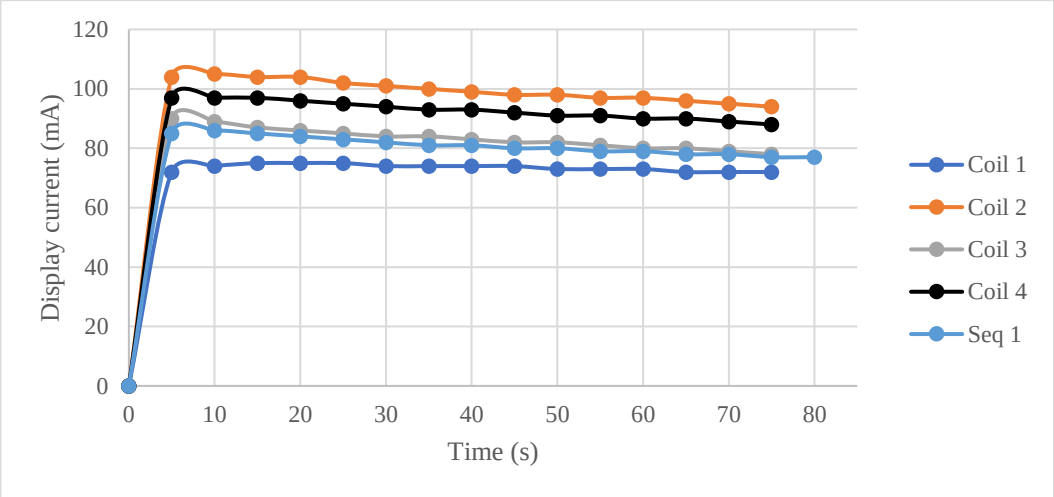


**Figure 48. Graphical representation of current transient through experiments**

Here, there is a marginal decrease in current but a layer weight that is in a similar range. Through literature (18,20,42), it is demonstrated that the current transient through the deposition of phosphors follows a similar trend of an initial spike followed by a gradual decrease in current over time. This can be attributed to the increase in deposit thickness and therefore resistance as the deposit has a much higher electrical resistance than the suspension (13). Photos of this sequenced coil are shown in Figure 49. Imagery shows that the phosphor will still deposit well atop the previous layers but there are spaces where the dielectric layer can be seen through. There is also still the preference for a deposit on the outer face with the thickness of the deposit decreasing towards the inner face of the coil.

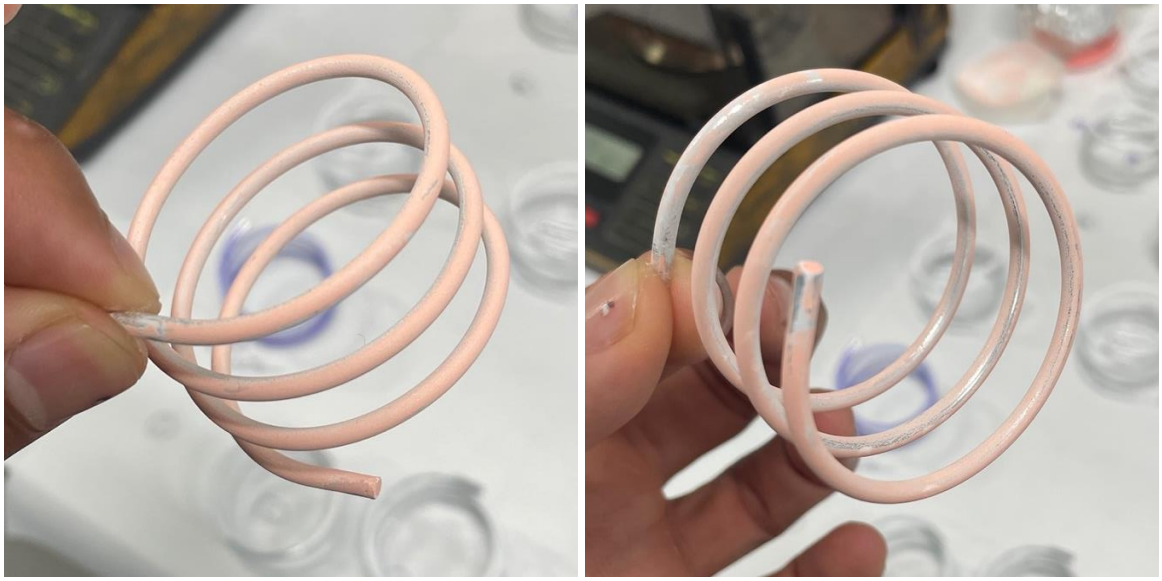

**Figure 49. Results of first dielectric-polymer-phosphor EPD**

From Figure 49**,** there is proof that the inner face has poor uniformity of phosphor whilst the outer face is an almost uniform deposit. The recurring evidence of poor coverage on the inside face of the coil proves there is room for improvement in the processing parameters and experimental setup. A lack of uniformity of electric field is highlighted further for this deposit as system resistance is increased. The low field strength inner faces would experience in the individual layer deposits is now even lower, so less material is deposited. Using the result for layer weight and the photos of the sequenced coil, the deposit is not very uniform with more material being deposited on the outermost face. The adhesion of the sequenced phosphor layer was like that of the deposit on the bare coil. With significant force and wiping, the material could be removed but material would not be lost to touch. Following the success of the initial sequencing test, further experiments were carried out as can be seen in Table 29.

Table 29**. Sequenced EPD results**

| ***Experiment number*** | ***Voltage (V)*** | ***Processing time (s)*** | ***Layer weight (g)*** | ***+/- (g)*** | ***R (g/min)*** |
|---|---|---|---|---|---|
| *1* | 200 | 120 | 0.0503 | -0.0287 | 0.0252 |
| *2* | 200 | 120 | 0.0541 | -0.0249 | 0.0271 |
| *3* | 200 | 120 | 0.0993 | 0.0203 | 0.0497 |
| *4* | 200 | 120 | 0.0351 | -0.0439 | 0.0211 |
| *5* | 200 | 120 | 0.0353 | -0.0437 | 0.0176 |
| *6* | 200 | 120 | 0.0334 | -0.0456 | 0.0167 |

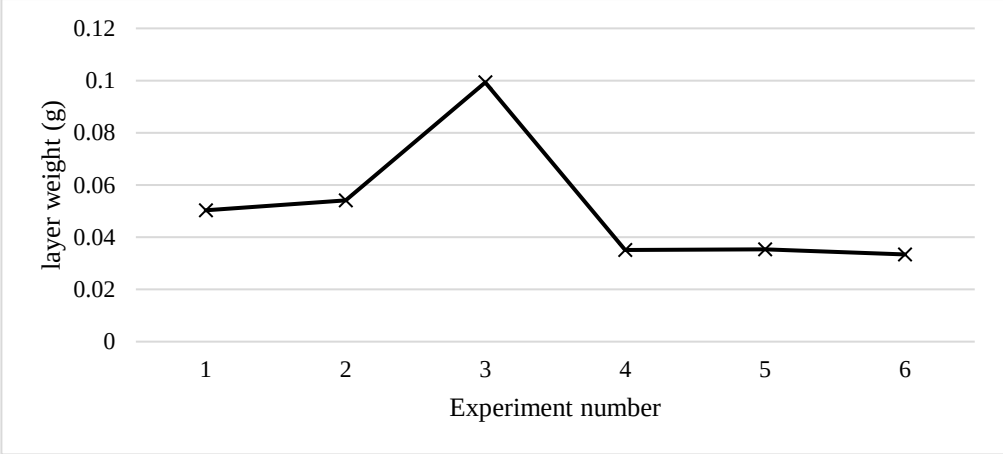


**Figure 50. Layer weight through sequenced EPD experimentation.**

The results from these tests exhibited a range of results and their reaction to the process can be characterized by the morphology of the previously deposited layers. Table 30 shows the layer weights of previous layers for each of these experiments.

**Table 30. Individual layer weights of experimented coils**

| *Experiment number* | *$BaTiO_3$ layer weight (g)* | *PMMA layer weight (g)* | *Phosphor layer weight (g)* |
|---|---|---|---|
| *1* | 0.2507 | 0.0037 | 0.0503 |
| *2* | 0.0725 | 0.0030 | 0.0541 |
| *3* | 0.1676 | 0.0020 | 0.0993 |
| *4* | 0.0485 | 0.0043 | 0.0351 |
| *5* | 0.0346 | 0.0031 | 0.0353 |
| *6* | 0.1200 | 0.0021 | 0.0334 |

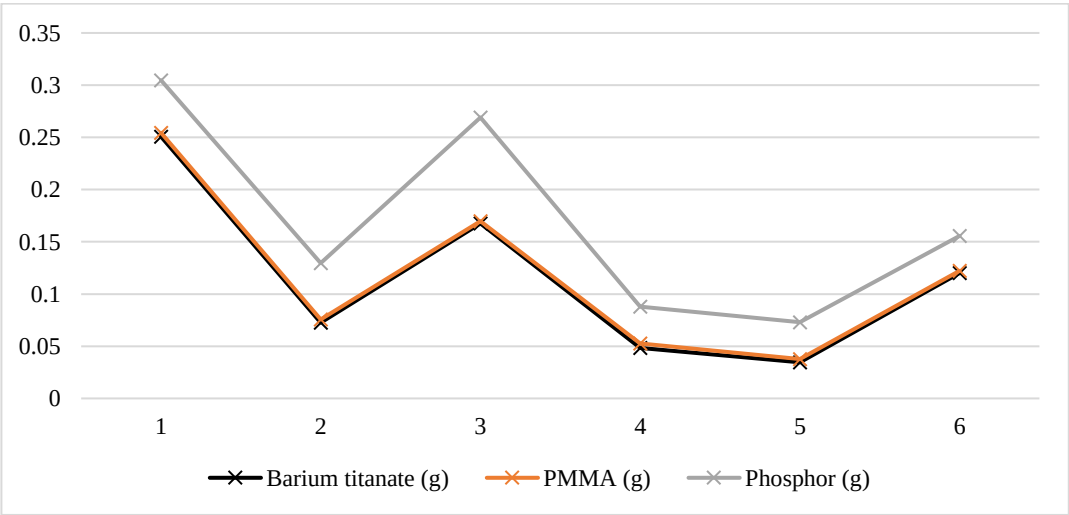


**Figure 51. Sequenced deposition of dielectric, polymer, and phosphor layers.**

This table is a good example of the effect of material deposit on sequencing and quality of the deposit. The uniformity of some of the deposits is shown in Figure 52. These can be paired with the individual layer weights to understand and explain morphology.

There are a few observations to be made from the documented data and photos. Firstly, coil 1 has a higher mass of deposited dielectric and a medium level of PMMA. From the photos, it is evident that the deposit shown is mostly due to gravity as there is no coating on the underside of the sample. This would suggest that electrophoretic mobility is decreased, and particles are instead mobilised by gravity. This is justified by the increased system resistance due to the thickness of the previous deposit showing that both an improvement in particle suspension and an increase in electric field strength are required.

**(a)**

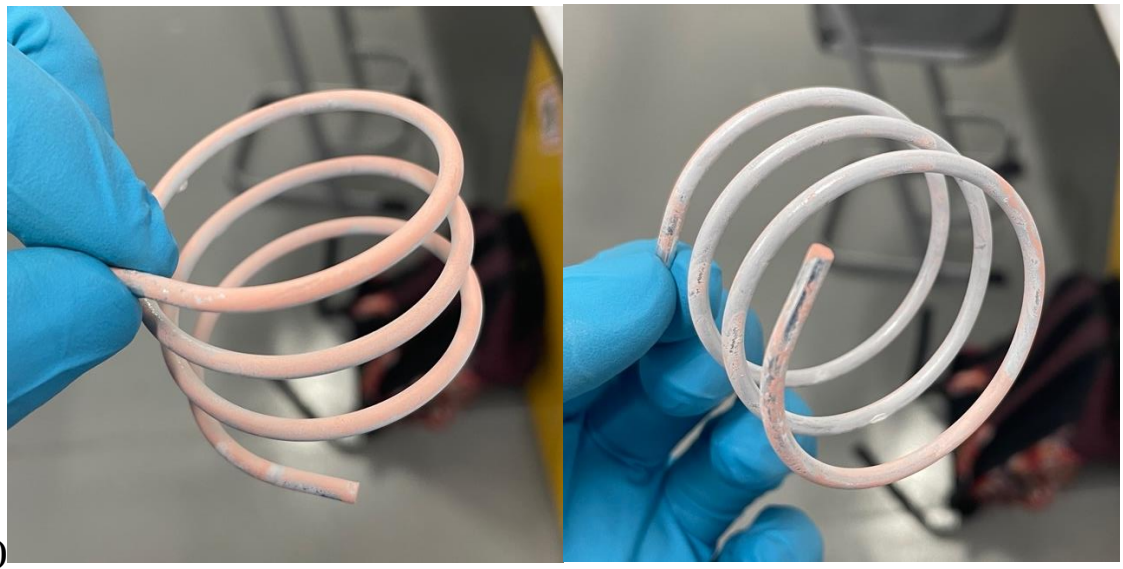

**(b)**

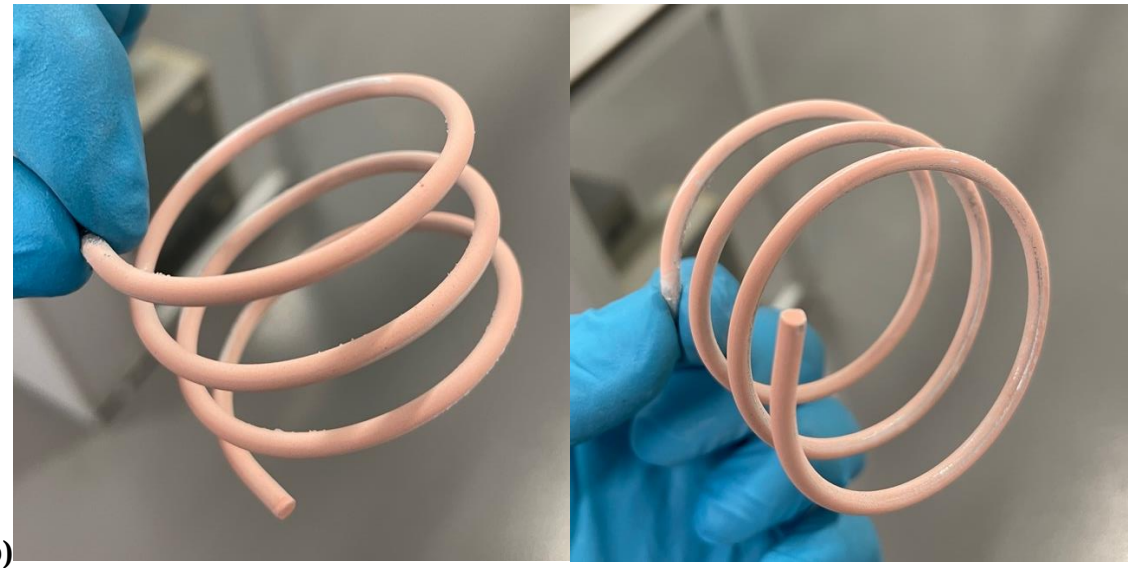

**(c)**

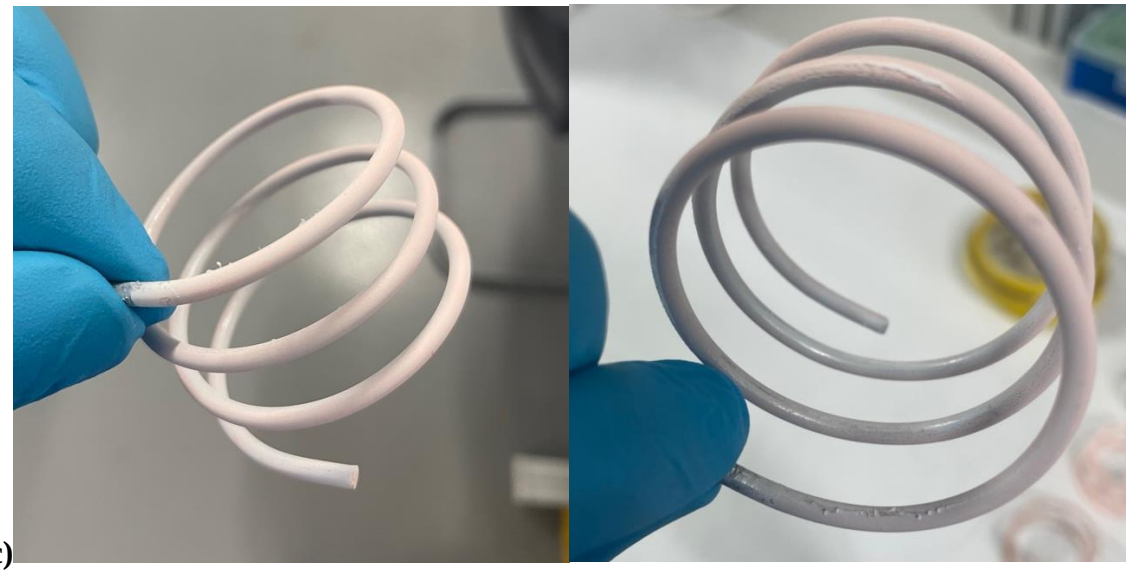

**Figure 52. Sequenced deposits of (a) coil 2, (b) coil 3 and (c) coil 4**

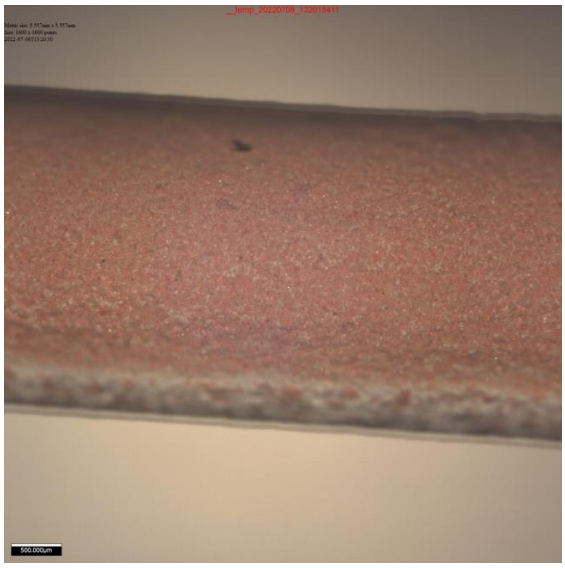

Outside face

Inner face

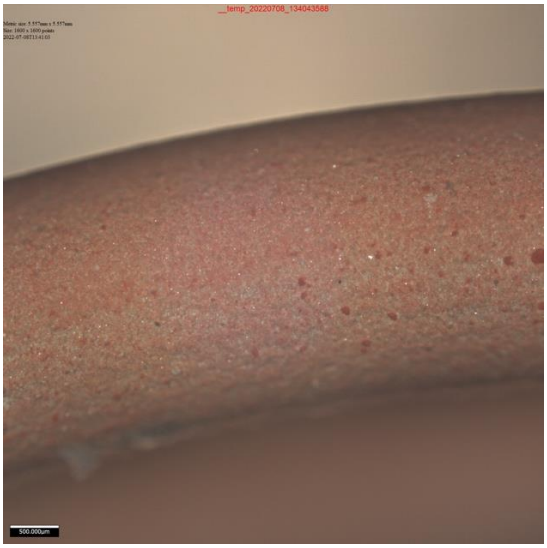

Top face

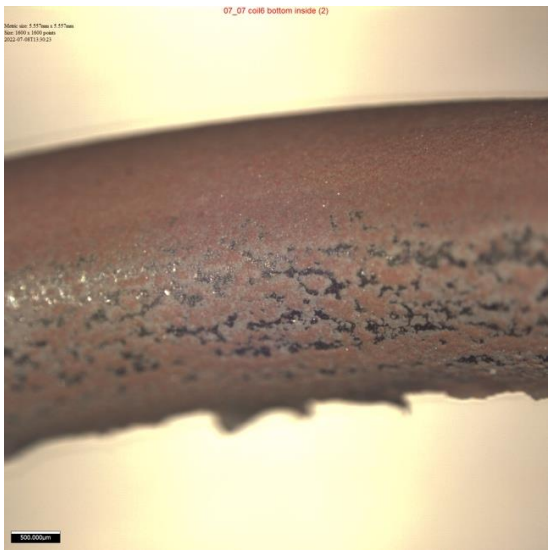

Bottom face

**Figure 53. Microscopy images of coil 3**

The inconsistency in layer thickness is revealed for coil 3. Here, the areas of the sample with a greater thickness have no deposit but the remainder of the surface is well coated. From this test, it is evident that inconsistency in the deposited layer gives a false value for layer weight as the mass is not evenly distributed. Aside from this area of thicker deposit, coil 3 showed a coating that resembled the results from previous phosphor layers. There is a slight lack of deposit on the inner faces of the sample, but this is characteristic of this study. The microscope imagery in Figure 53 shows areas of the substrate where there is no phosphor deposit but an even layer in surrounding areas. This is due to the inconsistency in the layer thickness of the dielectric and the piling effect. The outside face (upside down in imagery) shows evidence of piling and how this negatively affects the phosphor during sequencing experiments. Towards

the top of the coil, there is almost no deposited material, but the rest of the surface is uniform. The image of the inner face demonstrates the thinner deposit when compared to the outer face. This is visible by eye but more easily visualised here. The lack of deposit toward the inner faces of the coil is also shown by the bottom face image. Here there is a decrease in deposit material moving towards the inside of the sample. As stated previously, this is characteristic of these experiments. The comparison between the top and bottom faces finally demonstrates that there is still room for improvement in the suspension of the particles. From these two photographs, it is evident that there is less deposited material on the bottom face with spaces in the deposit.

Sequencing experiments have proved that it is possible to deposit a layer-by-layer device through electrophoretic deposition. The optimal parameters do require some adjustment to account for increased system resistance but, with deposited layers being very thin, this only requires a slight increase in certain parameters. With the design of experiments, it is possible to achieve almost total coverage, good adhesion, and relatively uniform thicknesses but the apparatus in use can be remodelled to improve this further.

## 5.6.Preliminary testing on PC coils and Ø4.7 mm samples

### 5.6.1. Deposition onto PC coils

As stated at the beginning of this thesis, testing onto aluminium substrates was used due to their low cost but aluminium-coated polycarbonate (PC) coils are to be used for the final product. These samples are much lighter in weight and are much more flexible than their aluminium counterparts due to PC having a lower elastic modulus. For primary testing of these samples, the same barium titanate bath formulation was used at a concentration of 25 g/L. As these samples would take another level of experimentation, optimal conditions for the aluminium coils were selected with the anticipation of alterations. Parameters were set at 260 V for a processing time of 60 s. Several tests were carried out with comparable results of deposit morphology. The resulting deposit from these experiments is shown in Figure 54.

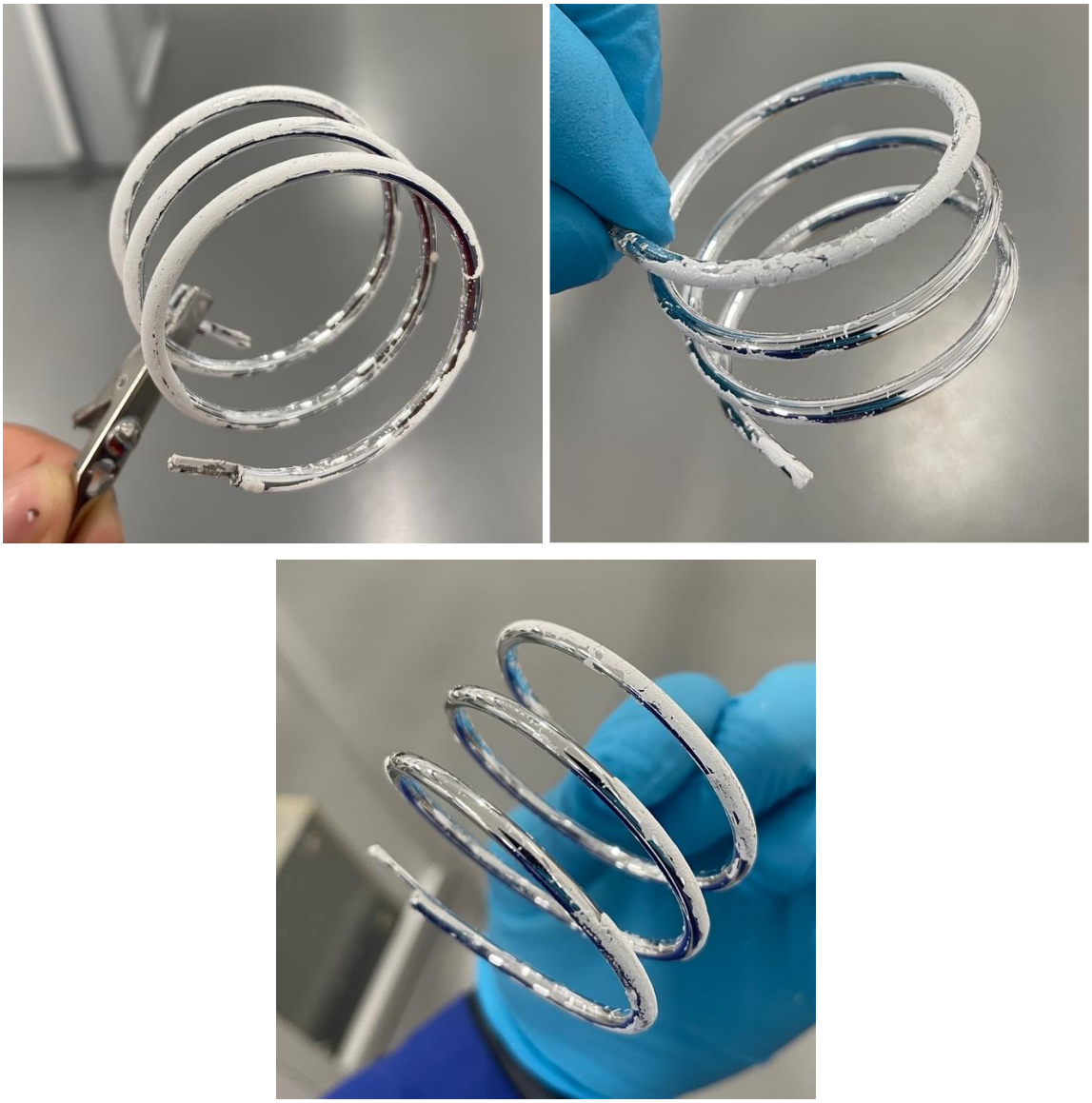

**Figure 54. Dielectric-coated PC coils**

Layer weight was not considered for these tests due to the obvious poor coverage of the substrate. Adhesion for these coils had decreased as any material that had been deposited through EPD would be easily knocked off with minimal force. For these tests, it was not so much an issue of the formulation but the sample itself and how it reacts under an electric field. Display current through these experiments also was of a much lower value, in the range of 4-6 mA. Low current density is due to the considerable decrease in conductive material in the substrate. The now thin coating of aluminium limited the current in the system and therefore would not demonstrate a good dielectric coating.

The surface of the PC coils was visibly much smoother and more reflective, so a sample was analysed under the 3D microscope to establish a surface roughness and view the surface at a

higher magnification. Figure 55 shows the comparison between the bare aluminium coil and the PC coil.

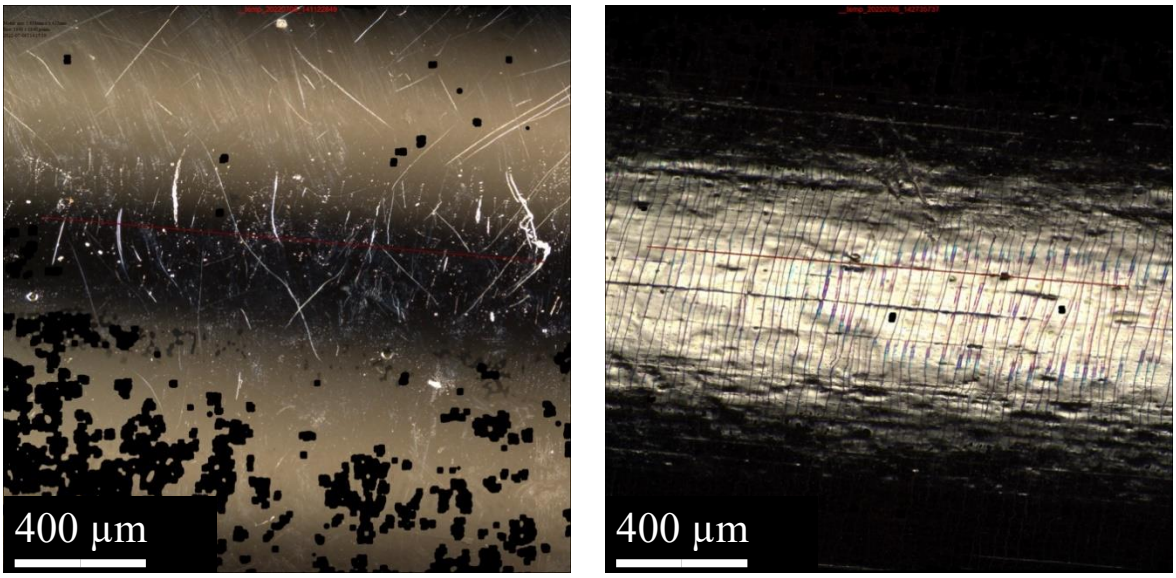


PC sample Aluminium sample

**Figure 55. Comparison of surface roughness of PC and aluminium samples**

The first issue faced with the PC coils was how reflective their surface is. This made analysis under the microscope much more difficult as is shown in the image render. By use of the 3D microscope, the surface roughness of the PC sample was measured as 0.278 µm whilst the aluminium coil was measured at 0.993 µm. This was a significant difference and can be one of the major reasons for poor layer uniformity and adhesion. Besra et al (2) alluded to the fact that the surface area of the counter electrode influences the mass of deposit following Hamaker's law. An increase in surface roughness increases the effective surface area of the substrate and therefore increases mass deposit. For the PC coil, processing parameters would need a major increase in magnitude, or the material could undergo some surface treatment. Zhang et al (77) document that sandblasting surface treatment effectively increases surface roughness and therefore increases the resulting mass of deposit.

Overall, the PC coil did not suit the experimental set-up for EPD as well as the aluminium samples. The validity of the deposition of all layers was proved through previous subsections so further alterations must be considered for the materials used in the emissive sources for successful deposition to occur.

### 5.6.2. Deposition onto Ø 4.7 mm aluminium samples

The sponsoring company have designed the product to be a lamp system consisting of a proprietary dual-channel geometric reflector, allied with two differing diameter low-power light emitting sources. The larger diameter source has been extensively tested throughout this thesis but parameters for experimentation still must be tested for the smaller diameter sample. The dimensions of this sample are 45 mm in height, 30 mm coil diameter, and 4.7 mm wire diameter with a surface area of 4.20 $cm^2$. Figure 56 displays a 3D render of the substrate.


**Figure 56. 3D render of the smaller emissive source.**

The first experiments on this sample required an adjustment of the experimental setup. Due to the diameter decreasing, the diameter of the counter electrode should also decrease to keep electrode spacing constant between experiments. Because of this, a smaller beaker of a diameter of 70 mm (FisherBrand FB33112) was used to design a new build. This build is shown in Figure 57**.**

The downsizing in beaker dimensions also came with the change to a smaller stirrer bar (20 mm). The counter electrode for these experiments was the same width as the height of the substrate stays the same. Because of this the counter electrode would be too large for the smaller beaker and had to be made slightly thinner (80 mm). With this sample the theory was, apart from the change in electrode spacing, experimental results should not be too dissimilar to that of the larger diameter coil. The thickness increase would account for the scaling down in diameter of the coil. As with the PC coils no results were guaranteed and the resulting deposits are shown in Figure 58 Processing parameters were set at 260 V and 45 s and identical tank formulation.

**Figure 57. Build used for initial, small-scale EPD.**

**Figure 58. First EPD results of dielectric onto small sample.**

Not visible in the images is the effect of piling which is more prominent in this experiment. As seen in the earliest experiments of this study, there is again a lack of deposited material on the bottom and innermost faces of the coil. Any material that is deposited has poor adhesion and can be easily wiped off. To solve this, an adjustment was made to a taller beaker of the same diameter (FisherBrand FB33124). This created more space in the beaker allowing for the counter electrode to be returned to 95 mm in width. The following experiments with the larger beaker used the same parameters and the resulting deposit is shown in Figure 59**.**

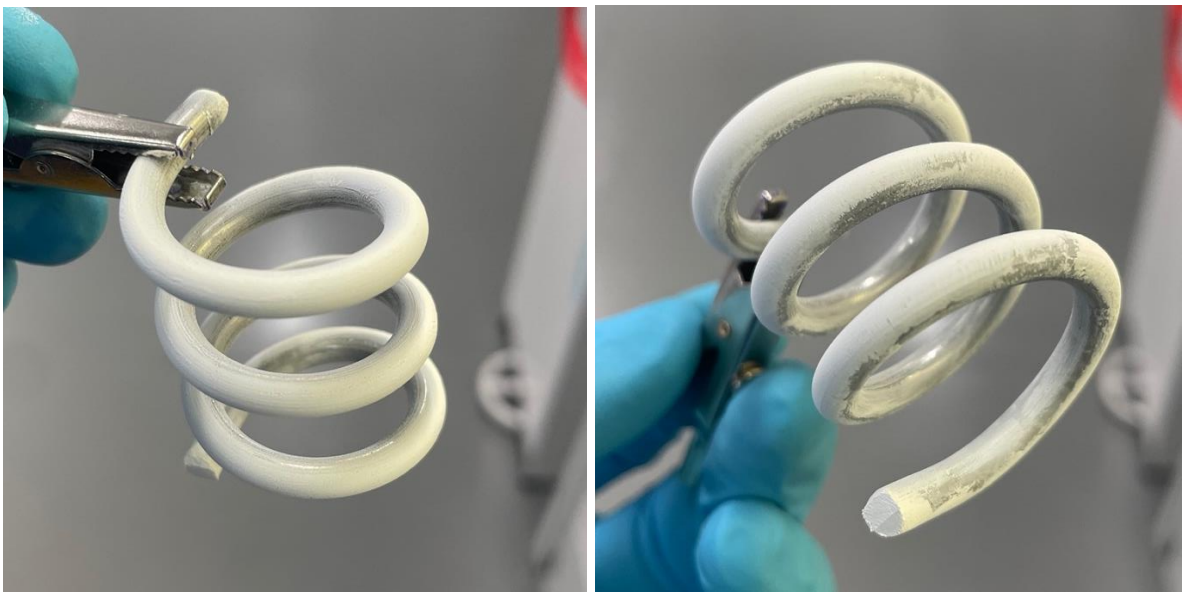

**Figure 59. EPD results of dielectric onto small sample with increased beaker dimensions.**

This gave a much-improved deposit but still displayed that there is room for optimisation of this process. The layer now exhibited no piling and good uniformity towards the upper side of the coil. There is still a poor coat deposited on the bottom and inner faces, but these results show promise for this layer. As proved through the earlier sections with the larger sample, electrodeposition is suited to the aluminium coil and gives results that exhibit good adhesion. The presumption is that phosphors would react in this way but due to time constraints, it was not possible to test the deposition of this material.

### 5.7.Discussion

This study allowed for an extensive investigation into the electrophoretic deposition of materials onto a 3D substrate to form the initial layers of an emissive source. It has been documented that the first 3 layers of this device will be dielectric, encapsulating polymer and phosphor. The investigation into the individual layers of the eventual device allowed for a wide range of processing parameters and conditions to be tested and analysed to establish optimal conditions for layer uniformity and coverage. Each of the layers demonstrated that there would be varying sets of optimal parameters which would depend on the material and the requirement of that layer. For example, the phosphor and dielectric materials are of different weights and target layer weights so would exhibit different requirements for processing parameters. Also, the encapsulating polymer would be deposited to assist in adhesion but also to make up for any spaces that may be left in the dielectric layer and therefore required much less material to be

deposited. These slight variations meant that assumptions could not be made for separate layers as they would not react in the same way to processing conditions.

### 5.7.1. Adjustments and challenges with equipment used for experiments.

Aside from the differences in layer requirements and materials, there was the issue of attempting to deposit on a complex 3D substrate. This is something that is not well documented through literature so would require significant experimentation to first establish trends so outcomes may be more predictable. Literature has shown the use of a circular counter electrode to exhibit an equal electric field (43), but these examples were onto a much simpler substrate. A complex shape like the coils used for this study would create a quite different electric field and for the electric field strength around the sample to be completely equal, a much more complex design of counter electrode would be required. In these experiments, the singular cylindrical electrode offered a reasonable alternative and allowed for good coatings to be achieved. An eventual increase in the width of the counter electrode proved to be beneficial, promoting a wider electric field and allowing for more areas of the coil to be coated. Along with the adjustment of the counter electrode, it was also important to ensure good suspension of particles in the tank with this being one of the main components of the EPD process (9). Particles must be well dispersed to avoid agglomeration which may be achieved through particle charging or agitation. Initially, stirring was used with agitation from the bottom of the tank but for the heavier particles, this would not promote vertical displacement of the particles and therefore poor suspension. To solve this, baffles would obstruct the horizontal flow and ensure particles were evenly spread through the formulation.

There was less coverage towards the inner face of the sample, but this was expected due to shadowing and a decrease in electrical field strength in these areas. To assist in increasing the electrical field strength towards the centre of the coil, a central counter electrode was tested. The theory here was that the material would now migrate from both the outer and inner electrodes and form a uniform deposit. The central electrode proved to be unnecessary for these experiments and cause deposit uniformity to decrease. Specifically with the dielectric layer, there was evidence of increased piling when the central counter electrode was in use. This concept of depositing onto a 3D substrate required innovation like this but in a capacity that would benefit the material deposit.

With improvements and innovation in the set-up of the experiments, there were also major drawbacks in the design. For the repeatability of these experiments to be improved, specific

experimental apparatus should be designed and manufactured to minimise the onset of error between experiments. The first issue met in these experiments was the deposition of material onto the crocodile clips. Initially, this would seem not very influential to the results but after consideration, it was something that needed to be rethought. Deposit of material onto the crocodile clips would increase the resistance at the junction between the sample and the clip and would therefore affect results from the following deposition tests. A slight change in the resistance here would cause experiments with identical parameters in every other respect to exhibit non-identical results. This type of discrepancy between individual tests was a recurring theme throughout the study as many parameters were controlled but not to a sufficient level. The second of these drawbacks came with the suspension of the coil in the fluid. The suspensions used for electrophoretic deposition were both opaque so once the entire coil was submerged in the fluid it was not visible to establish an equal electrode spacing. There are ways to solve this which are investigated in **Chapter 6** but for these rapid repeated experiments, it was rarely able to be effectively controlled. Unequal electrode spacing results in a non-uniform electrode field surrounding the coil which eventually results in an uneven coating.

### 5.7.2. Comparison of individual layers.

Of all the layers, the phosphor is the most widely documented (18–20,42)so formulations for experiments could be established without the need for experimentation. Validation experiments proved that the formulation would promote effective particle migration and deposition onto the substrate. Because of this, this layer quickly became the easiest to find optimal conditions for the deposit. As stated in **Section 5.7.1**, there is an element of unpredictability with a 3D substrate, so some changes were made with phosphor experiments, but formulation stayed constant with the only change coming with the sieving of the phosphors. This proved to assist with deposition because settling becoming less of an impact on experiments. After sieving was carried out, the mechanism of settling causing a mass gradient was no longer witnessed. The smaller particles also promoted better suspension in the formulation which improved the deposit onto all faces.

Comparatively, many more barriers were met in the electrophoretic deposition of the other two layers. Anodic deposition proved to be not suited to this project but had an element of success. Microscopy showed that material is deposited but the change in polarity through sequencing did not allow for this to be a viable process for the PMMA layer. After this, testing was carried out for cathodic deposition before eventually finding a suitable method of depositing material through dip coating. Dip coating is widely documented with parameters established for

maximising the quality of deposited material. With this, dip coating needed a few experiments before achieving the desired layer weight and effectively encapsulating the dielectric layer.

EPD of barium titanate was successful in the first experiments with the only issues being the deposited layer weight and spaces in the deposit. Apart from these spaces, the deposit was uniform in thickness, so steps were required to solely increase the deposit thickness and therefore weight. The dielectric layer was much greater in mass than the previous layers and particles being on the nanoscale would lead to a very dense deposit. Multiple bulk concentrations were tested to find a range that would demonstrate a layer with good coverage and uniform layer thickness. Contrary to the literature it was not possible to achieve films through sintering of the dielectric layer for this study as the PC coils that will be used in production would not be able to withstand temperatures this high. Because of this, drying was carried out at low temperatures causing very little change in the morphology of the deposited material. As is documented through literature (2,66), the higher material concentration decreased the uniformity but also negatively influences the adhesion of the layer. The poor adhesion was solved through the addition of PVP after testing alternative polymers (PVA) to find a compatible material.

Each of the layers has different requirements within the eventual EL device so, therefore, have different requirements for the deposit. The dielectric layer was targeted to be as thin a deposit as possible which would allow for a high capacitance within the device and acts as a protective layer from electric breakdown. Because of this the deposit should have minimal voids but the formation of voids is, in theory, solved by the deposition of an encapsulating polymer. Here, a thin, transparent layer protects and secures any dielectric to the substrate. As stated, a thin layer requirement suggests a much lower layer weight which is achieved through dip coating of the polymer. Finally, the phosphor layer was targeted to be a single particle in thickness by the sponsoring company. This was with the assumption particles are identical in size and shape so would not be possible with this deposition technique. Instead, the phosphor layer was targeted to achieve total coverage of the coil. This came with requirements to optimise particle suspension by the addition of baffles and investigation into optimal stirring rpm. The challenges of the separate layers were then elevated in the process of sequencing. Poor adhesion or uniformity of initial layers had a noticeable effect on the deposit of sequenced layers. This again revealed the importance of first achieving a dielectric deposit with optimal morphology so the following layers could demonstrate the same. Sequencing of layers came with an increase in substrate resistance. This is an effect that caused decreased deposited material and would require adjusted optimal values for processing parameters.

Constantly changing parameters and conditions like resistance and concentration made controlling the deposit of individual and sequenced layers much harder than anticipated and revealed that there would need to be further control measures put in place.

### 5.7.3. Final device considerations

The final build for these emissive sources will include two aluminium-coated PC coils and a further two layers so this study sets the base level of experiments which can be built on in future research. The knowledge of parameters that affect material deposit for each layer means that suitable adjustments can be made with sequencing onto the PC coils. The final two layers to be deposited will be the transparent electrode and a silver outer electrode. The outer layer is a semi-transparent conductor, made from Poly(3,4-ethylene-dioxythiophene) polystyrene sulfonate (PEDOT: PSS) with silver nanowires to improve conductivity but not at the expense of too much drop in transparency. The conductivity of the transparent electrodes is good but not to the extent of materials like silver. The role of this outer electrode is as a "current collector" or "bus bar" to help reduce the voltage loss across the relatively long length of the component ($\Delta V = IR$), as a support for the less conductive transparent layer but without blocking a large area of emitted light. The aim is to again use electrophoretic deposition for the transparent electrode which comes with its challenges as with the other layers. Once fully sequenced for the larger coil, experiments must also be carried out for the smaller sample. Some experiments were tested in this study on the smaller sample with limited success. Material was successfully deposited onto the coil but not to the uniformity and coverage of the larger coil that has been extensively tested throughout.

The PC coils were found to be too smooth a surface to deposit on so were not directly comparable to experiments on the aluminium samples. This was assumed to be down to the surface roughness decreasing the effective surface area of the coil but also due to the thin layer of metal compared to the solid metal in the samples. Surface treatment or remodelling of these components would need to occur for the parameters used in this study to be valid. Aside from the validity of the optimal parameters, this process revealed the effect of processing parameters and conditions on a 3D substrate. Formulations were proved to be suitable for the electrodeposition process therefore the only changes going forward should be to the substrate and the experimental set-up.

### 5.7.4. Evolution of experiments from the original build.

The original build designed for experiments for this project has drastically changed and allowed for a vastly improved resulting deposit. The change from a two-electrode to the singular electrode set-up has allowed for a new outlook on the build process for this device and will now look to further optimise the experimental set-up. The benefit of the electrodeposition process is its simplicity and the initial design of experiments overcomplicated this. The movement to a much simpler build proved beneficial and now more complex adjustments may be made to control the results of the experiment. The mounting frame in the original build made for extra obstruction in the process and ended up being detrimental to the resulting deposits. A benefit to take from this is the sealed mount that the samples are placed in. The non-conductive polymer sealing the electrical connection to the sample prevents the build-up of material deposits that are seen in the crocodile clips. This is a feature that can be used in future research to negate the build-up of resistance at the coil/connector interface. The considerable decrease in volume and voltage have also allowed for the process to be much safer and decrease the number of wasted materials were experiments to fail. Testing on a small scale as carried out through this research allows for rapid testing in a controlled laboratory environment. The decrease in operational volume also highlighted that there is no requirement for larger tanks for deposition to be improved. Tanks of this size may be used in future but for deposition onto multiple coils at once. Suspending multiple coils and fixed counter electrodes in a single tank allows for the repeatability of the tests to be improved. This is something that can be assessed in the future but for validation purposes, a 500 ml working volume has proved sufficient.

The suitability of this process and materials cannot yet be guaranteed to form effective devices to be used for lighting as further layers are to be deposited. These layers will also need to be deposited on a suitable substrate for the EL mechanism to be tested. Phosphor layers are prone to electrical breakdown at increased humidity so the layers' exposure should be kept to a minimum after deposition. Provided all layers are well deposited in a controlled environment, the layers should form a functioning emissive source due to the widespread usage of the individual materials in EL devices. Purpose-built experimental architecture should be established for the process to gain control of all stages of the process. These alterations and considerations will allow for the efficient production of these layers to test their electroluminescent properties.

# 6.Conclusions and recommendations

## 6.1.Conclusions

This study was carried out to primarily find suitable experimental parameters and conditions for electrophoretic deposition onto a 3D substrate. The success of these experiments would allow for each individual layer of an ACEL device to be tested to reach target values set by the sponsoring company. The refinement of these layers to find optimal parameters then allows for the preliminary stages of sequencing for the final ACEL device emissive source(s). The following notable observations were made through this study:

- Electrophoretic deposition onto a 3D substrate is made possible due to a novel apparatus build developed through extensive experimentation. Alterations to counter electrode dimensions from square to cylindrical and an increase in width ensured that it was now possible to coat an entire coil from outside to inside face simultaneously. There are some areas of the substrate where total uniformity has proved difficult to achieve but with further advancements in experimental design total uniform coverage is possible.
- Sequential deposition of dielectric, encapsulating polymer and phosphor was successful with coils exhibiting almost total coverage. Slight adjustments in previously established optimal conditions would allow for resistance to be compensated for. Increasing resistance of the system with increasing layer thickness must be considered in both the individual layer and sequencing stages.
- Sieving is a sensible step to improved deposition but cannot be fully proved until a full build has been fabricated. Sieving of phosphors narrowed their PSD, making their electrophoretic movement more predictable. The decrease in particle size allowed for particles to be better suspended in the formulation encouraging a more uniform deposit.
- Dip coating of PMMA in acetone successfully deposited material onto a 3D substrate. When sequencing onto a $BaTiO_3$-coated coil, adhesion of the coat improved and was a suitable encapsulation technique before the deposition of the phosphor layer.
- Anodic deposition is successful in the deposition of PMMA onto an Aluminium substrate but the phenomenon of electrolysis of water at the anode forms holes in the deposited layer. For a uniform deposit, further research must be carried out into alternate additives or solvents in the formulation and the removal of water. Anodic deposition also stripped the dielectric layer from the substrate due to opposite polarity.

- The electrophoretic deposition of barium titanate is suitable to be used in an EL device, but tank conditions must first be set at an optimal level. Concentration has the most noticeable effect on deposits with high concentrations demonstrating a non-uniform deposit with poor adhesion. Lower concentrations of material allow for a more uniform deposit with better adhesion to an extent. Exceptionally low concentrations exhibit spaces in the layer.
- The inability of sintering the deposited barium titanate layer prevents the formation of a smooth film and the deposited layer exhibits a higher surface roughness. This will cause a decrease in the luminance of emitted light if used in an EL device.
- PVP is a suitable additive to use to improve the adhesion of barium titanate. When comparing tests with and without the polymer, there is an obvious improvement in uniformity and adhesion with the PVP added.
- Stirring is an important parameter to be considered for EPD. Heavier particles in the phosphor formulation tend to settle so agitation is needed to prevent a deposit gradient. Baffles successfully suspend heavier particles equally in the formulation, promoting a vertical motion rather than solely rotational.
- Experimental design for aluminium-coated polycarbonate requires further testing. The smooth surface of the coils decreases their effective surface area, therefore, causing a poor deposit of material onto the coil. If these are to be used in the final device, they must undergo some form of surface treatment to increase roughness.

### 6.2.Recommendations

A prominent issue that was found with the experimental set-up through this study was the lack of control over certain distances and continuous movement of the apparatus. Figure 60 gives an example of an improved set-up that will allow for the components to be held in place more rigidly, ensuring better control of baffle placement and electrode spacing. Note that this design has the addition of the central electrode again. This is added to test deposition with the central counter electrode only. As experiments were carried out with both counter electrodes there was no opportunity to assess if, when connected on its own, the central electrode could assist in depositing material on the internal face. This experimental setup would allow for an initial test using just the outer counter electrode followed by a test with just the central counter electrode. Results could be assessed to understand if this is a viable way of achieving more total coverage of the coil.

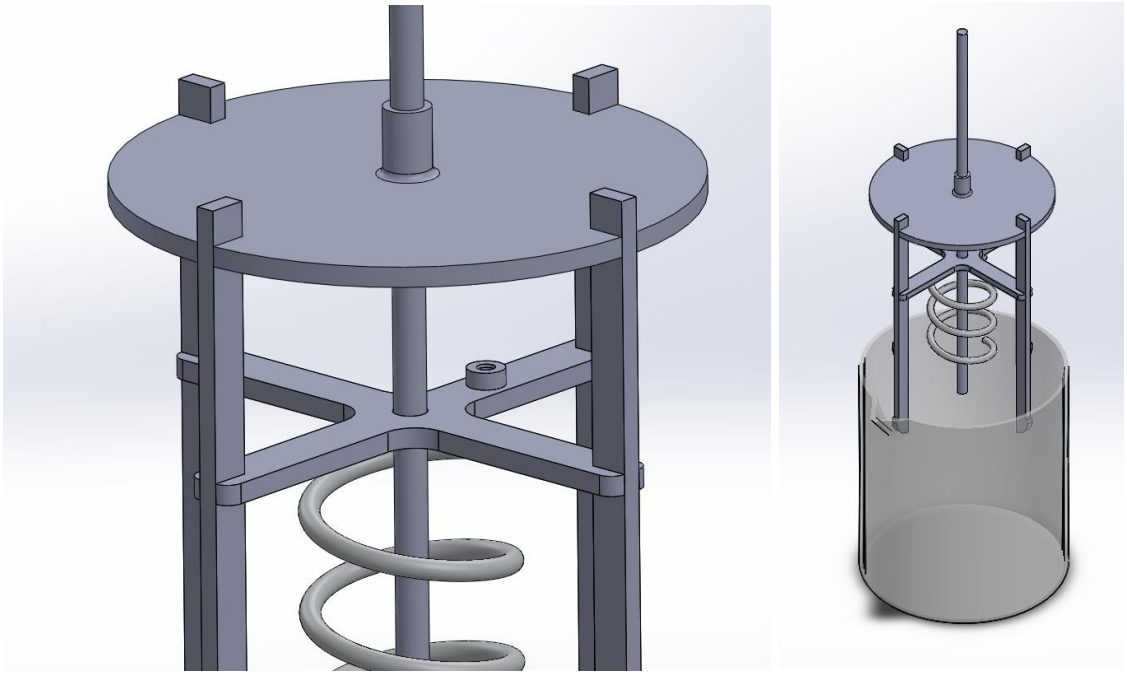

**Figure 60. Improved experimental design.**

As stated in **Section 5.7.4,** there are still further layers that must be deposited before the luminance of this device can be assessed. When the electrophoretic deposition of the PEDOT: PSS layer followed by the silver outer electrode is established and is successful, the device may then be tested for its validity as a light-emitting source. As with the layers investigated in this study, there is a considerable amount of experimentation that will be necessary to achieve a uniform deposit of these layers. To establish if the device will have success as a light emitting source, I also suggest deposition of all layers should first be tested onto a flat plate and luminance analysed. This way there are fewer variables in the process, and it is testing a process that has proven to work in a single plane. The materials used for this product have not been used together in an ACEL device and others haven't been at all deposited using electrophoretic deposition. Simplifying the process to a smaller scale, onto a less complex substrate allows for more aspects to be controlled and material selection to be validated. Small-scale experimentation will also allow for thorough instrumental analysis of deposited layers. Methods of analysing the Luxtec substrate are limited due to its complexity so a smaller flat substrate would prove beneficial at the initial stages. Alternative substrate design for small-scale testing would allow for several techniques to be employed that would benefit characterisation throughout the project. With methods already used through the project, surface roughness and topography can be quantitively analysed using 3D microscopy as values may be calculated over a flat area rather than a line. Improving the work done through this study, the 3D microscope can also produce a high-quality 3D render over a large area by combining

multiple scans into one image. This can also be used to calculate layer thickness over a larger area which was the main limitation of the complex geometry of the ‘coil’ substrate. Scanning electron microscopy (SEM) may be used to analyse the surface and cross-section of the deposit. As seen across the literature (2,10,18,20,42), it is possible to first analyse the surface of the deposit to assess the uniformity of the sequenced deposited layers and may be possible to introduce focussed ion beam (FIB) milling to form an image of the cross-section of the deposit. This then allows for a more accurate calculation of a dense deposit where a clear average layer thickness can be calculated. Photoluminescence (PL) analysis of the phosphor layer will also give a more in-depth understanding of the emission of the materials and compare this to the requirements and targets set by the sponsoring company. The combination of the three phosphors used through experimentation would, in theory, emit light at 6200K. The percentage distribution of the final deposit may not be identical due to differences in particle size or inaccurate measurements when replenishing material to the suspension. PL analysis would then be able to identify if there is an even spread of the individual phosphors and if more, or less material must be added. With this being identified at the preliminary stages of experimentation, there will be more confidence that the molar fraction of material in the suspension will form a deposit of the correct colour and luminance. For surface topography of individual layers and layers in sequence, atomic force microscopy (AFM) may be employed. AFM is based on the measurement of the variation of force between a sample surface and probe tip (78) and does not require a vacuum as in SEM so can be much more useful for rapid analysis. AFM can also produce a 3D image of the deposited surface on a nanometre scale and therefore can be slightly more beneficial than simple 3D microscopy.

An adjustment in the expectation for each deposited layer may also be necessary. Assumptions were made for each layer that are not realistic to experimental results. For example, the phosphor particles were assumed to be perfectly spherical and of identical sizes which would allow for a monolayer to be formed with ease. The actual result of this layer was a much broader PSD and the inability to form a monolayer with this simplified equipment. The simplicity of the counter electrode design meant that the inner face could not easily be deposited on to. This would then require an increase in processing time to account for the poor coverage which in turn creates a thicker layer on the outer face. First, total uniform coverage of the substrate should be the aim which can then be followed by refinement to decrease the layer weight and thickness as much as possible. Defining layer weight through PSD data and assumptions on particle weight makes the testing process much more difficult.

# 7.Appendix

## 7.1.Hoefer Tanks

SE600 Standard Dual Cooled Unit

## 7.2.Original tank configuration

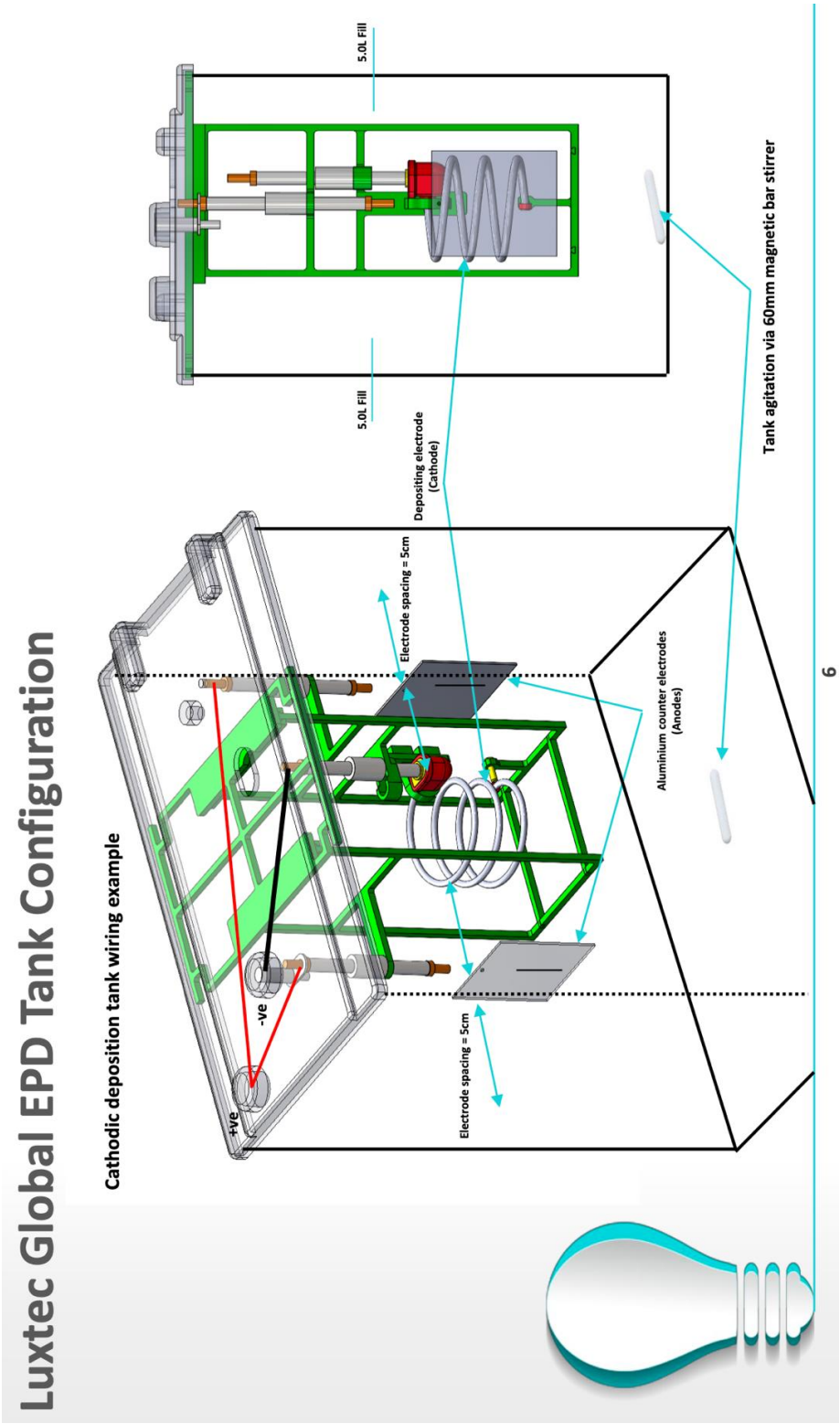

## 7.3.Glass tank build

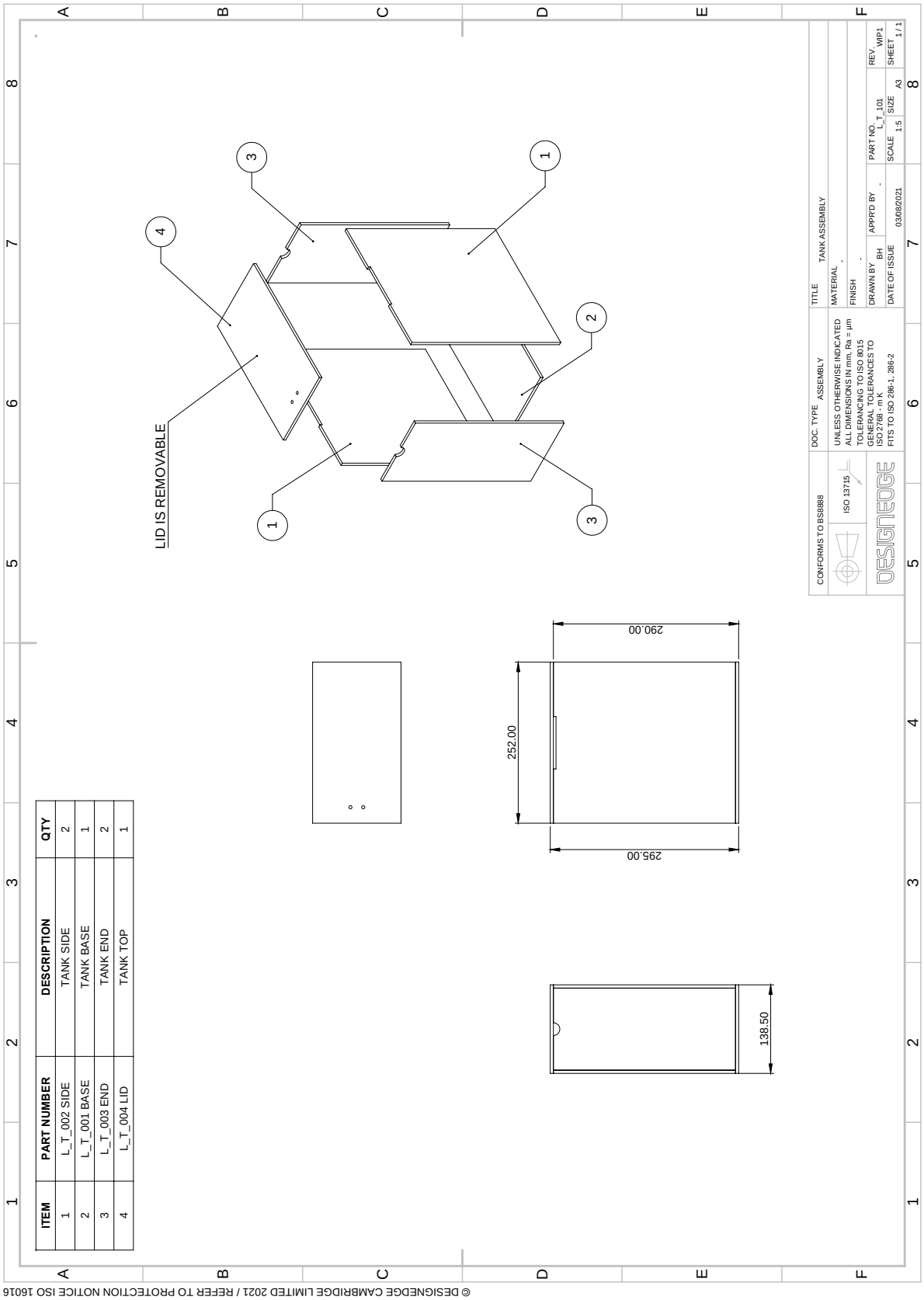


| ITEM | PART NUMBER | DESCRIPTION | QTY |
|---|---|---|---|
| 1 | L_T_002 SIDE | TANK SIDE | 2 |
| 2 | L_T_001 BASE | TANK BASE | 1 |
| 3 | L_T_003 END | TANK END | 2 |
| 4 | L_T_004 LID | TANK TOP | 1 |

### 7.4.PVA solubility testing

To improve the film of the barium titanate layer, the addition of PVA to the suspension was tested. To find out if PVA is suitable without damaging the already-made suspensions, solubility tests were carried out in small volumes of solvent. An IPA/Toluene solution was first tested with 30 ml and 20 ml of each solvent, respectively. 0.25 g of 80k Mw PVA was added and left to stir for 60-90 minutes. PVA at this molecular weight was not soluble so PVA with 9-10k and 20-30k molecular weight was added to 2 separate solutions of IPA/Toluene. These also were not soluble so another solvent is required that PVA will dissolve in. Testing of solubility using methanol with 1% 9-10k Mw PVA was carried out with no success.

## 7.5.EPD of barium titanate at 30 g/L (raw data)

| Experiment number | Voltage (V) | Dip time (s) | Layer weight (g) | +/- (g) | % | Rate of deposition (g/min) | Suspension Concentration (g/L) |
|---|---|---|---|---|---|---|---|
| 1 | 220 | 180 | 0.0850 | -0.0697 | -45.1% | 0.0283 | 30.0000 |
| 2 | 220 | 180 | 0.6342 | 0.4795 | 310.0% | 0.2114 | 29.9150 |
| 3 | 220 | 120 | 0.2726 | 0.1179 | 76.2% | 0.1363 | 29.2808 |
| 4 | 220 | 180 | 0.6299 | 0.4752 | 307.2% | 0.2100 | 29.0082 |
| 5 | 220 | 120 | 0.2606 | 0.1059 | 68.5% | 0.1303 | 30.0000 |
| 6 | 260 | 120 | 0.2196 | 0.0649 | 42.0% | 0.1098 | 29.7394 |
| 7 | 180 | 120 | 0.3009 | 0.1462 | 94.5% | 0.1505 | 29.5198 |
| 8 | 240 | 110 | 0.2957 | 0.1410 | 91.1% | 0.1613 | 29.2189 |
| 9 | 220 | 70 | 0.1584 | 0.0037 | 2.39% | 0.1358 | 29.2189 |
| 10 | 260 | 84 | 0.2200 | 0.0653 | 42.21% | 0.1571 | 29.0605 |
| 11 | 260 | 75 | 0.1321 | -0.0226 | -14.61% | 0.1057 | 28.8405 |
| 12 | 260 | 80 | 0.1643 | 0.0096 | 6.21% | 0.1232 | 28.7084 |
| 13 | 260 | 80 | 0.2300 | 0.0753 | 48.67% | 0.1725 | 28.5441 |
| 14 | 260 | 77 | 0.2507 | 0.0960 | 62.06% | 0.1954 | 28.3141 |
| 15 | 260 | 72 | 0.1540 | -0.0007 | -0.45% | 0.1283 | 28.0634 |
| 16 | 260 | 72 | 0.1222 | -0.0325 | -21.01% | 0.1018 | 27.9094 |
| 17 | 260 | 72 | 0.1535 | -0.0012 | -0.78% | 0.1279 | 27.7872 |
| 18 | 260 | 72 | 0.1454 | -0.0093 | -6.01% | 0.1212 | 27.6337 |
| 19 | 260 | 72 | 0.1267 | -0.0280 | -18.10% | 0.1056 | 27.4883 |

# 8.Bibliography


1. Blasse G, Grabmaier B. Luminescent Materials. Berlin: Springer-Verlag Berlin and Heidelberg GmbH & Co. KG; 1994. 210–213 p.
2. Besra L, Liu M. A review on fundamentals and applications of electrophoretic deposition (EPD). Vol. 52, Progress in Materials Science. 2007. p. 1–61.
3. Jayathilaka WADM, Chinnappan A, Tey JN, Wei J, Ramakrishna S. Alternative current electroluminescence and flexible light emitting devices. J Mater Chem C Mater. 2019;7(19):5553–72.
4. Zhang X, Wang F. Recent advances in flexible alternating current electroluminescent devices. APL Mater. 2021 Mar 1;9(3).
5. Hamaker HC. Formation of a deposit by electrophoresis. Transactions of the Faraday Society. 1940;35:279.
6. Avgustinik AI, Vigdergauz VS, Zharalev GI. Electrophoretic deposition of ceramic masses from suspensions and calculation of deposit yields. Journal of Applied Chemistry of the USSR (English translation). 1963;35(10):2175–80.
7. Antonelli E, Silva RS da, Bernardi MIB, Hernandes AC. Electrophoretic deposition of BaTi0.85Zr0.15O3 nanopowders. Materials Research. 2013 Jul 29;16(6):1344–9.
8. Hanaor D, Michelazzi M, Veronesi P, Leonelli C, Romagnoli M, Sorrell C. Anodic aqueous electrophoretic deposition of titanium dioxide using carboxylic acids as dispersing agents. J Eur Ceram Soc. 2011 Jun;31(6):1041–7.
9. Van Tassel JJ, Randall CA. Mechanisms of Electrophoretic Deposition. Key Eng Mater. 2006 Jul;314:167–74.
10. Amrollahi P, Krasinski JS, Vaidyanathan R, Tayebi L, Vashaee D. Electrophoretic Deposition (EPD): Fundamentals and Applications from Nano- to Micro-Scale Structures. In: Handbook of Nanoelectrochemistry. Springer International Publishing; 2015. p. 1–27.
11. Delgado A v., González-Caballero F, Hunter RJ, Koopal LK, Lyklema J. Measurement and interpretation of electrokinetic phenomena: (IUPAC technical report). Vol. 77, Pure and Applied Chemistry. 2005. p. 1753–805.
12. Hanaor D, Michelazzi M, Leonelli C, Sorrell CC. The effects of carboxylic acids on the aqueous dispersion and electrophoretic deposition of ZrO2. J Eur Ceram Soc. 2012 Jan;32(1):235–44.
13. Van der Biest OO, Vandeperre LJ. ELECTROPHORETIC DEPOSITION OF MATERIALS. Annual Review of Materials Science. 1999 Aug;29(1):327–52.
14. Grillon F, Fayeulle D, Jeandin M. Quantitative image analysis of electrophoretic coatings. J Mater Sci Lett. 1992;11(5):272–5.
15. Sarkar P, Nicholson PS. Electrophoretic Deposition (EPD): Mechanisms, Kinetics, and Application to Ceramics. Journal of the American Ceramic Society. 1996 Aug;79(8):1987–2002.
16. Fukada Y, Nagarajan N, Mekky W, Bao Y, Kim HS, Nicholson PS. Electrophoretic deposition—mechanisms, myths and materials. J Mater Sci. 2004 Feb;39(3):787–801.
17. Stappers L, Zhang L, van der Biest O, Fransaer J. The effect of electrolyte conductivity on electrophoretic deposition. J Colloid Interface Sci. 2008 Dec 15;328(2):436–46.
18. Talbot JB, McKittrick J. Review—Electrophoretic Deposition of Phosphors for Solid-State Lighting. ECS Journal of Solid State Science and Technology. 2016;5(1):R3107–20.

19. Shane MJ, Talbot JB, Sluzky E, Hesse KR. Zeta potential of phosphors. Colloids Surf A Physicochem Eng Asp. 1995 Mar;96(3):301–5.
20. Shane MJ, Talbot JB, Sluzky E, Hesse KR. Electrophoretic Deposition Of Phosphors For Display Technology. MRS Proceedings [Internet]. 1994 Feb 15;345:299. Available from: http://link.springer.com/10.1557/PROC-345-299
21. Goossen JD, Alizade A, Bredol M. Electrophoretic deposition of carbon/ZnS composite electrode layers. Mater Chem Phys. 2020 Jan;239:122083.
22. BYJUS. Dielectric Constant - Definition, Formula, Symbol, Units, Values. https://byjus.com/physics/dielectric-constant/. 2022.
23. Sarkar P, Nicholson PS. Electrophoretic Deposition (EPD): Mechanisms, Kinetics, and Application to Ceramics. Journal of the American Ceramic Society. 1996 Aug;79(8):3341–65.
24. Koura N, Tsukamoto T, Shoji H, Touru Hotta TH. Preparation of Various Oxide Films by an Electrophoretic Deposition Method: A Study of the Mechanism. Jpn J Appl Phys. 1995 Mar 1;34(3R):1643.
25. Ojo AA, Dharmadasa IM. Electroplating of Semiconductor Materials for Applications in Large Area Electronics: A Review. Coatings. 2018 Jul 27;8(262):1–12.
26. Binner J. Advanced Ceramic Processing and Technology. Vol. 1. Park Ridge, N.J., U.S.A: Noyes Publications; 1990. 255–283 p.
27. Sun J, Zhong DK, Gamelin DR. Composite photoanodes for photoelectrochemical solar water splitting. Energy Environ Sci. 2010;3(9):1252.
28. Rastogi AC, Balakrishnan KS. Growth, structure and composition of electrodeposited CdTe thin films for solar cells. Solar Energy Materials and Solar Cells. 1995 Feb;36(2):121–46.
29. Razmjoo O, Bahrololoom ME, Najafisayar P. The effect of current density on the composition, structure, morphology and optical properties of galvanostatically electrodeposited nanostructured cadmium telluride films. Ceram Int. 2017 Jan;43(1):121–7.
30. Sarkar P, De D, Rho H. Synthesis and microstructural manipulation of ceramics by electrophoretic deposition. J Mater Sci. 2004 Feb;(39):819–23.
31. Peng Z, Liu M. Preparation of Dense Platinum-Yttria Stabilized Zirconia and Yttria Stabilized Zirconia Films on Porous La0.9Sr0.1MnO3 (LSM) Substrates. Journal of the American Ceramic Society. 2004 Dec 20;84(2):283–8.
32. Kajikawa Y. Roughness evolution during chemical vapor deposition. Mater Chem Phys. 2008 Dec;112(2):311–8.
33. Komiyama H, Shimogaki Y, Egashira Y. Chemical reaction engineering in the design of CVD reactors. Chem Eng Sci. 1999 Jul;54(13–14):1941–57.
34. Jones AC, Hitchman ML, editors. Chemical Vapour Deposition. Vol. 1. Cambridge: Royal Society of Chemistry; 2008. 1–26 p.
35. Sivaram S. Chemical Vapour Deposition: Thermal and Plasma Deposition of Electronic Materials. 1st ed. Springer; 2013.
36. McHardy J, Ludwig F. Electrochemistry of Semiconductors and Electronics: Processes and Devices. 1st ed. Norwich, NY, USA: William Andrew; 1992.
37. Ojo AA. Engineering of Electroplated Materials for Multilayer Next Generation Graded Bandgap Solar Cells. Sheffield Hallam University; 2017.
38. Yasmeen S, Ryu SW, Lee S, Lee H. Atomic Layer Deposition Beyond Thin Film Deposition Technology. Adv Mater Technol. 2022 Oct 10;2200876.
39. Knoops HCM, Potts SE, Bol AA, Kessels WMM. Atomic Layer Deposition. In: Kuech T, editor. Handbook of Crystal Growth. 2nd ed. Elsevier; 2015. p. 1101–34.

40. Bernardin GA, Davies NA, Finlayson CE. Spray-coating deposition techniques for polymeric semiconductor blends. Mater Sci Semicond Process. 2017 Nov;71:174–80.
41. Noebels M, Cross RE, Evans DA, Finlayson CE. Characterization of spray-coating methods for conjugated polymer blend thin films. J Mater Sci. 2014 Jun 4;49(12):4279–87.
42. Russ BE, Talbot JB. A Study of the Adhesion of Electrophoretically Deposited Phosphors. J Electrochem Soc. 1998 Apr 1;145(4):1245–52.
43. Ozhukil Kollath V, Chen Q, Mullens S, Luyten J, Traina K, Boccaccini AR, et al. Electrophoretic deposition of hydroxyapatite and hydroxyapatite–alginate on rapid prototyped 3D Ti6Al4V scaffolds. J Mater Sci. 2016 Mar 16;51(5):2338–46.
44. Angel K, Tsang HH, Bedair SS, Smith GL, Lazarus N. Selective electroplating of 3D printed parts. Addit Manuf. 2018 Mar;20:164–72.
45. Wang L, Xiao L, Gu H, Sun H. Advances in Alternating Current Electroluminescent Devices. Adv Opt Mater. 2019 Apr 23;7(7):1801154.
46. Liu JM. Photonic Devices. 1st ed. Cambridge: Cambridge University Press; 2005. 816–820 p.
47. Wang K, Chen P, Chen J, Liu Y, Wu C, Sun J, et al. Alternating current electroluminescence from GaN-based nanorod light-emitting diodes. Opt Laser Technol. 2021 Aug;140:1–7.
48. Krasnov AN, Hofstra PG. Growth, characterization and modeling of alternating-current thin-film electroluminescent devices. Progress in Crystal Growth and Characterization of Materials. 2001 Jan;42(3):65–164.
49. Yang Z, Wang W, Pan J, Ye C. Alternating Current Electroluminescent Devices with Inorganic Phosphors for Deformable Displays. Cell Rep Phys Sci. 2020 Oct;1(10):1–27.
50. Krasnov AN. Selection of dielectrics for alternating-current thin-film electroluminescent device. Thin Solid Films. 1999 Jun;347(1–2):1–13.
51. Winscom C, Withnall R, Silver J. Handbook of Digital Imaging. 1st ed. Kriss M, editor. Chichester: John Wiley & Sons, Ltd; 2015. 1–18 p.
52. Gispert JR. Coordination Chemistry. 1st ed. Weinheim: Wiley-VCH; 2008. 483 p.
53. Tiwari S, Tiwari S, Chandra BP. Characteristics of a.c. electroluminescence in thin film ZnS : Mn display devices. Journal of Materials Science: Materials in Electronics. 2004 Sep;15(9):569–74.
54. Kamal ChS, Mishra RK, Patel DK, Rao KR, Sudarsan V, Vatsa RK. Effect of structure, size and copper doping on the luminescence properties of ZnS. Mater Res Bull. 2016 Sep;81:127–33.
55. Park KW, Jeong HS, Park JH, Deressa G, Jeong YT, Lim KT, et al. Flexible powder electroluminescent device on silver nanowire electrode. J Lumin. 2015 Sep;165:216–9.
56. Schrage C, Kaskel S. Flexible and Transparent SWCNT Electrodes for Alternating Current Electroluminescence Devices. ACS Appl Mater Interfaces. 2009 Aug 26;1(8):1640–4.
57. Stauffer F, Tybrandt K. Bright Stretchable Alternating Current Electroluminescent Displays Based on High Permittivity Composites. Advanced Materials. 2016 Sep 14;28(33):7200–3.
58. Gupta BK, Singh S, Kedawat G, Kanika K, Kumar P, Gangwar AK, et al. A novel electroluminescent device based on a reduced graphene oxide wrapped phosphor (ZnS:Cu,Al) and hexagonal-boron nitride for high-performance luminescence. Nanoscale. 2017;9(15):5002–8.

59. Hu L, Kim HS, Lee JY, Peumans P, Cui Y. Scalable Coating and Properties of Transparent, Flexible, Silver Nanowire Electrodes. ACS Nano. 2010 May 25;4(5):2955–63.
60. Hu L, Gruner G, Gong J, Kim CJ "CJ", Hornbostel B. Electrowetting devices with transparent single-walled carbon nanotube electrodes. Appl Phys Lett. 2007 Feb 26;90(9).
61. Wroblewski G, Kielbasinski K, Stapinski T, Jaglarz J, Marszalek K, Swatowska B, et al. Graphene Platelets as Morphology Tailoring Additive in Carbon Nanotube Transparent and Flexible Electrodes for Heating Applications. J Nanomater. 2015;2015:1–8.
62. En-on J, Sriprachuabwong C, Tuantranont A, Wongkokua W, Wongchoosuk C. Flexible alternating current electroluminescent display: Study of parameters on light emission. In: 2014 11th International Conference on Electrical Engineering/Electronics, Computer, Telecommunications and Information Technology (ECTI-CON). IEEE; 2014. p. 1–4.
63. de Vos M, Torah R, Tudor J. Dispenser printed electroluminescent lamps on textiles for smart fabric applications. Smart Mater Struct. 2016 Apr 1;25(4).
64. Angelo P. Inkjet-printed Light-emitting Devices: Applying Inkjet Microfabrication to Multilayer Electronics. [Toronto]: University of Toronto; 2013.
65. Lee TM, Hur S, Kim JH, Choi HC. EL device pad-printed on a curved surface. Journal of Micromechanics and Microengineering. 2010 Jan 1;20(1).
66. Louh RF, Hsu YH. Fabrication of barium titanate ferroelectric layers by electrophoretic deposition technique. Mater Chem Phys. 2003 Apr;79(2–3):226–9.
67. Louh RF, Ku Y, Tsai I. Rapid prototyping technique for ceramic mini-devices containing internal channels with asymmetrical contour. J Eur Ceram Soc. 2010 Oct;30(14):2841–7.
68. Negishi H, Yamaji K, Imura T, Kitamoto D, Ikegami T, Yanagishita H. Electrophoretic Deposition Mechanism of YSZ/n-Propanol Suspension. J Electrochem Soc. 2005;152(J16).
69. James B. Mixing 101: Baffled by Baffles? DYNAMIX AGITATORS. 2012.
70. M M. Agitation, Mixing & Dispersion. Asiantech.
71. Kamla Y, Bouzit M, Ameur H, Arab MI, Hadjeb A. Effect of the Inclination of Baffles on the Power Consumption and Fluid Flows in a Vessel Stirred by a Rushton Turbine. Chinese Journal of Mechanical Engineering. 2017 Jul 12;30(4):1008–16.
72. Sato N, Kawachi M, Noto K, Yoshimoto N, Yoshizawa M. Effect of particle size reduction on crack formation in electrophoretically deposited YBCO films. Physica C Supercond. 2001 Aug;357–360:1019–22.
73. Basu RN, Randall CA, Mayo MJ. Fabrication of Dense Zirconia Electrolyte Films for Tubular Solid Oxide Fuel Cells by Electrophoretic Deposition. Journal of the American Ceramic Society [Internet]. 2001 Jan;84(1):33–40. Available from: https://onlinelibrary.wiley.com/doi/10.1111/j.1151-2916.2001.tb00604.x
74. Tatiparti SS v., Ebrahimi F. Potentiostatic versus galvanostatic electrodeposition of nanocrystalline Al–Mg alloy powders. Journal of Solid State Electrochemistry. 2012 Mar 17;16(3):1255–62.
75. Vandeperre L, van der Biest O, Clegg WJ. Silicon Carbide Laminates with Carbon Interlayers by Electrophoretic Deposition. Key Eng Mater. 1996 Nov;127–131:567–74.
76. Grosso D. How to exploit the full potential of the dip-coating process to better control film formation. J Mater Chem. 2011;21(43):17033.

77. Zhang H, Liu Y, Yuan J, Zhu M, Chen J, Wang Z. The influence of substrate surface treatment on the electrodeposition of (Co,Mn) $_3$ O $_4$ spinel precursor coatings. Mater Res Express. 2020 Jul 1;7(7):076405.
78. Chatterjee S, Biswas N, Datta A, Dey R, Maiti P. Atomic force microscopy in biofilm study. Microscopy. 2014 Aug;63(4):269–78.